

CHARLES UNIVERSITY IN PRAGUE

Faculty of Science

Developmental and Cell Biology



The role of transcriptional factor Tcf7l1 and Wnt/ β -catenin signaling pathway during differentiation of the head ectoderm.

Ph.D. Thesis

Jan Mašek

Supervisor: Zbyněk Kozmik, Ph.D.

Co-supervisor: Ondřej Machoň, Ph.D.

Department of Transcriptional regulation

Institute of Molecular Genetics of the ASCR, v. v. i.

Prague, 2016

Declaration

I declare that I wrote the thesis independently and that I cited all the information sources and literature. This work was not presented to obtain another academic degree or equivalent.

Prague, 10.2.2016

Jan Mašek

Acknowledgments

Firstly, I would like to express my sincere gratitude to my supervisor Zbyněk Kozmik for supporting my research both mentally and materially and for allowing me to grow as a research scientist. Special appreciation and thanks to my co-supervisor Ondřej Machoň for being positive and ready to help during all the ups and downs of this project. I am very thankful to our technicians Veronika Nosková, Jitka Láchová, Lucie Svobodová, Jindra Pohořelá, Anna Zittová and Katarina Kováčova who let me focus on experimental work, bearing the burden of endless genotyping and preparation of the common, yet indispensable, reagents on their backs. I consider myself extremely lucky since I always had really great fellow labmates around. My Ph.D. studies were no exception and I hope that people from Lab 29 enjoyed our time together as much as I did. From all the present and former members of the lab I want to namely thank Peter Fabian, Jiří Pergner, Lucie Žilova, Barbora Antošová, Vladimír Soukup, Kamil Matulka and Pavel Vopálenky for, apart from being great fun, they shared their knowledge and lab experience with me. In addition, special thanks to Chrysa Pantzartzi for proofreading this and other manuscripts. I would like to thank Hynek Strnad and his team for analysis of the microarray samples and him and Michal Kolář for their patience in answering of my bio-statistical questions. From all the nice colleagues at the Institute of Molecular Genetics I want to thank Vladimír Kořínek, Bohumil Fafílek, Vendula Pospíchalová, Lucie Janečková, Jana Balounová and Ondřej Svoboda for friendly sharing of both lab material and experience.

Finally, I would like to thank my family, my parents who let me decide what I want to do in my life and together with my sister supported me in all my pursuits. Words cannot express how grateful I am to my wife Daniela, for being my partner, friend, and mother to our beloved son Vitek. I would not be able to finish this project without the energy they gave me every moment we spent together.

Table of contents

Declaration	2
Acknowledgments	3
Table of contents	4
List of abbreviations	5
Abstract (English)	8
Abstrakt (Czech)	9
Introduction	10
Wnt/ β -catenin signaling pathway.....	10
Wnt/ β -catenin signaling in the nucleus and transcription factors Tcf/Lef	12
Differentiation of the head ectoderm	13
Anterior neural fold and Wnt/ β -catenin signaling	14
Role of the Wnt/ β -catenin signaling in neural crest formation	16
Wnt/ β -catenin signaling in placodal development.....	17
Tcf711: a potential regulator of the Wnt activity during mouse embryonic development.....	18
Aims of the study	20
Materials and Methods	22
Results	27
1) Manipulation of the Wnt/β-catenin signaling in the mouse neural crest and anterior neural fold via conditional deletion of <i>Tcf711</i> gene and subsequent analysis of the phenotype	27
AP2 α -Cre mediated deletion of <i>Tcf711</i> during mouse NC specification results in exencephaly.	27
Tcf711 is required for the expression of anterior neural markers	30
Tcf711 deletion results in aberrant trans-differentiation of the ANF cells into NC	32
Trans-differentiation of the ANF is driven by aberrant Wnt/ β -catenin signaling	34
The phenotype can be rescued with a truncated form of TCF4 but not with Tcf711 fused with β -catenin	39
2) Investigation of the effects of <i>Tcf711</i> deletion on the anterior pre-placode, with the focus on lens placode development in mouse	43
<i>Tcf711</i> positively regulates expression of the anterior PPR and ANF specifiers	43
Conditional deletion of <i>Tcf711</i> in the lens placode causes severe defects in lens development.....	46
<i>Tcf711</i> is not required during early differentiation of the developing lens.....	47
Absence of <i>Tcf711</i> results in the cell cycle imbalance and apoptosis of the fiber cells	49
<i>Tcf711</i> is negative regulator of the Cdkn1a ^{P21/Waf} expression during lens development	51
Discussion	55
Conclusions	63
List of publications	64
References	65
Appendix	72

List of abbreviations

4-OHT	4-hydroxitamoxifen
aa	amino acid
ANF	anterior neural fold
ANF	anterior neural fold
A-P	anterio-posterior
APC	adenomatous polyposis coli
APC	adenomatous polyposis coli
Axin	axis inhibition
Axud	Axin-1 up-regulated gene protein
BAT-gal	β -catenin activated transgene driving expression of nuclear β -galactosidase reporter
Bcl	B-Cell CLL/Lymphoma
BMP	bone morphogenic protein
BrDU	5-Bromo-2'-deoxyuridine
Brna3a	POU class 4 homeobox 1
BSA	bovine serum albumin
CBP	CREB binding protein
Cdkn1a	cyclin dependent kinase inhibitor 1
CK	casein kinase
cMaf	V-maf musculoaponeurotic fibrosarcoma oncogene homolog
c-Myc	avian myelocytomatosis viral oncogene homolog
CNS	central nervous system
C-term	carboxy-terminus
Dkk	dickkopf
Dlx	distal-less homeobox
Dvl	dishevelled
Eya	eyes absent
EYFP	enhanced yellow fluorescent protein
FGF	fibroblast growth factor
FLP	LoxP-flippase
Fox	forkhead box
Fzd	frizzled

Gbx	gastrulation brain homeobox
GRG	groucho-related gene
GRN	gene regulatory network
GSK3	glycogen synthase kinase 3
H&E	hematoxylin & eosin
H3-K4me3	tri-methylation of lysine 27 on histone H3
Hesx	homeobox expressed in ES cells
ICAT	inhibitor of β -catenin and Tcf
Irx	iroquois homeobox
Lef	lymphoid enhancer-binding factor
LoxP	locus of crossover in P1
Lrp	low density lipoprotein receptor-related protein
MEF	mouse embryonic fibroblast
Meis	myeloid ecotropic viral integration site homeobox
MHB	midbrain-hindbrain boundary
MLL	methyltransferases mixed-lineage-leukemia
MO	morpholino
NC	neural crest
Neo	neomycine resistance
NeuroD	neuronal differentiation
NNE	non-neural ectoderm
NPB	neural plate border
Oct	octamer-binding protein
Otx	orthodenticle homeobox
p21	protein 21
p57	protein 57
Pax	paired box
PBS	phosphate buffer solution
PCNA	proliferating cell nuclear antigen
PFA	paraformaldehyde
PGK	phosphoglycerate kinase promoter
PP	protein phosphatase
PPR	pre-placodal region

Prox	prospero homeobox
ROSA	reverse orientation splice acceptor
Rx	retina and anterior neural fold homeobox
SFRP	secreted frizzled-related protein
Six	sine oculis homeobox
Sox	SRY(Sex Determining Region Y)-Box
Tcf	T Cell-specific factor
Tfap2 α	transcription factor AP-2 Alpha
TLE	transducin-like enhancer of split
Wif	Wnt inhibitory factor
Zic	zinc finger protein of the cerebellum
β -TrCP	F-box containing β -transducin repeat containing

Abstract (English)

Differentiation of the head ectoderm is crucial for the evolutionary diversification of vertebrates. Expression of the genes responsible for this process is orchestrated throughout complex gene regulatory networks that are induced and modulated by Wnt, FGF and BMP signaling pathways. In addition, Wnt/ β -catenin signaling, in combination with expression of the Wnt antagonists from the rostral-most part of the head ectoderm, represent a key source of information for the regionalization of the tissue along the antero-posterior axis. This allows the differentiation of the anterior ectoderm that gives rise to the anterior neural fold (ANF) and anterior part of the presumptive placodal region (PPR), and more posterior ectoderm where higher levels of active Wnt/ β -catenin signaling promote differentiation into the neural crest (NC) and posterior PPR. Although the requirement of Wnt/ β -catenin signalling for ANF, PPR and NC development has been intensively studied in non-mammalian vertebrate model organisms, we lack a clear picture about the situation in mammals. Furthermore, current knowledge in mammals has been gathered via experiments on the level of β -catenin and very little is known about the individual roles of the Tcf/Lef transcription factors. Thereby, we decided to manipulate the Tcf711, member of the Tcf/Lef family with unique ability to act as a strong transcriptional repressor even in the presence of β -catenin. Through conditional deletion of the *Tcf711* gene in neural plate border of developing mouse embryo, we managed to describe function of the Tcf711 protein as well as the role of the Wnt/ β -catenin signaling in the process of mammalian head ectoderm specification. Absence of Tcf711 led to aberrant activation of the Wnt/ β -catenin signaling in the anterior neuroectoderm and its conversion into the NC. As a result, cell populations of the developing prosencephalon and anterior PPR were restrained. Importantly, this phenotype was not accompanied by changes of the anterior-posterior neural character. Thus, Tcf711 defines the border between the region of prospective forebrain and anterior placodes on one hand and the neural crest on the other, via restriction of the Wnt/ β -catenin signaling gradient.

Abstrakt (Czech)

Jedním z klíčových momentů v evoluci obratlovců bylo bezpochyby rozrůznění funkcí hlavového ektodermu. Genové regulační sítě využívané během tohoto procesu, jsou tvořeny množstvím genů jejichž exprese je spouštěna, a dále modulována pomocí signalizačních drah Wnt, FGF a BMP. K tomu je třeba přičíst i vliv signalizace Wnt/ β -kateninu a jejích antagonistů přítomných v rostrální části hlavového ektodermu, kteří jsou klíčoví pro regionalizaci tkání v rámci antero-posteriorní osy embrya. Kombinace těchto faktorů umožnila diverzifikaci anteriorního ektodermu na anteriorní neurální val (ANV) a rostrální preplakodální oblast (PPO), zatímco v posteriornějším ektodermu vznikají působením signální dráhy Wnt buňky neurální lišty (NL) a posteriorní PPO. Přestože byl vliv signalizační dráhy Wnt/ β -katenin detailně studován v kontextu vývoje ANV, PPO a NL u nesavčích modelových organismů, její vliv na vývoj těchto tkání u savců je stále nejasný. Navíc bylo současných poznatků u savců dosaženo pomocí experimentálních zásahů na úrovni β -kateninu, v důsledku čehož zůstává úloha transkripčních faktorů z rodiny Tcf/Lef v těchto procesech takřka neznámá. Z těchto důvodů jsme se rozhodli studovat transkripční represor *Tcf711*, který je členem rodiny Tcf/Lef a vyznačuje se schopností potlačovat genovou expresi i za přítomnosti β -kateninu. Pomocí cílené delece genu *Tcf711* v oblasti lemující neurální ploténku se nám podařilo objasnit funkci proteinu Tcf711 během specifikace hlavového ektodermu a zároveň charakterizovat význam, který při tomto procesu hraje signalizační dráha Wnt/ β -katenin. Nepřítomnost proteinu Tcf711 vedla k zvýšené aktivaci signalizace Wnt/ β -katenin v buňkách předního neuroektodermu, která měla za následek jejich přeměnu v buňky NL. Tento zásah negativně ovlivnil vývoj buněčných populací ANV a PPE. Je důležité zmínit, že embrya s tímto fenotypem nevykazovala změny v antero-posteriorním charakteru neurální tkáně. Souhrnem lze říct, že *Tcf711* definuje hranici mezi budoucím předním mozkem a anteriorními plakodami na jedné straně a neurální lištou na straně druhé, a to pomocí restriktivní kontroly gradientu aktivity signalizační dráhy Wnt/ β -katenin.

Introduction

Wnt/ β -catenin signaling pathway

The first mammalian gene coding for Wnt ligand was identified more than 30 years ago (Nusse and Varmus, 1982) and since then the Wnt signaling pathway became one of the most extensively studied phosphorylation cascade in general. The term “Wnt signaling” does not imply a single biochemical signal transduction pathway. Rather, it refers to a collection of signaling cascades triggered by Wnt ligand-receptor interactions that can affect key cellular processes: cell polarity, movement, proliferation, differentiation, survival and self-renewal. Due to its important role in maintaining homeostasis during adulthood, deregulation of the Wnt signaling activity is often connected with carcinogenesis and therefore it is of great interest for the whole field of biomedical research (reviewed in Clevers and Nusse (2012); Holland et al. (2013); Krausova and Korinek (2013)). Wnt/ β -catenin (also mentioned as Wnt Canonical pathway signaling) is being referred when the signal from phosphorylation cascade is integrated at the level of cytoplasmic β -catenin protein. Changes in the concentration of β -catenin subsequently affect the gene expression via transcription factors from the Tcf/Lef protein family.

Wnt/ β -catenin signaling pathway occurs in all the phyla of the animal kingdom, including metazoan animals with primitive body plan such as *Trichoplax* from Placozoa (Srivastava et al., 2008). Despite various differences between individual species, the core mechanism of the signal transduction of the Wnt/ β -catenin signaling pathway remains highly conserved. In the absence of the Wnt ligand, cytosolic β -catenin is marked for degradation by the so-called “destruction” complex of proteins, consisting of two serine/threonine kinases, namely casein kinase 1 alpha (CK1 α) and glycogen synthase kinase 3 (GSK3) and two tumor suppressors, the axis inhibition (Axin) and the adenomatous polyposis coli (APC) proteins (Ikeda et al., 1998; Rubinfeld and Martin, 1993; Siegfried et al., 1994). As a result, N-terminally phosphorylated β -catenin is ubiquitinated by the F-box containing β -transducin repeat containing (β -TrCP) E3 ubiquitin protein ligase and subsequently degraded by the proteasome (Aberle et al., 1997; Kitagawa et al., 1999). Without nuclear β -catenin, Tcf/Lef proteins associate with the transcriptional repressors from the Groucho/transducin-like enhancer of split (TLE) family (Roose and Clevers, 1999; Roose et al., 1998) that block expression of Wnt-responsive genes.

When the Wnt ligand (19 in mammals) is present, it binds to a seven-pass-transmembrane receptor from the Frizzled family (11 in mammals) and its co-receptor

- low density lipoprotein receptor-related protein 5/6 (Lrp5/6) (Schweizer and Varmus, 2003). Ligand-receptor interaction triggers a complex cascade of intracellular events leading to the stabilization of the β -catenin. This process involves phosphorylation of the adaptor protein Disheveled (Dvl) by casein-kinase 1 γ/ϵ (CK1 γ/ϵ) (Bernatik et al., 2011). Additionally, the intracellular portion of the Lrp 5/6 is phosphorylated by CK1 γ and GSK3, recruiting Axin from the cytosol to the intracellular part of the plasmatic membrane (Bilic et al., 2007). This can be further potentiated by additional phosphorylation of the PPPS/TP motif on the intracellular part of the Lrp5/6 by mitogen activating protein kinases (MAPKs) (Cervenka et al., 2011). Simultaneously, the Axin protein becomes dephosphorylated by the protein phosphatase 1 (PP1) (Kim et al., 2013; Luo et al., 2007). The subsequent change in its conformation prevents further phosphorylation, leading to β -catenin accumulation in the cytoplasm and its translocation to the nucleus (Kim et al., 2013) (Fig. 1).

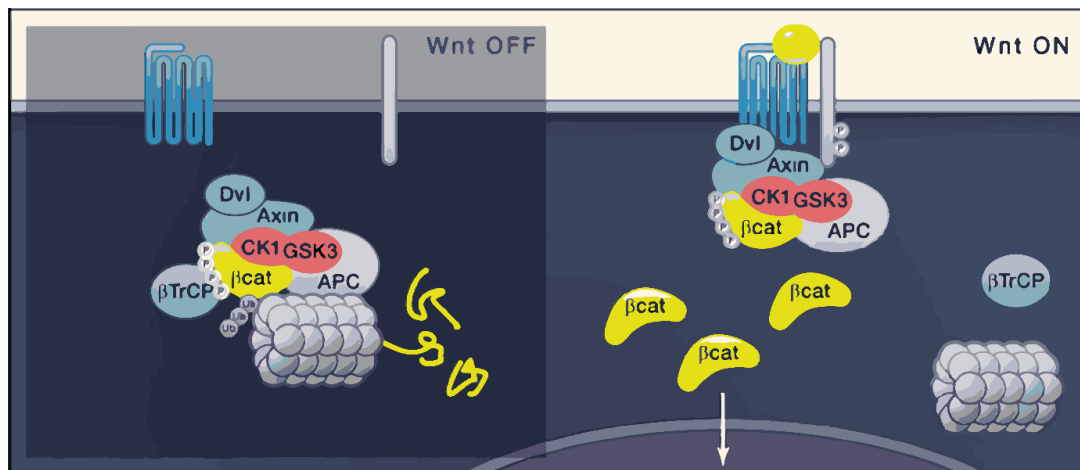


Figure 1: Model of the current view on the Wnt/ β -catenin signaling pathway. Left: Without presence of the Wnt ligand β -catenin is constitutively marked by destruction complex for degradation in the proteasome. Right: Binding of the secreted Wnt proteins to their Frizzled receptors and Lrp5/6 co-receptors recruits the destruction complex to the plasmatic membrane, allowing stabilization of the β -catenin. Stabilized β -catenin accumulates in the cytoplasm and enters the nucleus where it binds to the Tcf/Lef family of transcription factors, thereby regulating the expression of Wnt target genes. (Adapted from Clevers and Nusse (2012)).

Wnt/ β -catenin signaling in the nucleus and transcription factors Tcf/Lef

Nuclear β -catenin does not only compete out the Groucho/TLE corepressors from Tcf/Lefs, but its carboxy-terminus (C-term) acts also as a transcriptional activation domain (van de Wetering et al., 1997). Additionally, it recruits several modulators of transcription. Among these, B-Cell CLL/Lymphoma 9 (Bcl9) and Pygopus, were found to be indispensable for Wnt/ β -catenin signaling in *Drosophila* (Kramps et al., 2002; Parker et al., 2002; Thompson et al., 2002), however knock-out studies in mice suggest that these proteins do not play equally important role in mammals (Brack et al., 2009; Deka et al., 2010; Schwab et al., 2007). β -catenin also serves as a scaffold protein for histone modifiers, such as CREB binding protein (CBP) and its close relative p300, both linked to activation of Wnt target gene expression (Mosimann et al., 2009; Teo and Kahn, 2010). Presence of the CBP/p300 on Wnt target gene chromatin positively correlates with an increase in H3 and H4 acetylation (Kioussi et al., 2002; Parker et al., 2008; Sierra et al., 2006). Furthermore, active Wnt/ β -catenin signaling causes an elevation of the H3-K4me3 at various target promoters (Blythe et al., 2010; Chen et al., 2010; Parker et al., 2008). The methyltransferases mixed-lineage-leukemia proteins (MLL1/2), catalyzing this modification, seems to be required for complete activation of several Wnt targets (Chen et al., 2010; Sierra et al., 2006) (Fig. 2) (Reviewed in Cadigan and Waterman (2012); Clevers and Nusse (2012); Mosimann et al. (2009)).

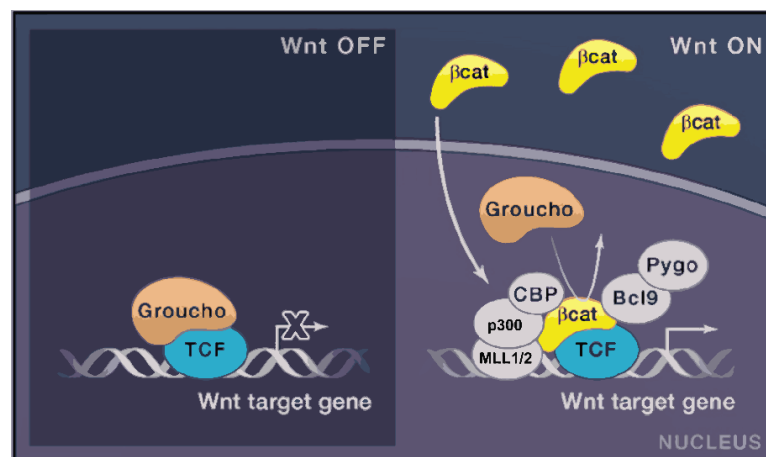


Figure 2: Model of the Wnt/ β -catenin signaling in the nucleus. Left: Without presence of the β -catenin, Tcf/Lef proteins are bound by co-repressor Groucho/TLE and act as transcriptional repressors. Right: Binding of the β -catenin to the Tcf/Lef family of transcription factors prevents the binding of co-repressor Groucho/TLE, promotes the recruitment of chromatin remodeling proteins, transcription modulators and induces Tcf/Lef mediated expression of the Wnt target genes. (Adapted from Cadigan and Waterman (2012); Clevers and Nusse (2012)).

Four Tcf/Lef genes have been identified in vertebrates; *Lef1* (alias *Lef1*) (Travis et al., 1991), *Tcf7* (alias *Tcf1*) (van de Wetering et al., 1991), *Tcf711* and *Tcf712* (alias *Tcf3* and *Tcf4*) (Castrop et al., 1992). Tcf/Lefs share several characteristic protein features, such as the N-terminal β -catenin binding motif, Groucho-related gene (GRG) motifs for binding of Groucho/TLE co-repressors and the HMG box containing the DNA binding domain. The consensus TCF cognate motif for vertebrate and *Drosophila* Tcf/Lef is AGATCAAAGG. Moreover, *Tcf7* and *Tcf712* contain a C-clamp, i.e. a second DNA binding motif that further modulates gene target specificity (Arce et al., 2006; Cadigan and Waterman, 2012; van de Wetering et al., 1997).

Unlike invertebrates, where a single TCF is typically present, individual Tcf/Lefs in vertebrates have different, context-dependent potential to activate or repress target genes. In *in vivo* experiments in mouse and *Xenopus* *Lef1* and *Tcf7* identified as activators of the Wnt target genes (Galceran et al., 1999; Kratochwil et al., 2002; Liu et al., 2005; Reya et al., 2000), *Tcf712* can act both as a repressor or an activator depending on the developmental context (Korinek et al., 1997; Liu et al., 2005; Nguyen et al., 2009; Tang et al., 2008), while *Tcf711* represents the least potent activator but the strongest repressor from the whole family (Cole et al., 2008; Liu et al., 2005; Ombrato et al., 2012). Taken together, distinct expression patterns of individual Tcf/Lefs and their unequal capability to activate/repress Wnt target genes, represent the ultimate regulatory step of the Wnt/ β -catenin signaling pathway.

Differentiation of the head ectoderm

Diversification of the developing epiblast cells into the three primary germ layers is one of the key developmental features of the Bilateria. It takes place during gastrulation (embryonic day E6.5 to E7.5 in mouse) and is directly followed by formation of the neural plate (E7.5-E8.5), and finally neurulation (E8.5-E9.25). During this time, emergence of the prospective head from the head ectoderm and underlying mesoderm takes place (Fossat et al., 2012). Correct differentiation of this region is achieved through differential gene expression orchestrated in complex gene regulatory networks (GRNs) that are responsive to stimuli from Wnt, FGF and BMP signaling pathways (Garnett et al., 2012). As a result, head ectoderm gives rise to four distinct cell populations: placodes, neural plate, non-neural ectoderm, and neural crest (NC) cells, that later form sensory organs; brain; epidermis; and sensory neurons, cartilage and bone of the skull, respectively (Fig. 3) (Groves and LaBonne, 2014; Litsiou et al., 2005; Simoes-Costa and Bronner, 2015; Steventon et al., 2009).

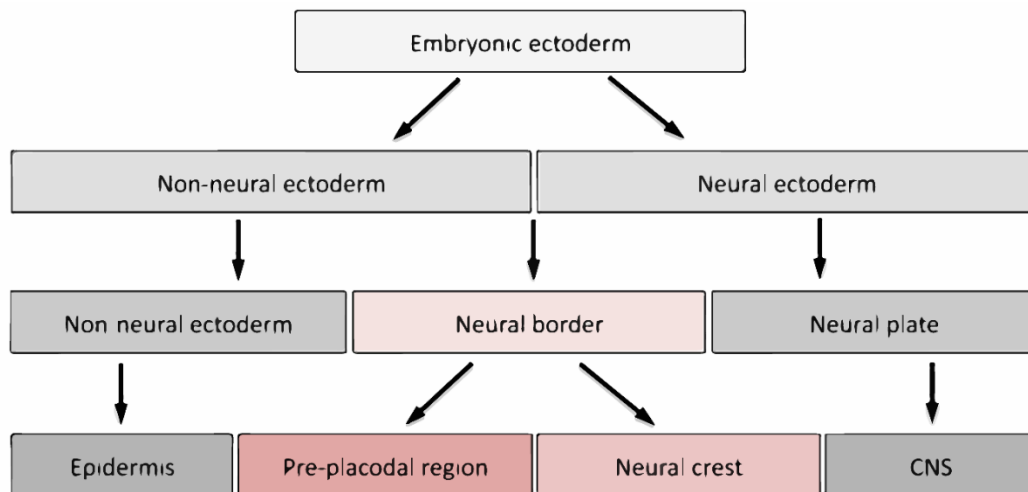


Figure 3: Scheme of the embryonic ectoderm differentiation. During gastrulation, embryonic ectoderm is subdivided into the non-neural ectoderm, later forming the epidermis, and the neural ectoderm, which gives rise to the central nervous system (CNS). A neural border zone appears at their boundary and gives rise to cell populations of the neural crest and pre-placodal region (PPR). Adapted from (Saint-Jeannet and Moody, 2014).

Anterior neural fold and Wnt/ β -catenin signaling

The anterior neural fold (ANF), the most rostral region of the neural plate, serves as a regional organizer secreting signaling molecules that generate the spatial patterning of the forebrain. Wnt/ β -catenin signaling controls A-P identity during body plan formation in most bilaterally symmetric animals, as has been demonstrated both in deuterostomes and protostomes (reviewed in (Petersen and Reddien, 2009). Unlike the rest of the body, the anterior patterning appears to proceed correctly only in the absence of the Wnt stimuli. Ectopic overactivation of the Wnt/ β -catenin signaling pathway results in aberrant expansion of the posterior character of the embryonic tissue anteriorly, compromising or completely diminishing head formation, as has been demonstrated in mouse, zebrafish and *Xenopus* (Fossat et al., 2011; Kiecker and Niehrs, 2001; Kim et al., 2000; Popperl et al., 1997). On the contrary, depletion of the Wnt/ β -catenin pathway showed the opposite phenotype i.e. expansion of the head neuroectoderm (Galceran et al., 1999; Kiecker and Niehrs, 2001; Shimizu et al., 2005). A-P gradient of the Wnt/ β -catenin pathway activation can be nicely visualised using BAT-gal reporter mouse strain (Maretto et al., 2003) (Fig.

4). Collectively, tight control of the Wnt/ β -catenin signaling activity is a key prerequisite for proper development of the ANF.

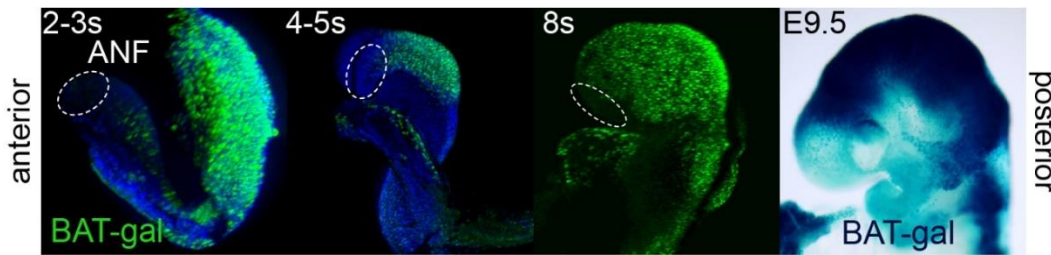


Figure 4: Gradient of Wnt/ β -catenin signaling in developing head of the mouse embryo. With the progress of the embryogenesis, a wave of Wnt/ β -catenin signaling activity proceeds from posterior towards anterior portion of the embryo, as can be visualized using Wnt reporter mouse strain BAT-gal (Maretto et al., 2003). The ANF region, however, stays devoid of the BAT-gal signal. More precise staging in somite pairs(s) has been used between E8.0-E8.5. (Adapted from Masek *et al.*, in revision) ANF – anterior neural fold (marked with dashed ellipse)

Wnt signaling in the ANF is restrained through expression of a set of Wnt antagonists, acting at different levels of the signal transduction cascade. Secreted molecules, including secreted frizzled-related protein (SFRP), Dickkopf-1 (Dkk1), Wnt inhibitory factor-1 (Wif1) or Cerberus, negatively regulate Wnt signaling activity by preventing the ligand-receptor binding (Kawano and Kypta, 2003). SFRPs diminish the signal activity presumably by competing with Wnt ligands for physical interaction with the Fzd receptor (Kawano and Kypta, 2003), while Dkk1 interferes with the interaction of Lrp5/6 co-receptor with Fzd and Wnt ligands, disrupting the activation of the receptor complex (Mao et al., 2001; Semenov et al., 2001).

The inhibitor of β -catenin and Tcf (ICAT), an 81aa protein, is another antagonist of the Wnt signaling pathway, acts in the nucleus, and intervenes in the interaction between β -catenin and Tcf/Lef (Tago et al., 2000). Whole body deletion of the *Dkk1* (Mukhopadhyay et al., 2001) and *ICAT* (Sato et al., 2004) results in defects in A-P patterning and exencephaly, which results from aberrant Wnt/ β -catenin signaling. Several other genes, such as *sine oculis homeobox 3 (Six3)* (Lagutin et al., 2003) or *homeobox expressed in ES cells 1 (Hesx1)* (Andoniadou et al., 2007), which are required for proper development of the ANF, are probably also involved in repression of the Wnt/ β -catenin signaling, since their deletion results in upregulation of the Wnt reporter and/or increased expression of the Wnt target genes along with severe reduction of the ANF tissue. This further demonstrates distinct requirement of

the Wnt/ β -catenin signaling during the ANF patterning and the A-P patterning of the whole body.

Role of the Wnt/ β -catenin signaling in neural crest formation

Neural crest (NC) cells are vertebrate-specific, multipotent, highly migratory cells originating from the ectoderm of the neural plate border (NPB) (Fig. 3). NC cells possess the ability to differentiate into a wide range of cell types, including the bone and cartilage of the skull, sensory neurons, outflow tract of the heart, enteric ganglia and pigment cells. NC originate from a border region of the neural plate and surrounding non-neuronal ectoderm along the dorsal part of the embryo.

Experiments in *Xenopus*, zebrafish and chicken have shown a requirement for Wnt/ β -catenin signaling even from the earliest steps of neural crest development. During gastrulation, Wnt/ β -catenin signaling drives the expression of the NC specifier genes *paired box 3 (Pax3)* (Bang et al., 1999; Garnett et al., 2012; Taneyhill and Bronner-Fraser, 2005; Zhao et al., 2014), *forkhead box D3 (FoxD3)* (Janssens et al., 2013) and *gastrulation brain homeobox 2 (Gbx2)* (Li et al., 2009). Later on, during NC maintenance (Kleber et al., 2005; Steventon et al., 2009) and the epithelial-to-mesenchymal transition (EMT), it triggers the *Slug* gene expression (Burstyn-Cohen et al., 2004; Sakai et al., 2005; Vallin et al., 2001). Compared to non-mammalian experimental models, no clear picture about the role of Wnt/ β -catenin signaling in early NC cell populations in mammals is shaped. This is partly caused by a lack of appropriate Cre drivers for the early pre-migratory NC lineage. The widely used mouse strain Wnt1-Cre targets the NC population after its induction and specification (Danielian et al., 1998; Lewis et al., 2013). Depletion of β -catenin using Wnt1-Cre leads to malformations of the craniofacial structures, accompanied with a deficiency in sensory neurons (Brault et al., 2001; Gay et al., 2015). Similar phenotypic changes have been observed in compound Wnt1/Wnt3a mutants that also show impaired formation of sensory neurons and defects in several bones and cartilage originating from the NC (Ikeya et al., 1997). Ectopic Wnt1-Cre driven expression of stabilized β -catenin (β -cat^{Ex3fl/+}) results in excessive differentiation of NC progenitors into sensory neurons expressing neuronal differentiation (NeuroD) and POU class 4 homeobox 1 (Brn3a) proteins, thus limiting multipotency of the NC cells (Lee et al., 2004). Collectively, these data confirm the requirement of Wnt/ β -catenin signaling in NC maintenance and differentiation, nevertheless, they do not clarify the role of Wnts in NC induction and specification. The apparent inconsistency may be explained in two ways. Either the signaling pathway network governing NC induction and specification differs between mouse and other species (Barriga et al., 2015) or, more likely, the

Wnt1-Cre driver targets the already specified NC, thus not allowing the investigation of the earlier events of NC development.

Wnt/ β -catenin signaling in placodal development

Patches of thickened ectoderm, called placodes, recruit originate from U-shaped domain of the head ectoderm that lines the outer edge of the anterior NPB. This domain, called pre-placodal region (PPR), is characterized by expression of members of the *six homeobox (six)*, *eyes absent (eya)* and *distal-less homeobox (dlx)* gene families (Schlosser and Ahrens, 2004). At the onset of neurulation Pre-placodal region could be divided into the anterior and posterior PPR; the former gives rise to adeno-hypophyseal, olfactory, and lens placodes and the latter forms the cranial sensory ganglia (together with NC cells), lateral line (in fishes), epibranchial, and otic placodes (Reviewed in Grocott et al. (2012); Saint-Jeannet and Moody (2014)).

Similarly to the case of ANF and NC, spatio-temporal different levels of Wnt, FGF and BMP signaling activity are responsible for expression of specific sets of genes that define PPR induction, A-P polarization and later differentiation into individual placodal subtypes. Experiments in *Xenopus* (Ahrens and Schlosser, 2005; Pieper et al., 2012), zebrafish (Bhat et al., 2013), and chicken (Litsiou et al., 2005) revealed that high levels of FGF but low levels of BMP and Wnt/ β -catenin signaling are necessary for expression of the genes *orthodenticle homeobox 2 (otx2)*, *paired box 6 (pax6)*, *six3*, *six6* that define anterior PPR. On the other hand *gbx2* and *iroquois homeobox (Irx1-3)* positive posterior PPR fate is induced by combination of high levels of the FGF and Wnt/ β -catenin but low BMP signaling during onset of neurulation (Ahrens and Schlosser, 2005; Schlosser and Ahrens, 2004; Steventon et al., 2012).

Far less is known about involvement of the Wnt/ β -catenin signaling during placodal development in mammals. Conditional loss of β -catenin using Pax2-Cre results in the otic placode size reduction while activation of the pathway through aberrant stabilization of the β -catenin, using the same cre-line, causes the opposite phenotype (Ohyama et al., 2006). The different size of the otic placode, is accompanied with changes in expression of the *Dlx5*, *Pax8*, results of the changes in ratio of ectodermal differentiation into placodal and epidermal fates (proliferation and apoptosis were not affected) (Ohyama et al., 2006). Conversely, β -catenin deletion in lens placode using the LR-Cre, where three copies of Pax6 lens enhancer were cloned upstream of the Cre gene (Kreslova et al., 2007; Smith et al., 2005), results in formation of ectopic lenses (Machon et al., 2010). β -catenin stabilization, using the same driver of recombination, prevents the lens placode formation through

downregulation of the lens specifiers *Meis2* and *Pax6* expression (Machon et al., 2010). Transcription factor *Pax6* activates expression of the Wnt antagonists *Dkk1* and *Sfrp2*, thus its absence further potentiates the phenotype in *Lens-Cre;β-cat^{Ex3fl/+}* mutants (Machon et al., 2010). Based on additional studies focusing on NC development in other vertebrate model organisms, we can conclude, that Wnt inhibition through the soluble antagonists secreted from the cells of the anterior neural plate and underlying mesoderm during ANF development, such as *Dkk1*, *Sfrps*, and *Cerberus*, is also important for the anterior PPR formation in mouse (Carmona-Fontaine et al., 2007; Kawano and Kypta, 2003; Litsiou et al., 2005; Monaghan et al., 1999). Figure 5 summarizes the effects of Wnt/β-catenin signaling pathway on differentiation of the head ectoderm, with focus on ANF, NC, PPR regions and genes involved in their specification.

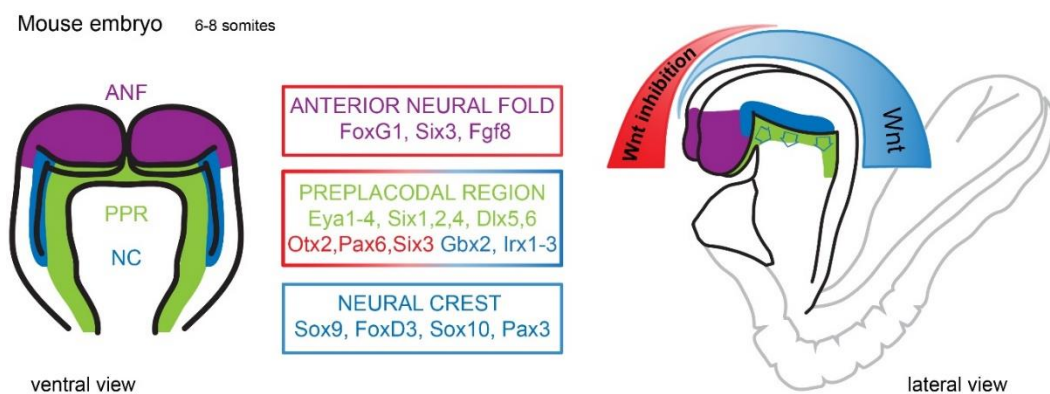


Figure 5: Schematic overview of the embryonic head ectoderm differentiation in relation to Wnt/β-catenin signaling. Ventral (left) and lateral (right) view of the head region of the whole developing mouse embryo at 6-8 somite stage. A→P gradient of the Wnt antagonists promotes differentiation of the most anterior ectoderm into *foxg1*, *six3*, *fgf8* expressing ANF and *otx2*, *pax6* and *six3* anterior PPR. A←P gradient of the active Wnt/β-catenin signaling induces formation of the *gbx2*, *irx1-3* positive posterior PPR and *pax3*, *sox9*, *foxd3* and *sox10* expressing NC.

ANF- anterior neural fold, PPR- preplacodal region, NC- neural crest

Tcf711: a potential regulator of the Wnt activity during mouse embryonic development

As mentioned above, Tcf711 represents the least potent activator but the strongest repressor from the whole family (Cole et al., 2008; Liu et al., 2005; Ombrato et al., 2012). This has been verified *in vivo*, using genetically modified mice that express only the N-terminally truncated form (lacking β-catenin binding domain) of the Tcf711. The mutant mice display defective eyelid closure and develop only four fingers, they do not, however, show any defects in differentiation of the anterior ectoderm or A-P patterning in general (Wu et al., 2012). Tcf711 deficient mice, on the other hand, die shortly after gastrulation displaying elevated levels of the Wnt/β-catenin signaling

activity, duplicated axis and a severely reduced anterior part of the embryo (Merrill et al., 2004), suggesting that Tcf711 function lays predominantly in repression of the Wnt/ β -catenin signaling.

The repressor activity of Tcf711 has been shown to be crucial for maintaining the balance between pluripotency and differentiation in various stem cells. For instance in ES cells, Tcf711 reduces the levels of transcription factors responsible for pluripotency, such as Oct4, Sox2 and Nanog (Cole et al., 2008; Cole and Young, 2008). In Tcf711 mutant ES cells (or after *tcf711* mRNA knockdown), Nanog expression is increased and self-renewal of ES cells is enhanced at the expense of cell differentiation. This phenotype can be rescued using small molecular inhibitors of the Wnt/ β -catenin pathway (Pereira et al., 2006; Tam et al., 2008; Yi et al., 2008).

During mouse embryogenesis, Tcf711 is expressed in the anterior ectoderm at E7.5 and the ANF at E8.5 (Korinek et al., 1998; Merrill et al., 2004). Tcf711 inactivation seems to allow spreading of Wnt/ β -catenin signaling towards the anterior neural fold in both zebrafish and mouse. This leads to a deficiency in expression of the ANF specific genes accompanied with severe defects in head formation (Andoniadou et al., 2011; Dorsky et al., 2003; Kim et al., 2000). All these data have been interpreted in a manner consistent with the fact that repression of Wnt signaling in the ANF is required for A-P axis determination of the neural tube. However, complete understanding of on the role of Tcf711 in the differentiation of the mammalian head ectoderm is still missing.

Aims of the study

Although the requirement of Wnt/ β -catenin signalling for ANF, PPR and NC development has been studied intensively in non-mammalian vertebrate model organisms, we lack a clear picture about the situation in mammals. Current knowledge was collected via experiments at the level of β -catenin and very little is known about the individual roles of the Tcf/Lef transcription factors. Therefore, we decided to abolish Tcf711, member of the Tcf/Lef family with unique ability to act as transcriptional repressor even in the presence of β -catenin. Through conditional deletion of the *Tcf711* gene in mouse, we would attempt to describe the function of both the Tcf711 and Wnt/ β -catenin signaling in the context of the head ectoderm differentiation in mammals.

According to available data, the signaling pathway network governing NC induction and specification differs significantly between mouse and other species (Barriga et al., 2015). There is a high probability that this inconsistency is due to the wide usage of the Wnt1-Cre driver of recombination. Wnt1-Cre targets already specified NC and thereby is not suitable for studying early events of the NC formation (Danielian et al., 1998; Lewis et al., 2013). In order to investigate the role of Wnt/ β -catenin signaling in the earliest possible steps of the NC development, we decided to conditionally delete Tcf711 using Ap2 α -Cre line. This mouse Cre-expressing mouse strain was derived from a NC inducer gene Tfp2 α and delivers recombination during NC induction (Macatee et al., 2003). Since the expression pattern of this Cre-line covers entire NPB (and therefore a significant part of the anterior ectoderm) resulting phenotype should provide information not only about the Tcf711 function in NC development, but also about its role during specification of the ANF and PPR.

Tight control of Wnt/ β -catenin signaling is also essential for the formation of the vertebrate eye. In mouse, down-regulation of the Wnt signaling in the lens surface ectoderm is a key prerequisite for lens placode specification; aberrant activation of the pathway in that stage completely disrupts eye development (Machon et al., 2010). Tcf/Lef transcription factors, differentially expressed in the embryonic eye structures, may further fine-tune the transcriptional response to Wnt/ β -catenin signaling, yet their function during mouse eye development remains unknown. The most abundant members of the Tcf/Lef family in developing lens tissue are Tcf711 and Tcf7 (Liu et al., 2006). In order to understand the role of Tcf711 during lens placode development, we specifically deleted *Tcf711* by employing a lens placode specific Cre expressing mouse strain, namely Lens-Cre (Ashery-Padan et al., 2000).

Specific aims:

1) Manipulation of the Wnt/ β -catenin signaling in the mouse neural crest and anterior neural fold via conditional deletion of *Tcf711* gene and subsequent analysis of the phenotype

2) Investigation of the effects following *Tcf711* conditional inactivation on the anterior pre-placode, with the focus on lens placode development in mouse

Materials and Methods

Mouse strains

Housing of mice and *in vivo* experiments were performed in compliance with the European Communities Council Directive of 24 November 1986 (86/609/EEC) and national and institutional guidelines. All procedures involving experimental animals were approved by the Institutional Committee for Animal Care and Use (permission PP-071/2011, PP-281/2011). This work did not include human subjects. LR-Cre and Rx-cre were produced in our laboratory (Klimova et al., 2013; Kreslova et al., 2007). AP2 α -IRESCre (AP2 α -Cre) was described previously (Macatee et al., 2003), Cre reporter lines Rosa26^{EYFPfl/+} (B6.129X1-Gt(ROSA)26Sor^{tm1(EYFP)Cos/J}, stock No: 00614) and ROSA26 (B6.129S4-Gt(ROSA)26Sor^{tm1Sor/J}, stock No: 003474) were purchased from The Jackson Laboratory. Tcf711^{fl/+} strain (Tcf711^{tm1a(EUCOMM)Wtsi}) was purchased from the EUCOMM. Transgenic mouse strain BAT-gal (Maretto et al., 2003) was kindly provided by S. Piccolo. The Lens-Cre was kindly provided by Dr. Ashery-Padan (Ashery-Padan et al., 2000). Mice with a conditional “floxed” β -catenin (β -cat^{Ex3fl/+}) were kindly provided by Dr. M. M. Taketo (Harada et al., 1999). Generation of Rosa26^{dnTCF4fl/fl} was described in (Janeckova et al., in press). Briefly, human TCF7L2 coding sequence lacking N-terminal domain (aa 1-31) was cloned into the ROSA26 targeting vector containing arms for homologous recombination into ROSA26 locus in a same way as when generating the Rosa26^{ct β cat-Tcf711fl/+}. Details about the Rosa26^{ct β cat-Tcf711fl/+} mouse line generation are present in Fig. S4. A C-terminal part of β -catenin (aa 696-781) was fused with the mouse full length Tcf711 and inserted into ROSA26 locus using homologous recombination in ES cells. The construct carries tdTomato coding sequence flanked with the LoxP sites serving as a stop cassette for ct β cat-Tcf711. Excision of the tdTomato cassette via Cre-mediated recombination, allows transcription of ct β cat-Tcf711 mRNA (Fig. 5A). PGK-Neo cassette was removed using FLP-FRT recombination, F1 animals were crossed to the Actb:FLPe strain (Rodriguez et al., 2000) and kept on a C57BL/6J background. Primers for genotyping Rosa26^{ct β cat-Tcf711fl/+} allele: JM21F GAGGAGCCATAACTGCAGAC, JM23R CCTGGCTATCCTAGATAGAAC and JM27R GTACTGTTCCACGATGGT the expected size of the PCR product is 965bp in the mutant and 300bp in the wild-type.

Morpholino mediated knock-down in zebrafish

Zebrafish wild-type, single-cell embryos were injected with combination of previously described Tcf7l1a (5' CTCCGTTTAACTGAGGCATGTTGGC 3') and Tcf7l1b (5' CGCCTCCGTTAAGCTGCGGCATGTT 3') morpholinos (Dorsky et al., 2003), in 1:1 ratio at a final concentration of 1.6ng/nl (1-2nl injected) (Gene Tools). Embryos were raised at 28°C and harvested at 12hpf.

Immunohistochemistry and RNA in situ hybridization

At least three embryos of each genotype and similar developmental stage were analyzed per staining. All used primary antibodies are listed in Table 1. Secondary antibodies: anti-mouse (-chicken, -rabbit, -goat) Alexa Fluor488 or 594 (dilution 1:500, Life Technologies), Biotinylated anti-rabbit (Vector Laboratories), Vectastain ABC Elite kit and ImPACT DAB substrate (all Vector Laboratories). For wholemount immunohistochemistry we used the protocol published by Sandell et al. (Sandell et al., 2014). Briefly, embryos were fixed overnight in 4% PFA, permeabilized using Dent's bleach and 100% methanol and rehydrated. Blocking for 2 hours and antibody incubation overnight were performed in 3% BSA in 0.1M Tris-Cl, pH 7.5, 0.15 M NaCl, 0.03% Triton X-100. After 5 times of 1-hour washing in PBS, overnight incubation with secondary antibody in the blocking buffer followed. The next day, embryos were stained for nuclei using Hoechst (dilution 1:1000, Life technologies), washed three times in PBS (20 minutes each) and stored in 2% formaldehyde (Sigma). Whole-mount immunofluorescence was captured using binocular microscope Apotome.2 Ax10 zoom.V16 (Zeiss). Fluorescence and bright-field light images were acquired in Nikon Diaphot 300 with objectives 4x/0.1 and 10x/0.25 and confocal Leica SP5.

In case of staining on section, following protocol was utilized. Embryos of desired age were dissected, fixed in 4% paraformaldehyde (PFA) from for up to 4 hours at 4°C, washed with PBS, cryopreserved in 30% sucrose and frozen in OCT (Sakura). The cryosections (10-12 µm) were permeabilized with PBT (PBS with 0.1% Tween), blocked with 10% BSA in PBT and incubated with primary antibody (1% BSA in PBT) overnight at 4°C. Sections were washed with PBS, incubated with fluorescent secondary antibody (Life Technologies, 1:500) for one hour at room temperature, washed with PBS, counterstained with DAPI and mounted in Mowiol. When paraffin sectioning was employed, embryos were fixed ON at 4-8% PFA, dehydrated, embedded in paraffin, sectioned (4-8 µm) rehydrated and antigens were retrieved by boiling in Citrate Buffer (Citric acid monohydrate, final concentration 0.1mM, pH 6.0) for 15 minutes in high pressure pot, prior staining as described above for cryosections.

Pregnant mice were injected with 100ug of 5-Bromo-2'-deoxyuridine (BrdU) into peritoneal cavity 1 hour prior sacrifice. Samples were processed by paraffin sectioning and stained using anti-BrdU antibody (Abcam).

Whole-mount *in situ* hybridization was performed using standard protocols. Riboprobes were cloned into pGEM-T-easy vector (Promega) using primers specified in the Table 1.

ISH probes		
Gene	forward	reverse
FoxD3	GGACCGCAAGAGTTCGCGGA	TCCGGAGCTCCCGTGTCGTT
Sox9	GAGCACTCTGGGCAATCTCAG	CTCAGGGTCTGGTGAGCTGTG
Gbx2	Gift from Peter Rathjen	Adelaide University
Sp5	CGTGAAGACGCACCAAATA	TATTTTCACGCTGCCAACTG
Fgf8	CAGGTCCTGGCCAACAAG	GAGCTCCCGCTGGATTCT
Sox10	Gift from Anthony Firulli	Indiana University, USA
Sox2	Open Biosystems	BC057574
FoxG1	Gift from Stefan Krauss	OUS, Oslo, Norway
Six3	Gift from Guillermo Oliver	St. Jude Hospital, Memphis, USA
Wnt1	Gift from Andy McMahon	USC, USA
Tcf7l1	Open Biosystems	BC128306
Tcf7l2	Open Biosystems	BC052022
Antibodies		
Gene	Company	Dilution
Sox1	R&D AF3369	1:1000
Tfap2 α	Santa Cruz Biotech SC-184	1:1000
Sox10	Santa Cruz Biotech SC-17342	1:1000
Sox9	Millipore AB5535	1:1000
N-cadherin	BD Transduction Lab. 610920	1:2000
GFP	Life Technologies A11122	1:1000
β -galactosidase	Abcam ab9361-250	1:1000
Lef1	Cell Signaling C12A5	1:1000
α -BrdU	Abcam AB6326	1:100
E-cadherin	Invitrogen 13-1900	1:400
Pax6	AF-1 custom made	1:4000
FoxE3	Gift from Peter Carlsson	1:500
Prox1	Abcam 11941	1:1000

PCNA	DSHB	1:1000
cMaf	Bethyl Laboratories BL662	1:500
cleaved caspase 3	Cell Signaling 9664	1:350
Tcf7l1	Santa Cruz Biotech SC-M-20	1:2000
γ -crystalline	Gift from Hisato Kondoh	1:400
p21	Santa Cruz Biotech SC-471	1:1000
plasmids		
SuperTopFlash	AddGene	12456
Renilla pRL-SV40P	AddGene	27163
pCI-neo	Promega	E1841
Tcf7l1	Open Biosystems	BC128306
Tcf7l2	Open Biosystems	BC052022
Tcf7	Open Biosystems	BC057543
Lef1	Open Biosystems	BC138596
Dn-b-catenin	modified gift from V. Korinek	IMG, Prague
β -gal	Clontech	631719
p21Luc	Gift from H.Clevers	Hubrecht Institute, Netherlands

Table 1: list of used reagents

SuperTop Flash reporter assay

HEK293 cells (30 000 cells/well/96-well plate) were transiently transfected using Lipofectamine 2000 (Invitrogen) with 30 ng of Super8X TopFlash and 1 ng of Renilla luciferase constructs and indicated amount of the expression vector, filled with mock DNA to final concentration of 200ng DNA per well. Luciferase assays were performed 48h later with a Dual-Glo luciferase kit (Promega). The luciferase signal was normalized to a co-transfected Renilla readout. Experiments were performed on at least 6 biological replicates per condition.

P21-luc reporter assay

MEF cells from Ert2-Cre;Tcf7l1^{fl/fl} embryos at E13.5 were isolated using protocol described by Bryja *et al.* (Bryja *et al.*, 2006). After first two passages were cells seeded on 10cm dish and treated with 4-hydroxitamoxifen (4-OHT). Cells were detached by trypsin treatment (1% in DMEM without serum) and transfected in GT porator solution

(Biologicals) by Amaxa Nucleofector (Lonza). 2×10^6 cells and 3ug of total DNA (p21-Luc, Tcf711, β -gal) were used per condition. Cells were re-plated at 6-well dishes and after 36 hours lysed subjected for luciferase assays were One-Glo luciferase kit (Promega), absorbance of the β -gal was used for normalization. Experiment was repeated at least three times on biological duplicates.

Results

1) Manipulation of the Wnt/ β -catenin signaling in the mouse neural crest and anterior neural fold via conditional deletion of *Tcf711* gene and subsequent analysis of the phenotype

Results presented in this chapter were included in a manuscript entitled “**Tcf711 protects the anterior neural fold from adopting the neural crest fate**” by **Jan Mašek, Vladimír Kořínek, M. Mark Taketo, Ondřej Machoň, and Zbyněk Kozmik**; submitted to the journal *Development*, potentially accepted after major revision

AP2 α -Cre mediated deletion of *Tcf711* during mouse NC specification results in exencephaly.

Tcf711 is detected in the developing mouse ectoderm prior to gastrulation, and later, at E7.5, it is expressed in the anterior ectoderm and mesoderm (Korinek et al., 1998; Merrill et al., 2004). Expression of *Tcf711* during neurulation was characterized using whole mount *in situ* hybridization. *Tcf711* mRNA was detected in the anterior neural plate at the 1 somite pair (s) stage, being further restricted to the ANF region and along the anterior NPB with the progress of neurulation 3-4s (Fig. 6A). We next wanted to relate the expression pattern of *Tcf711* to that of known NC-specific genes and the area of Wnt/ β -catenin signaling. *Tfap2 α* is one of the key genes involved in the NC induction, while *FoxD3*, *Sox9*, *Sox10* have been associated with the NC specification (Groves and LaBonne, 2014; Simoes-Costa and Bronner, 2015). During neurulation, the Tfap2 α protein is continuously expressed along the whole NPB (Fig. 6B). *Sox9* and *FoxD3* transcripts were initially detected in the neural plate, as early as at the 1-2s stage (Figs 6C, 7A), while at 3-4s they were expressed robustly in characteristic stripes along the anterior neural plate border (Figs 6C, 7A). The onset of *Sox10* mRNA expression was detected later (4-5s) and slightly more caudally (Fig. 7B), in a very similar pattern as the expression of *Sox9* (Fig. 6C). To map the activity of the Wnt/ β -catenin pathway, we used the BAT-gal reporter mice (Maretto et al., 2003). Starting from the 2-3s stage, the BAT-gal signal, spread across the prospective mesencephalon and metencephalon, but did not reach the ANF at the 4-5s stage (Fig. 6D). In conclusion, *Tcf711* expression in the ANF is reciprocal to that of *Sox9*, *FoxD3*,

Sox10 and *BAT-gal*, which reside in the caudal areas of the neural plate, but overlaps with *Tcf7l1* in the anterior part of the NPB.

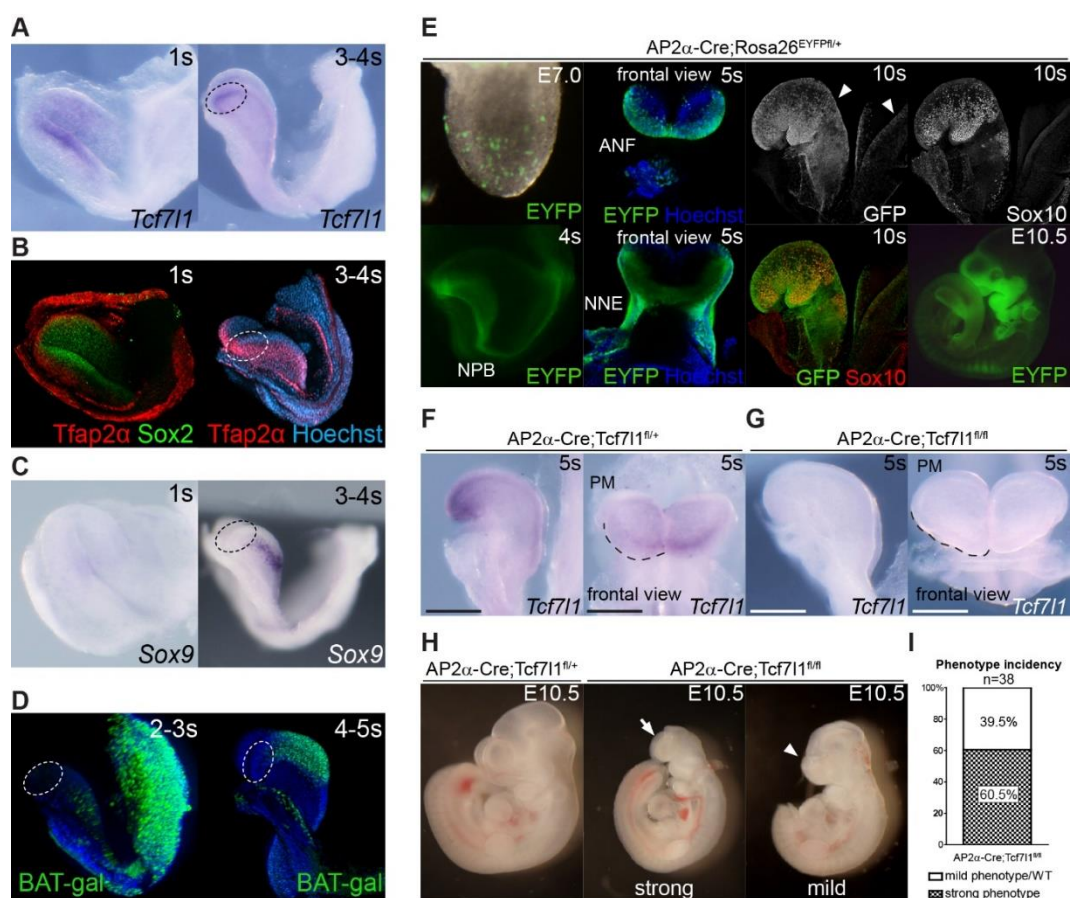


Figure 6: *Tcf7l1* is expressed in a mutually exclusive manner with markers of specified NC and is required for proper forebrain development. (A-D) Expression of (A) *Tcf7l1*, (B) *Tfap2α*, early NC marker, (C) *Sox9*, marker of specified NC and (D) Wnt reporter *BAT-gal*, in the NPB and the ANF (encircled) of developing mouse embryo. Please note the overlap of *Tcf7l1* transcript and *Tfap2α* protein, and of *Sox9* mRNA and *BAT-gal* signal. **(E)** Mapping of recombination delivered by *AP2α-Cre*, using *Rosa26^{EYFPfl/+}* reporter mouse at various stages (E7.0-E10.5). EYFP was detected either directly or using anti-GFP antibody. The recombination occurred along the entire NPB (arrowheads, 10s stage). Co-staining of GFP with anti-*Sox10* antibody revealed recombination in the whole cranial NC population at 10s stage. **(F-G)** *In situ* hybridization shows loss of *Tcf7l1* mRNA expression in *AP2α-Cre;Tcf7l1^{fl/fl}* mutants. ANF in mutant is wider at PM, but narrower towards anterior tip of the ANF (dashed line) than in the control at 5s stage (scale 30μm). **(H)** Control embryo (left) and typical examples of strong (middle) and mild (right) *AP2α-Cre;Tcf7l1^{fl/fl}* phenotype. **(I)** Quantification of strong and mild phenotype incidence between E10.5-E13.5. ANF (encircled) - anterior neural fold, NPB-neural plate border, NC-neural crest, NNE-non-neural ectoderm, PM-prosencephalic-mesencephalic boundary, s-somite pairs. All embryos are shown from a lateral view if not stated otherwise. Nuclei were stained with Hoechst.

In order to study the function of *Tcf7l1* during NC induction and specification, *Tcf7l1* was inactivated, by crossing *Tcf7l1* conditional knock-out mice (EUCOMM) with *AP2α-IRES-Cre* (*AP2α-Cre*) transgenics (Macatee et al., 2003). Tracing of the *AP2α-Cre*-driven recombination using the *Rosa26^{EYFPfl/+}* reporter strain revealed the

first EYFP-positive cells scattered throughout the embryo at E7.0 (Fig. 6E). The EYFP signal became focused along the entire NPB at the 4s stage, while the highest levels were detected rostrally, in the neural- and non-neural ectoderm of the ANF, at the 5s stage. AP2 α -Cre most probably mediates the recombination in the entire NC population, as the recombined EYFP-positive cells included the entire Sox10-positive NC population of the AP2 α -Cre;Rosa26^{EYFPfl/+} embryos at the 10s stage (arrowheads, Fig. 6E). At E10.5, the EYFP signal was present in NC derivatives (brachial arches, dorsal root ganglia and sensory neurons), the head ectoderm, lens placodes, and in the anterior telencephalon (Fig. 6E, Fig. 7C).

In AP2 α -Cre;Tcf711^{fl/fl} mutants, *Tcf711* mRNA expression was completely abolished, whereas high levels were detected along the anterior NPB, including the ANF, in control embryos at the 5s stage (Fig. 6F-G). At this stage, phenotypical changes following *Tcf711* deletion became apparent; the shape of neural folds changed from rounded into more a narrow morphology and the neural plate expanded laterally at the prosencephalic-mesencephalic boundary (dashed lines in frontal views in Fig. 6F,G). At later stages (E10.5), we observed a variability in the penetrance of morphological changes among individual mutants. Therefore, we decided to classify the defects into two categories: (i) a strong phenotype, represented by a severe reduction of the telencephalic tissue and exencephaly (arrow, Fig. 6H) and (ii) a mild phenotype, with reduced telencephalon and bilateral anophthalmia (arrowhead, Fig. 6H). Quantification of phenotype incidence, between E10.5-E13.5, revealed that the strong phenotype was present in 60.5% and the mild phenotype in 39.5% of the analyzed embryos (n=38) (Fig. 6I). Mutant embryos with the strong phenotype exhibited massive exencephaly and severe defects in craniofacial structures and did not survive beyond E13.5 (Fig. 7D, E). These data demonstrate that *Tcf711* function in the ANF is crucial for the development of the mouse forebrain.

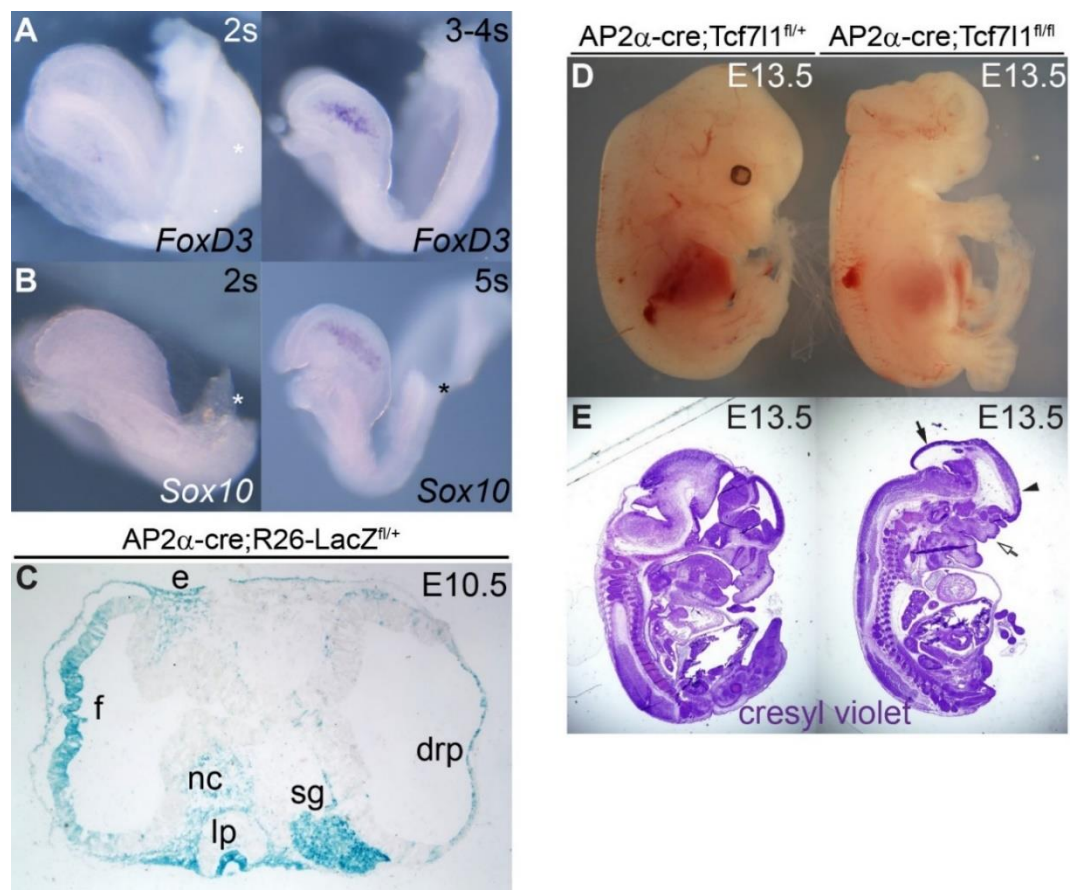


Figure 7: Expression of NC genes during early mouse embryogenesis. (A-B) RNA *in situ* hybridization of *FoxD3* and *Sox10* transcripts, at 2s and 3-4s, and at 2s and 5s stages, respectively. Asterisks mark artifacts caused by sample preparation. **(C)** Mapping of AP2α-Cre delivered recombination. Coronal section of AP2α-Cre;Rosa26^{LacZ}^{fl/+}, at E10.5 stage. Recombination was detected enzymatically with β-galactosidase. drp-dorsal roof plate, e-ectoderm, f-forebrain, lp-lens pit, nc-neural crest, sg-sensory ganglion. **(D, E)** RNA *in situ* hybridization of *FoxD3* and *Sox10* transcripts, at 2s and 3-4s, and at 2s and 5s stages, respectively. Histological analysis of sagittal sections, stained with cresyl violet, from the AP2α-Cre;Tcf711^{fl/fl} ‘strong’ mutant at E13.5, shows severe defects in the splanchnocranium (white arrow), forebrain (black arrowhead) and midbrain (black arrow) of the mutant embryo.

Tcf711 is required for the expression of anterior neural markers

Tcf711 has been implicated in A-P patterning of the developing brain in both zebrafish and mouse, since its loss-of-function mutations result in severe reductions of anterior neural regions, accompanied with apparent expansion of midbrain and hindbrain markers towards the anterior (Dorsky et al., 2003; Merrill et al., 2004). In contrast to published data, we did not observe any A-P shift in mRNA expression of the core regulators of the midbrain-hindbrain boundary (MHB), namely *Fgf8*, *Gbx2* and *Wnt1*, between Tcf711 conditional mutant embryos and controls at E9.0 (E9.0 in the figure) (arrowheads Figs 8A-B', 12D). Remarkably, we observed a progressive loss of the posterior prosencephalon marker *Tcf712* (*Tcf4*) mRNA (Fig. 8C-C'),

accompanied by gradual loss of anterior neural tissue in AP2 α -Cre;Tcf711^{fl/fl} mutants with mild (C') or strong (C'') phenotype at E9.0. Furthermore, the expression of the ANF specific transcripts, *Six3* (Lagutin et al., 2003), *FoxG1* (Hanashima et al., 2004) and *Fgf8* (Meyers et al., 1998) was lost or strongly reduced in the mutants when compared with controls of appropriate stage (Fig. 8D-F'). Next we tested whether *Tcf711* deletion affected the neural character the ANF cells. RNA *in situ* hybridization revealed reduced expression of the neural marker *Sox2*, and an expansion of *Sox2* negative cells along the whole lateral border of the ANF in AP2 α -Cre;Tcf711^{fl/fl} mutants (Fig. 8G,G'), suggesting that the cells had lost their neural identity.

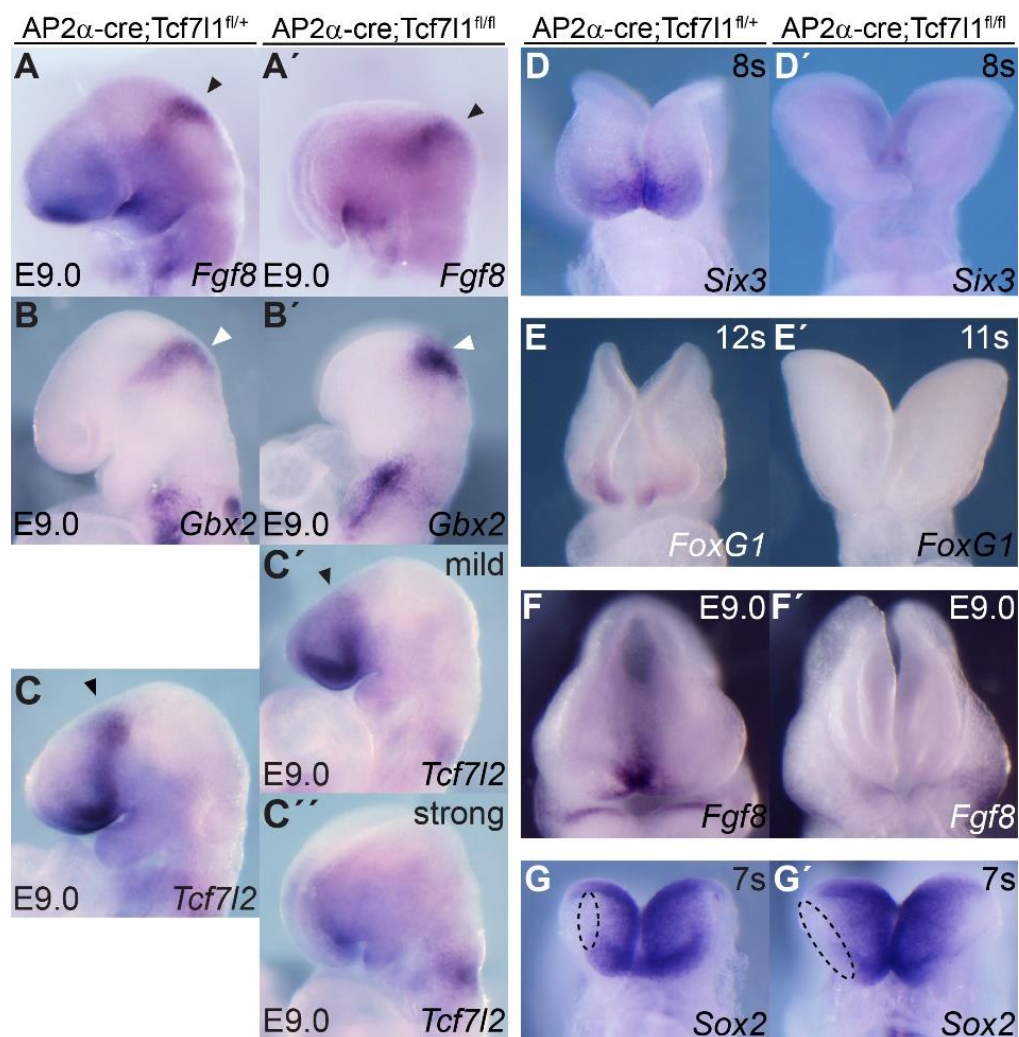


Figure 8: *Tcf711* deletion induces loss of ANF specifiers, without affecting more posterior brain structures. (A-B') RNA *in situ* hybridization shows unchanged expression of *Fgf8* and *Gbx2* in MHB (arrowheads) at E9.0, all lateral view. **(C-C')** *Tcf712* expression in the posterior prosencephalon of control and AP2 α -Cre;Tcf711^{fl/fl} embryos displaying mild and strong phenotype at E9.5, all lateral view. **(D-G')** *Tcf711* deletion resulted in marked reduction of endogenous expression of *Six3* and *Sox2* at 7-8s stage, of *FoxG1* at 11-12s stage and of *Fgf8* at E9.0 in the ANF of AP2 α -Cre;Tcf711^{fl/fl} embryos, all frontal view.

Tcf711 deletion results in aberrant trans-differentiation of the ANF cells into NC

NC cells need to lose their neuroepithelial character in order to undergo EMT and migrate towards their target destinations. NC specification, which precedes the EMT in *Xenopus* and chicken, is regulated by transcription factors FoxD3, Sox9 and Sox10 (Cheung et al., 2005; Dottori et al., 2001; Liu et al., 2013). Therefore, we decided to investigate expression of these three factors in the absence of Tcf711.

As can be seen in the whole-mount immunostaining, Sox9 positive NC cells expanded into the Sox1 positive ANF region in AP2 α -Cre;Tcf711^{fl/fl} mutants compared with controls at the 5s stage (Fig. 9A). Examination under higher magnification revealed decreased neural Sox1 staining towards the anterior part of the mutant embryo (Fig. 9A). A frontal view on the same embryos clearly showed ectopic Sox9-positive NC cells along the ANF in mutants (Fig. 9B). This was further confirmed by *in situ* hybridization of Sox9 mRNA (arrowhead Fig. 10A). Consistently, the expression of FoxD3 mRNA also shifted anteriorly in mutant embryos compared to controls at the 10s stage (Fig. 9C). Later at E9.0, aberrant Foxd3 mRNA was detected in the rostral part of the head in mutants (arrowhead, Fig. 10B), while it was completely absent in controls. Expression of Sox10 mRNA was apparently delayed in the absence of Tcf711, being barely detectable at the 6s stage (Fig. 9D). Two days later, at E9.5, however, RNA *in situ* hybridization revealed robust ectopic expression of Sox10 in the anterior part of the head of mutant embryos (arrowhead, Fig. 9D). Interestingly, we also observed a cell fate shift, characterized by the change from Sox1 to Sox9, in caudal neural tissue. Coronal sectioning of the developing hindbrain at E9.0 also uncovered aberrant Sox9-positive/Sox1-negative cells in the mutants (arrowheads, Fig. 10C).

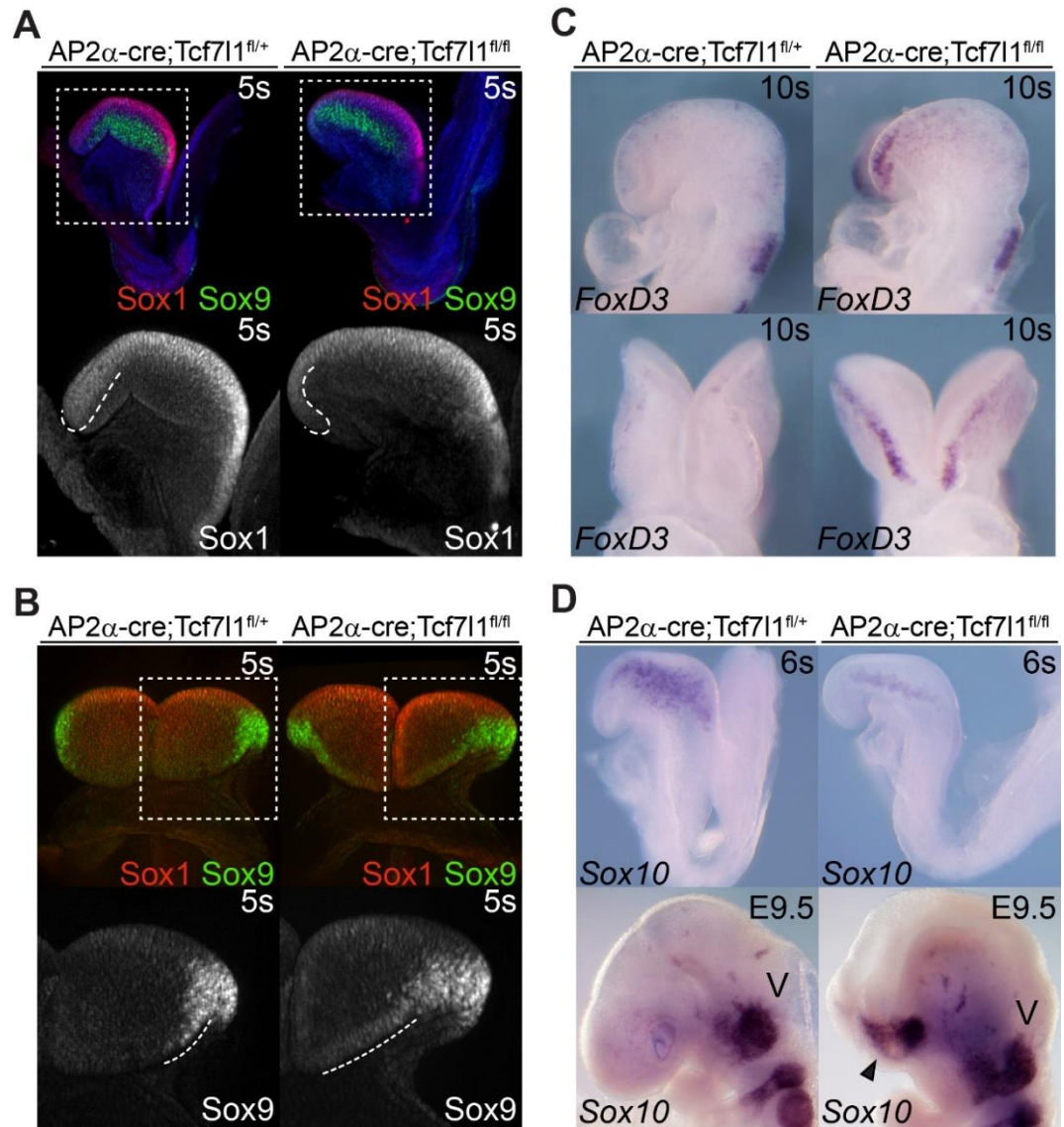


Figure 9: The NC population expands anteriorly in the absence of *Tcf711*. **(A)** Whole mount immunohistochemical staining of Sox1 and Sox9 protein at 5s stage, lateral view. Higher magnification reveals reduction of Sox1 staining in the ANF (dashed line) of the AP2 α -Cre;Tcf711^{fl/fl} mutants. Nuclei were stained with Hoechst. **(B)** Same embryos as in (A), frontal view; higher magnification (bottom) documents the expansion (dashed line) of Sox9 positive cells along the ANF border in mutants. **(C)** Lateral (top) and frontal (bottom) views revealed aberrant expression of the NC marker *FoxD3* along the ANF in the mutants, while it is absent in the control embryos at 10s stage. **(D)** *Sox10* mRNA is less abundant in the *Tcf711* mutants at 6s stage but becomes ectopically expressed later in anterior head (arrowhead) of AP2 α -Cre;Tcf711^{fl/fl} embryos at E9.5. V-trigeminal ganglion.

Analogously to the NC expansion in AP2 α -Cre;Tcf711^{fl/fl} mice mutants, we observed ectopic expression of *FoxD3*, *Pax3* and *Sox9* mRNA along the entire anterior NPB, upon MO-mediated knock-down of both *Tcf711a* and *Tcf711b* in zebrafish embryo (arrowheads, Fig. 10D), this fact denotes the conservation of *Tcf711* function across vertebrate species. Taken together, the expression of several genes responsible for the NC specification and EMT initiation is expanded towards ANF in the AP2 α -Cre;Tcf711^{fl/fl} mutants, suggesting that *Tcf711* maintains the neuroepithelial character of the ANF and restricts spreading of NC fate within the anterior head.

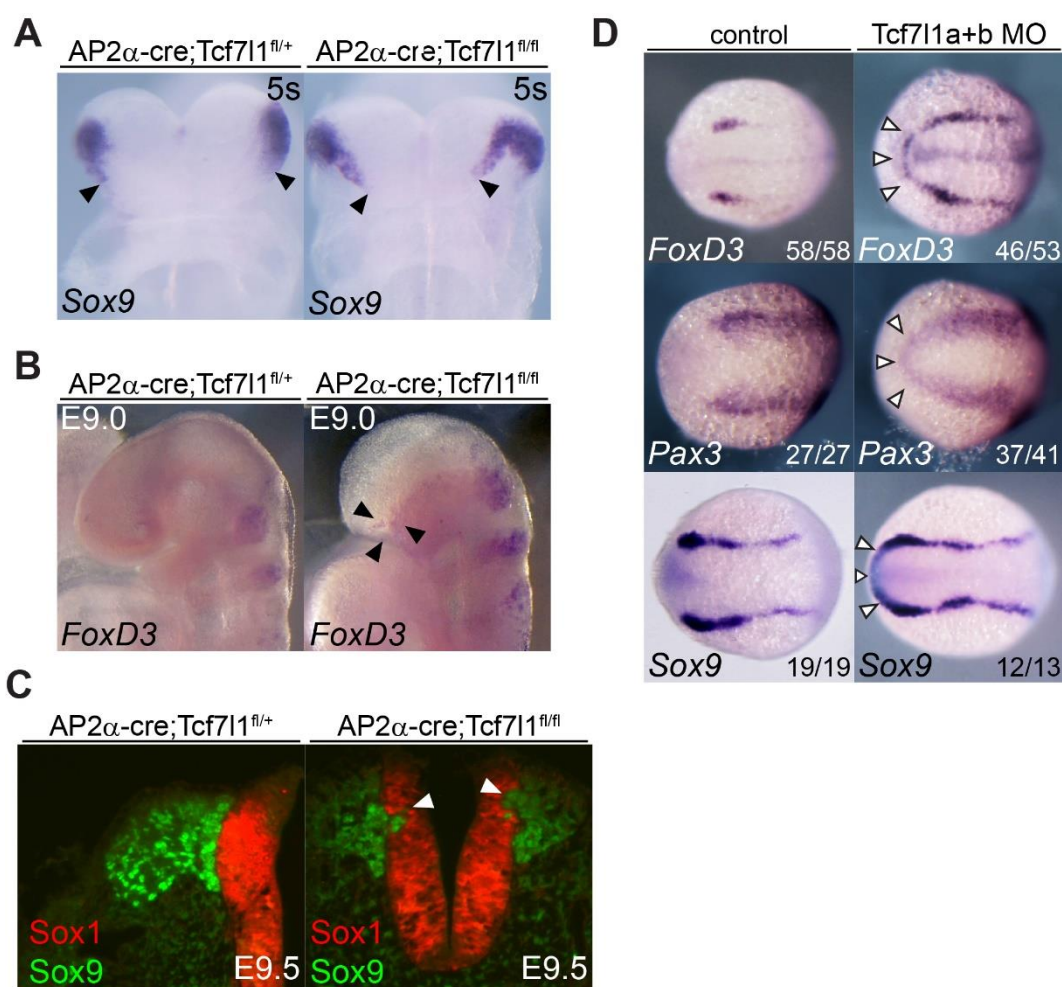


Figure 10: Expansion of NC markers follows *Tcf711* deletion in mouse and zebrafish. (A-C) Expression of *Sox9* mRNA expanded rostrally in AP2 α -Cre;Tcf711^{fl/fl} mutant at 5s stage. Aberrant *FoxD3* mRNA expressing cells are present in the *Tcf711* mutant at E9.0. Immunohistological staining of coronal sections from the E9.0 hindbrain revealed ectopic *Sox9*-positive/*Sox1*-negative cells in AP2 α -Cre;Tcf711^{fl/fl} mutants. **(D)** Expression of *FoxD3*, *Pax3* and *Sox9* mRNA expands along the anterior NPB upon MO-mediated knock-down of both *Tcf711a* and *Tcf711b* variants in zebrafish at 12h stage.

Trans-differentiation of the ANF is driven by aberrant Wnt/ β -catenin signaling

Tcf711 is a very efficient repressor of Wnt/ β -catenin signaling target genes, as has been shown both in mouse embryonic stem cells and *in vivo* (Cole et al., 2008;

Shy et al., 2013; Wu et al., 2012). Gain- and loss-of-function experiments in non-mammalian vertebrates have shown that the Wnt/ β -catenin pathway is required for physiological, and sufficient for ectopic induction and expansion of the NC (Garcia-Castro et al., 2002; Heeg-Truesdell and LaBonne, 2006; Steventon et al., 2009; Taneyhill and Bronner-Fraser, 2005; Wu et al., 2005). In our transient reporter assays, using the SuperTopFlash reporter in HEK293 cells, *Tcf711* was able to compete out other Tcf/Lefs, significantly reducing Wnt reporter signal (Fig. 12A). Therefore we questioned whether the expansion of NC cells in AP2 α -Cre;*Tcf711^{fl/fl}* mutants was caused by upregulation of Wnt/ β -catenin signaling. We crossed BAT-Gal reporter mice with *Tcf711* conditional mutants and stained whole-mount embryos with anti-galactosidase and anti-Sox9 antibodies.

As expected, the Wnt reporter BAT-gal immunofluorescence expanded anteriorly in the AP2 α -Cre;*Tcf711^{fl/fl}* mutants (arrow, Fig. 11A). This was accompanied with a high number of ectopic Sox9-positive cells, as clearly visible from the frontal view of the 8s stage embryos (white arrowheads, Fig. 11A). The co-expression of Sox9 and BAT-gal positive cells does not seem to be aberrant, as cross-sections from the 8s old wild-type embryos showed large overlaps between the Sox9 and BAT-gal immunofluorescence (Fig. 12B), indicating that Sox9 may be induced by Wnts. Furthermore, expression of *Sp5*, a known Wnt/ β -catenin target gene, was also upregulated and expanded rostrally in the mutant embryos at 6s stage (arrowheads, Fig. 11B), confirming the ectopic increase of the Wnt/ β -catenin signaling activity in the anterior neuroectoderm. Apart from its role in MHB formation (McMahon and Bradley, 1990; Thomas and Capecchi, 1990), *Wnt1* is also required during NC development (Ikeya et al., 1997; Saint-Jeannet et al., 1997). Interestingly, we found aberrant *Wnt1* expression in the ANF of the *Tcf711* mutants at the 5-6s stage (Fig. 11C). The ectopic pattern of *Wnt1* mRNA expression along the NPB of the prosencephalon was even more obvious at E9.0 (arrowheads, Fig. 11C). We observed no difference in *Wnt1* mRNA expression in the MHB between controls and *Tcf711* mutants (arrowheads, Fig. 12D) at the same stage, suggesting that the aberrant expression of *Wnt1* reflects the NC phenotype, rather than changes in A-P patterning.

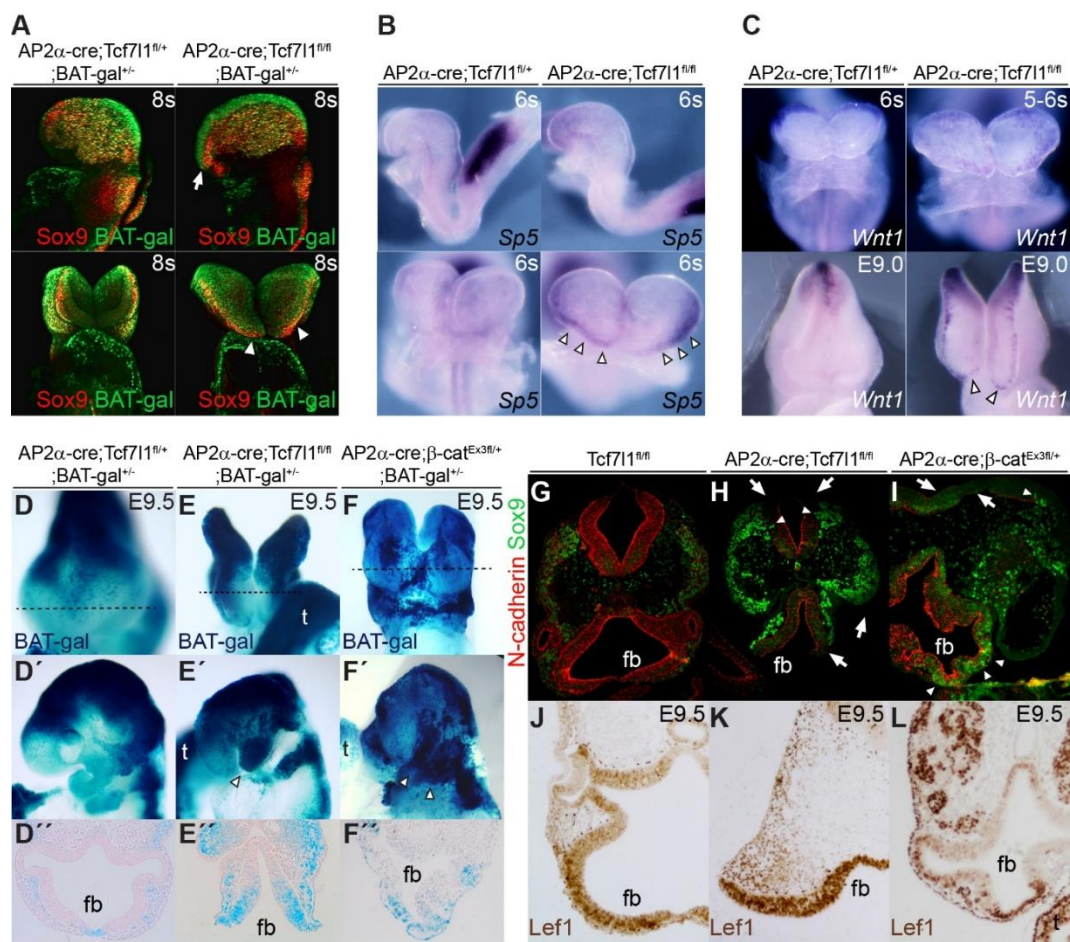


Figure 11: The ectopic activation of Wnt/β-catenin pathway promotes NC formation in mouse. (A) BAT-gal signal (detected with β-galactosidase antibody) and Sox9 staining expands anteriorly in AP2α-Cre;Tcf711^{fl/fl} mutants at the 8s stage. **(B, C)** *In situ* hybridization shows upregulation of the Wnt target *Sp5* and Wnt ligand *Wnt1* along the NPB of the ANF in Tcf711 mutants at 5s and E9.5 stage. **(D-F)** Frontal (top) and lateral (middle) view on the whole mount BAT-gal staining of the control, AP2α-Cre;Tcf711^{fl/fl} and AP2α-Cre;β-cat^{Ex3fl/+} embryos at E9.5. **(D''-F'')** Coronal sections in the dashed line shown in **(D-F)**. Different embryos were used in F, F' and F''. **(G-I)** Coronal sections immunostained with antibodies against N-Cadherin and Sox9 at E9.5. Sox9⁺ population is increased and N-Cadherin staining decreased in the AP2α-Cre;Tcf711^{fl/fl} and AP2α-Cre;β-cat^{Ex3fl/+} mutants, but not in control embryos. **(J-L)** Lef1 immunostaining of coronal sections of the control **(J)**, AP2α-Cre;Tcf711^{fl/fl} **(K)** and AP2α-Cre;β-cat^{Ex3fl/+} **(L)** embryos at E9.5. fb-forebrain, t-tail.

To confirm that the phenotype observed in AP2α-Cre;Tcf711^{fl/fl} mutants resulted from an aberrant activation of the Wnt/β-catenin pathway, we activated the signaling using β-cat^{ΔEx3fl/fl} mice (Harada et al., 1999), in which a truncated, non-degradable form of β-catenin is produced upon AP2α-Cre-mediated recombination. The AP2α-Cre;β-cat^{ΔEx3fl/+} embryos exhibited neural tube closure defects and did not survive beyond E10.5 (data not shown). The crossing of the BAT-gal reporter strain with the AP2α-Cre;Tcf711^{fl/fl} revealed activation of the reporter in the forebrain; this was even more pronounced in AP2α-Cre;β-cat^{ΔEx3fl/+};BAT-gal^{+/-} mutants that also showed a strong over-activation of the signal in most of the head ectoderm when

compared with controls (Fig. 11D-F). A lateral view of the *Tcf711* and β -cat ^{Δ Ex3fl/+} mutants clearly showed an aberrant population of BAT-gal-positive cells migrating towards the branchial arches (arrowheads, Fig. 11D'-F'). Cross sections of these embryos uncovered aberrant BAT-gal staining in the forebrain of both *Tcf711* and β -cat^{Ex3} mutants (Fig. 11D''-F'').

Next we assayed the EMT using immunofluorescence of neuroepithelial cells marked with N-cadherin and migrating NC cells labelled with Sox9 antibodies. In control embryos, only a thin layer of Sox9 positive cells between the N-cadherin positive forebrain tissue and the epidermis was observed. The hindbrain in controls labeled with N-cadherin was found to be completely devoid of Sox9 positive cells at E9.5. (Fig. 11G). In contrast, AP2 α -Cre;*Tcf711*^{fl/fl} mutants clearly displayed aberrant Sox9-positive cells in the hindbrain prior to EMT (arrowheads, Fig. 11H). Concomitantly, N-cadherin expression was weaker in the anterior forebrain and the dorsal hindbrain mutants with "strong" phenotype (arrows, Fig. 11H). Intriguingly, the same analysis of AP2 α -Cre; β -cat^{Ex3fl/+} embryos revealed that almost the whole mutant forebrain converted into Sox9 positive NC (arrowheads, Fig. 11I). Similarly to *Tcf711* conditional mutants, we also detected aberrant Sox9 expressing cells in the hindbrain, together with a massive decrease in the levels of N-cadherin (arrows, Fig. 11I). Furthermore, protein levels of Lef1, the Wnt/ β -catenin transcriptional activator and target gene (Galceran et al., 1999; Kratochwil et al., 2002; Liu et al., 2005), were increased in the forebrain of the *Tcf711* mutants in comparison with controls (Fig. 11J, K). β -cat^{Ex3} mutants displayed very strong upregulation of Lef1 in the mesenchyme adjacent to the hindbrain, as well as in the forebrain (Fig. 11L). Whole-mount immunofluorescence of wild-type embryos revealed co-localization of Lef1 and Sox10-positive cells at the 8s stage (arrowhead, Fig. 12C). It should be noted that in addition to the effects on NC population, the strong activation of the Wnt/ β -catenin pathway in the AP2 α -Cre; β -cat^{Ex3fl/+} mutants disorganized both the A-P patterning of the neural tissue and the non-neural ectoderm surrounding the NC. This was clearly visible from the expansion of *Gbx2* and *Fgf8* mRNA expression domains at E9.5 (Fig. 12E,F). Collectively, deletion of *Tcf711* resulted in the ectopic activation of the Wnt/ β -catenin pathway, suppression of neuroepithelial character and premature initiation of NC cell fate. Similar observations were made in conditional AP2 α -Cre; β -cat^{Ex3fl/+}

mutants that yielded even more profound changes in the expression of described cell markers and in more extended areas than in *Tcf711* mutants.

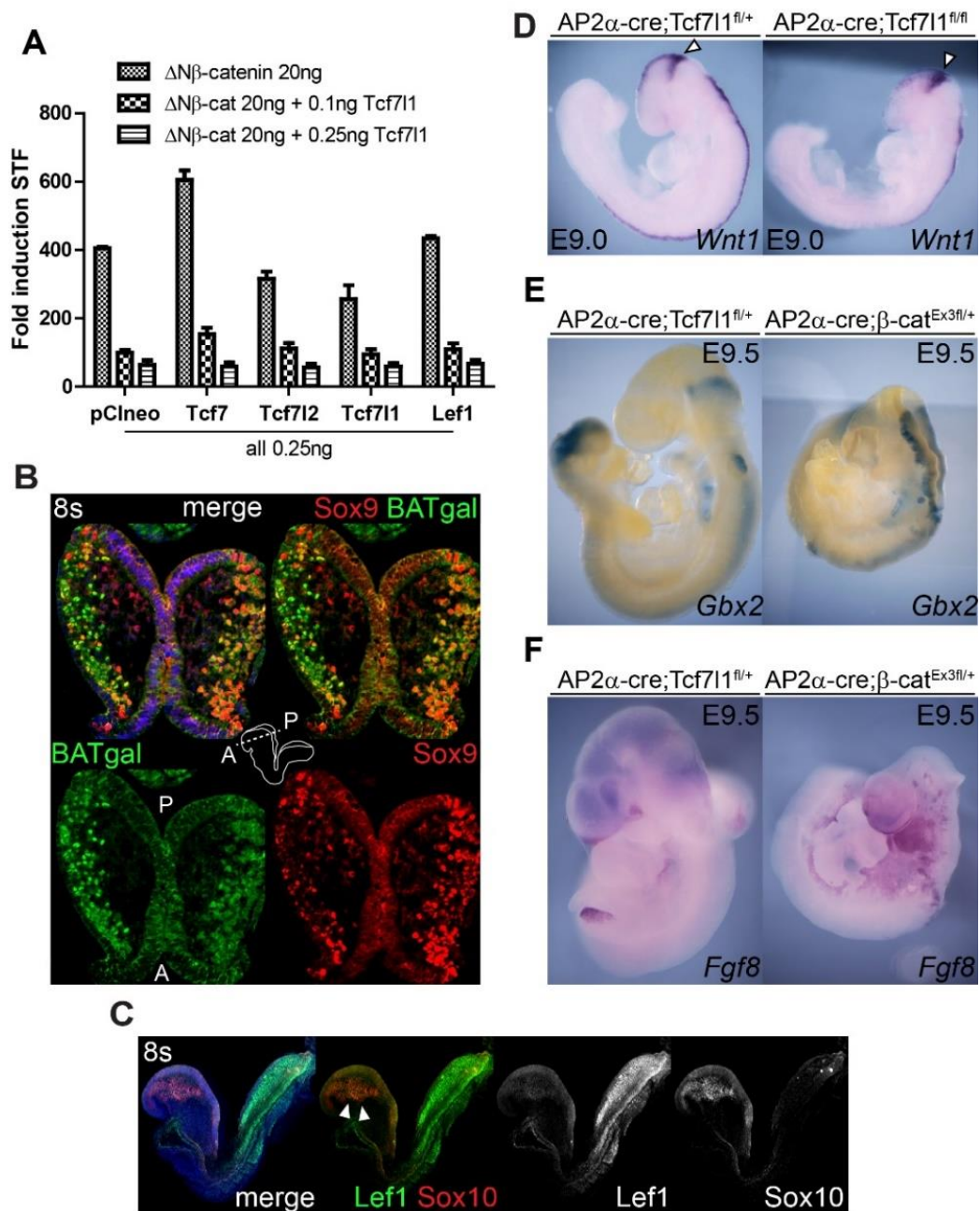


Figure 12: Balance between Wnt/ β -catenin pathway activation and Tcf711 delivered repression regulates NC specification. (A) SuperTopFlash luciferase reporter assay in HEK293 cells documents Tcf711 ability to repress Tcf/Lef driven gene expression. Activation of the pathway was achieved by co-transfection with non-degradable form of β -catenin ($\Delta N\beta$ -catenin). **(B)** Immunostaining of coronal sections from 8s stage wild-type embryos, A-anterior, P-posterior. Please note a large overlap between the Sox9-positive and BAT-gal-positive delaminating cells. Nuclei were stained with DAPI. **(C)** Whole mount immunofluorescence revealed overlap of Lef1 and Sox10-positive cells in wild-type embryo at 8s stage (arrowheads). Nuclei were stained with Hoechst. **(D)** The expression of *Wnt1* transcripts is unchanged in the MHB of AP2 α -Cre;Tcf711^{fl/fl} mutants at E9.0 (arrowheads). **(E-F)** RNA *in situ* hybridization of the MHB markers *Gbx2* (E) and *Fgf8* (F) in controls and the AP2 α -Cre; β -cat^{Ex3fl/+} mutants at E9.5.

The phenotype can be rescued with a truncated form of TCF4 but not with Tcf711 fused with β -catenin

Our data suggest that the loss of Tcf711-mediated repression of Wnt targets is the primary cause of NC cell fate expansion. In order to verify this hypothesis, we performed rescue experiments using two mouse strains, conditionally expressing either dominant Tcf repressor or activator. As a dominant repressor we used the mouse strain Rosa26^{dnTCF4fl/+}, which contains the N-terminally truncated form of the human TCF7L2 (TCF4) targeted into the ROSA26 locus, 3' to the lox-STOP TdTomato (TdT) cassette (originally referred to as Rosa26^{+/tdTomato}). This form cannot bind β -catenin and thus acts as dominant repressor of Wnt/ β -catenin targets (Janeckova et al., in press). Secondly, we generated the mouse strain Rosa26^{ct β cat-Tcf711fl/+}, to allow for conditional expression of full-length mouse Tcf711 fused with the transactivation domain of β -catenin (aa696-781), analogous to the described Cat-Lef fusion (Hsu et al., 1998). This construct (ct β cat-Tcf711), that mimics the β -catenin binding to Tcf711, was able to deliver activation of the Wnt reporter (Fig. 13A). Fig. 13B represents a scheme of the Rosa26 locus and targeted construct, where primers for genotyping and Southern blot analysis are also depicted. We have confirmed correct targeting of the construct into mES cells using Southern blotting. Autoradiograph showed bands of predicted size for short arm (5.9kb) and long arm (9.9kb) (Fig. 13C). We have confirmed production of the ct β cat-Tcf711 fusion protein using Western blot analysis on mouse embryonic fibroblasts (MEFs) isolated from R26^{ERT2-cre};Rosa26^{ct β cat-Tcf711fl/+} (Fig. 13D). Addition of 4-hydroxitamoxifen resulted in expression of the protein of the desired size (aprox. 110 kda) that is detected both by Tcf711 antibody and a-Flag antibody (Fig. 13D). Furthermore, we see ubiquitous expression of the fluorescent protein tdTomato in the Tcf711^{fl/+};Rosa26^{ct β cat-Tcf711fl/+} mice (Fig. 13E), yet the expression disappears in the AP2 α -Cre;Tcf711^{fl/fl}; Rosa26^{ct β cat-Tcf711fl/+} compound mutants in the regions where recombination occurs (Fig. 13G); AP2 α -Cre;Tcf711^{fl/fl} serves as a negative control (Fig. 13F). In brief, following Cre recombination, the TdT cassette is excised, allowing production of either dnTCF4 or ct β cat-Tcf711 mRNA (Fig. 14A).

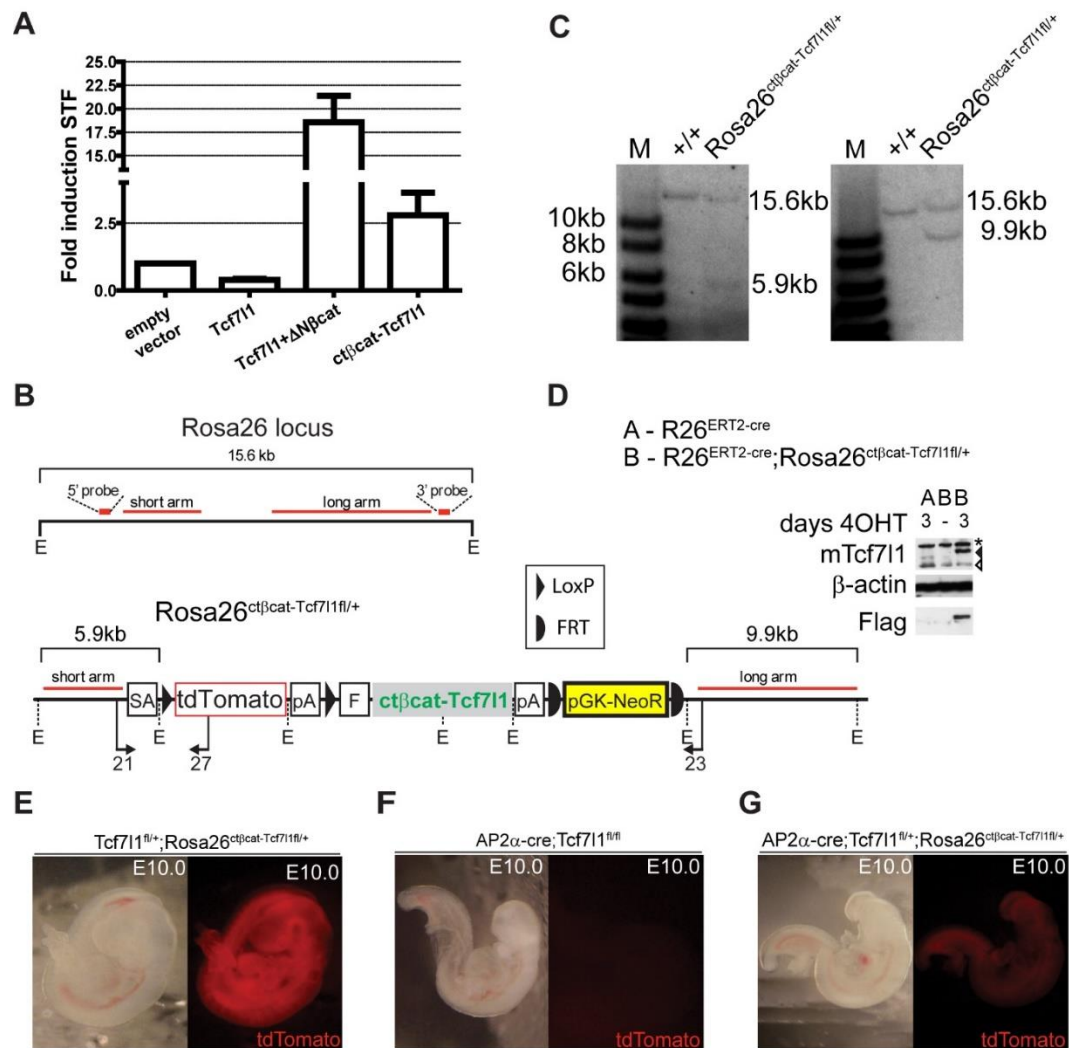


Figure 13: Generation and validation of the mouse strain $Rosa26^{ct\beta cat-Tcf711fl/+}$. (A) SuperTopFlash assay in HEK293 cells showed $ct\beta cat-Tcf711$ mediated activation of the Tcf/Lef driven luciferase reporter. (B) Scheme of the $Rosa26$ locus and the targeting vector, homology arms are depicted in red. E-EcoRI cleavage site, SA-splice acceptor, pA-poly-adenylation signal, pGK-NeoR-neomycin expressing cassette, F-Flag tag sequence, primers for genotyping 21-JM21F, 23-JM23R and 27-JM27R. (C) Southern blotting analysis confirms correct homologous recombination into mES cells, short arm is on the left. (D) Western blotting of lysates from mouse embryonic fibroblasts (MEFs) isolated from the $R26^{ERT2-cre}; Rosa26^{ct\beta cat-Tcf711fl/+}$ embryos revealed presence of the $ct\beta cat-Tcf711$ fusion protein (black arrowhead approx. 115kDa), 3 days after administration of 4-OHT (*4-hydroxitamoxifen*). Black and white arrowhead marks endogenous Tcf711 (aprox. 80kDa). * marks nonspecific binding of the antibody. (E-G) $Tcf711^{fl/+}; Rosa26^{ct\beta cat-Tcf711fl/+}$ mice ubiquitously express fluorescent protein tdTomato, the expression is lost in the regions where recombination occurs, visible in the $AP2\alpha-Cre; Tcf711^{fl/fl}; Rosa26^{ct\beta cat-Tcf711fl/+}$ compound mutants. $AP2\alpha-Cre; Tcf711^{fl/fl}$ serves as a negative control.

We crossed the $Tcf711^{fl/fl}; Rosa26^{dnTCF4fl/fl}$ and $AP2\alpha-Cre; Tcf711^{fl/+}$ strains and evaluated the strength of the phenotype in $AP2\alpha-Cre; Tcf711^{fl/fl}; Rosa26^{dnTCF4fl/+}$ compound mutants at E10.5 stage (scheme Fig. 14A). Intriguingly, overexpression of the dnTCF4 was able to reduce the occurrence of the strong phenotype by more than

half (27.3%), compared with the 60.5% incidence in the AP2 α -Cre;Tcf711^{fl/fl} mutant (Fig. 14D). The effect of the rescue on NC population was further analyzed by *in situ* hybridization showing no or very little ectopic Sox10 mRNA in the AP2 α -Cre;Tcf711^{fl/fl};Rosa26^{dnTCF4fl/+} 'rescued' mutants (arrowheads, Fig. 14B,C). On the contrary, the β cat-Tcf711 fusion protein showed significantly ($P=0.049$, Fishers test) decreased capability to rescue the phenotype than the dnTCF4; 85.7% of analyzed embryos displayed the strong phenotype in the AP2 α -Cre;Tcf711^{fl/fl}; Rosa26^{ct β cat-Tcf711fl/+} compound mutants (Fig. 14D). Expression of ct β cat-Tcf711 was also unable to reduce the aberrant Sox10-positive NC population (Fig. 14B,C). In summary, using transgenic mice strains, we have genetically confirmed that Tcf711, acting as a repressor of Wnt/ β -catenin signaling, protects anterior neural tissue from conversion to a NC cell fate.

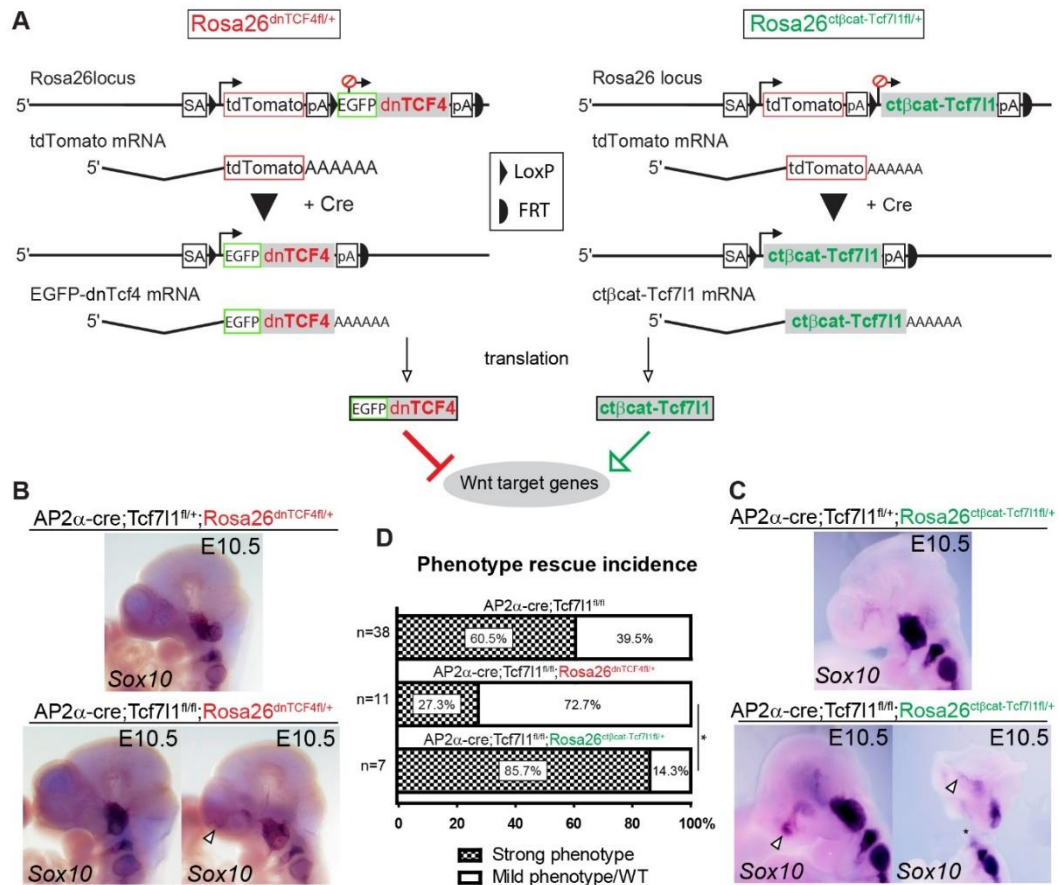


Figure 14: A constitutively expressed repressive form of Tcf is able to rescue the ANF absence in *AP2α-Cre;Tcf711^{fl/fl}* mutants. (A) Diagram describing *Rosa26^{dnTCF4fl/+}* and *Rosa26^{ctβcat-Tcf711fl/+}* mouse strains used in the rescue experiments. SA-splice acceptor, pA-poly-adenylation signal. (B,C) Expression of *Sox10* transcripts was either unaffected or only mildly affected in the *AP2α-Cre;Tcf711^{fl/fl};Rosa26^{dnTCF4fl/+}* compound mutants (arrowheads), confirming the rescue capability of dnTCF4. *AP2α-Cre;Tcf711^{fl/fl};Rosa26^{ctβcat-Tcf711fl/+}* compound mutants displayed no rescue or even stronger phenotype. Asterisk (*) marks artifact caused during sample preparation. (D) Quantification of the strong and mild phenotype incidence and rescue capability of dnTCF4 and ctβcat-Tcf711, scored at E10.5-13.5. *(P=0.049, Fishers test), n-number of embryos analyzed.

2) Investigation of the effects of *Tcf7l1* deletion on the anterior pre-placode, with the focus on lens placode development in mouse

Jan Mašek, Barbora Antošová, Hynek Strnad, Ondřej Machoň, Zbyněk Kozmik

Results presented in this chapter are unpublished data

Tcf7l1 positively regulates expression of the anterior PPR and ANF specifiers

In order to better characterize the global effects of *Tcf7l1* deletion, we employed differential gene expression analysis. We took advantage of the EYFP fluorescence of the Rosa26^{EYFP^{fl/+}} mouse strain and isolated the NPB cells from the 6-8s Rosa26^{EYFP^{fl/+}};AP2 α -Cre;Tcf7l1^{fl/fl} mutant and Rosa26^{EYFP^{fl/+}};AP2 α -Cre;Tcf7l1^{fl/+} control embryos using FACS sorting (scheme of the experimental workflow is in Fig. 15A). RNA isolated from sorted cells was amplified and processed on Illumina MouseRef-8v2.0 Expression BeadChip, while collected data were analyzed in R-environment using Bioconductor packages.

Expression profiling (Fig. 15B) revealed downregulation of several Wnt antagonists, among which *Dkk1* and *Tcf7l1*, while various components of the Wnt/ β -catenin pathway, such as *Wnt1* and *Lef1*, were upregulated, confirming the whole mount RNA *in situ* hybridization and BAT-gal reporter data shown in previous section of the results (Fig. 11). Analysis also confirmed the previously shown (Fig. 8A) downregulation of *Six3* and *Fgf8* and enriched the list of the compromised ANF specifiers with *Zic1*, *Zic5*, and *Hesx1* genes, whose expression was more than 4 times downregulated. We did not observe many changes in the expression of the NC specifiers (with the exception of a 1.84 and 0.76 fold increase case of *Foxd3* and *Pax3*, respectively). This could be attributed to the fact that their relatively high expression along the entire NPB masks the effects of *Tcf7l1* deletion in the most anterior part of the NPB.

Next, we focused on genes connected with PPR development. Unfortunately, combination of variability between different stages, penetrance of the phenotype and the subsequent amplification step introduced inconsistency into the data set that hampered the statistical significance of the accumulated data. Nevertheless, the overall changes in the expression levels of several key regulators of the placodal

development from the Six, Eya and Dlx gene families as well as like *Pax6* and *Otx2* (Fig. 15B), suggest an important role of *Tcf7l1* in expression of the anterior PPR genes. The most pronounced changes were observed for those genes that specify anterior PPR (normally devoid of active Wnt/ β -catenin signaling), i.e. *six5*, *otx2*, *pax6*, *six4*, *six3*, *eya2* and *eya3*, which were downregulated in *Rosa26^{EYFPfl/+};AP2 α -Cre;Tcf7l1^{fl/fl}* mutants. On the other hand, the expression of more posteriorly localized genes, such as *foxi1*, *dlx1*, and *pitx2*, which are normally exposed to intermediate levels of Wnt/ β -catenin signaling activity, remained unchanged.

It has been shown that *Pax6* and genes from Six and Eya families play important role in development of adeno-hypophyseal, nasal and lens placodes during mouse embryogenesis (Chen et al., 2009; Dellovade et al., 1998; Grindley et al., 1995; Hogan et al., 1986; Lagutin et al., 2003; Purcell et al., 2005). Gross morphology of the *AP2 α -Cre;Tcf7l1^{fl/fl}* “strong” mutants (Fig. 6H) at embryonic day 9.0-9.5 prevented analysis of these structures, so we decided to score the placodal defects of the “mild” mutants. EYFP signal in the *Rosa26^{EYFPfl/+};AP2 α -Cre;Tcf7l1^{fl/fl}* “mild” mutants and *Rosa26^{EYFPfl/+};AP2 α -Cre;Tcf7l1^{fl/+}* control embryos at E10.5 stage allowed us to identify recombined tissue and compare its morphology (Fig. 16A,B). Mutant embryos did not develop nasal structures and eyes, the trigeminal ganglion was not formed properly, but the otic vesicle appeared to be without obvious defects (Fig. 16B) when compared with the control embryos from the same stage (Fig. 16B). Immunohistochemical staining of the sections from the *AP2 α -Cre;Tcf7l1^{fl/fl}* mutants confirmed expected absence of Tcf7l1 protein in the region of future lens placode (arrows, Fig. 16D), while it is present in the controls at embryonic stage E9.5 (arrows, Fig. 16C). Immunostaining with antibody for ectodermal marker Tfp2 α revealed complete absence of ectodermal thickening and failure in lens pit formation in *AP2 α -Cre;Tcf7l1^{fl/fl}* mutant (Fig. 16F,F'), when compared to *AP2 α -Cre;Tcf7l1^{fl/+}* controls (Fig. 16E,E') at E10.5 stage. Even though these results looked promising, low overall incidence of the “mild” mutants (39.5%) (Fig. 6I) and substantial variability in observed defects caused by broad region of *AP2 α -Cre* activity, led us to employ different Cre

expressing mouse strain and focus on the effects of *Tcf7l1* deletion during lens placode development.

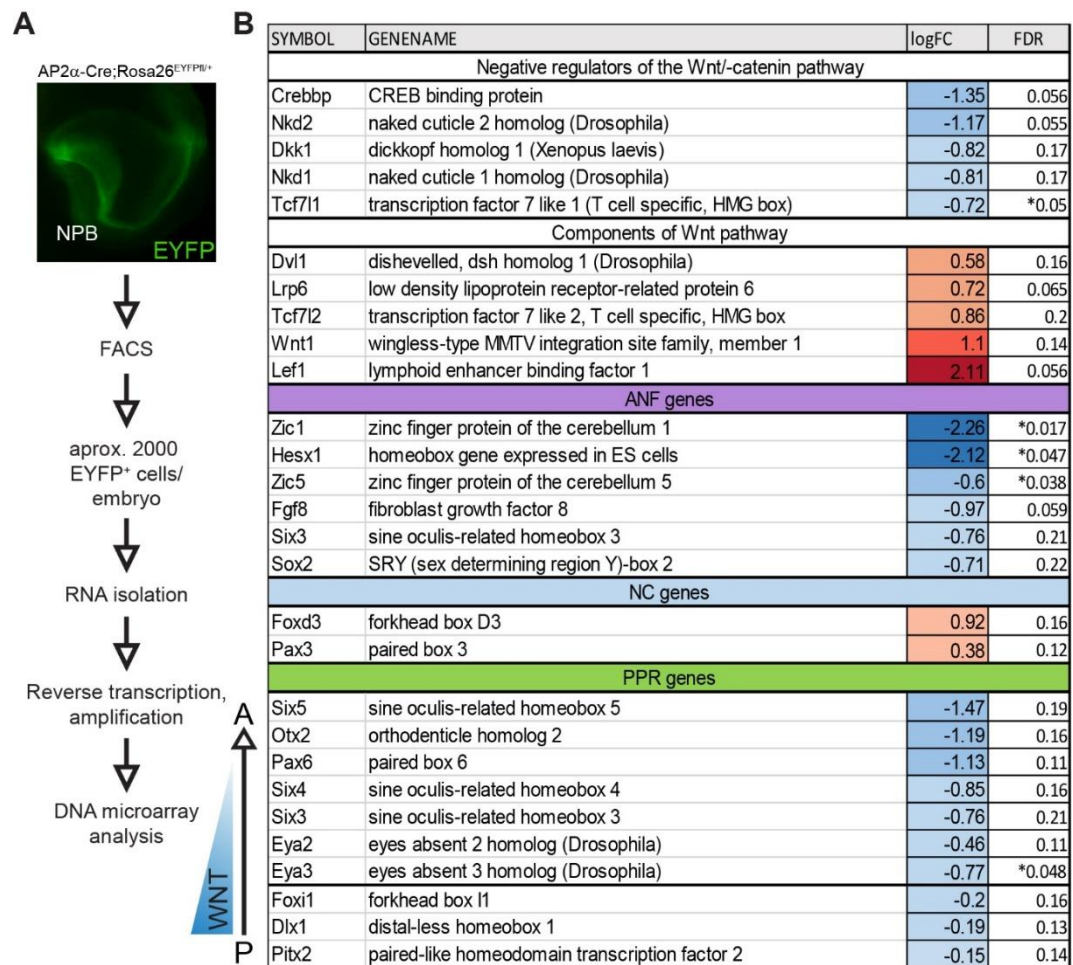


Figure 15: *Tcf7l1* deletion results in reduced expression of the ANF and anterior PPR genes. (A) Scheme of the experimental workflow. RNA isolated from sorted EYFP⁺ cells of the Rosa26^{EYFPfl/+};AP2 α -Cre;*Tcf7l1*^{fl/fl} mutants (n=4) and Rosa26^{EYFPfl/+};AP2 α -Cre;*Tcf7l1*^{fl/+} controls (n=4) at 6-8s stage was amplified and subjected to processing on Illumina MouseRef-8v2.0 Expression BeadChip. **(B)** Data from the DNA microarray analysis were analyzed in R-environment using Bioconductor packages. Elimination of the most outlying values for mutant and control datasets was performed. Red and blue colors represent upregulated and downregulated genes in the mutants, respectively. A-anterior, P-posterior, FDR-False discovery rate.

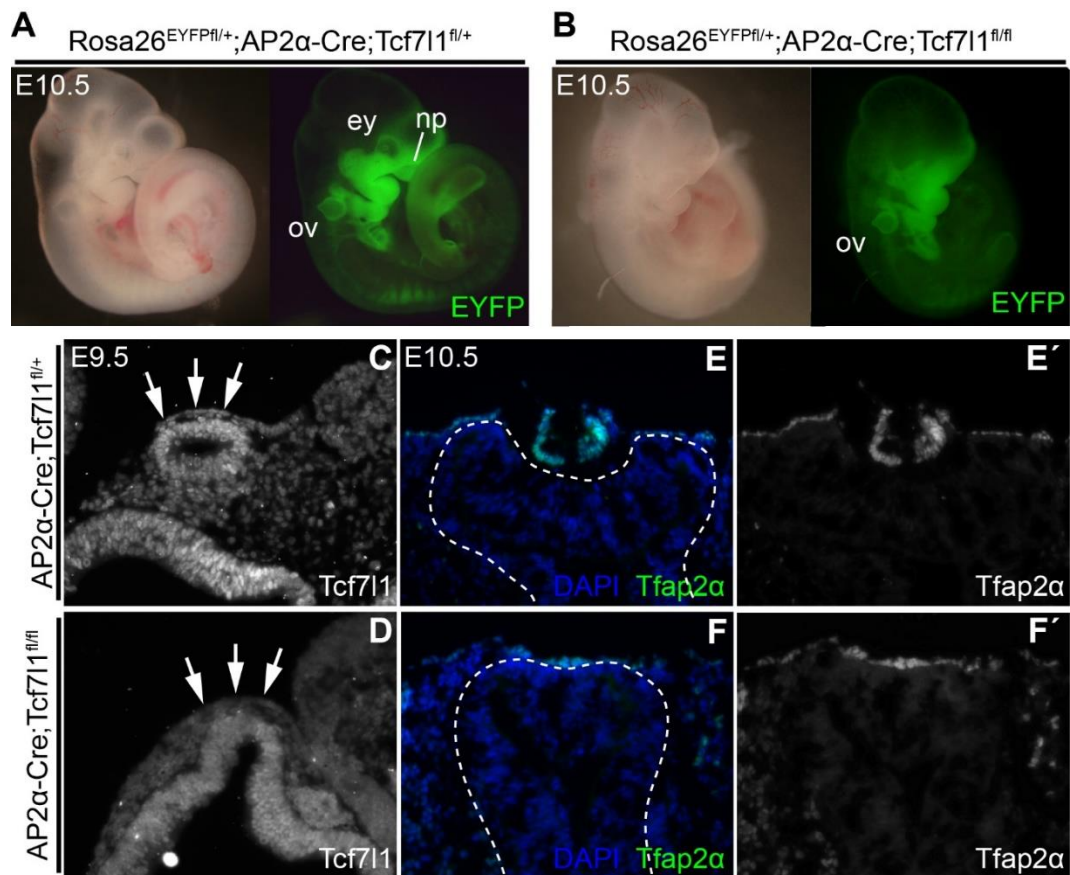


Figure 16: Placodal defects resulting from *Tcf711* deletion. (A,B) Comparison of morphology between Rosa26^{EYFP}^{fl/+};AP2α-Cre;Tcf711^{fl/+} controls (A) and Rosa26^{EYFP}^{fl/+};AP2α-Cre;Tcf711^{fl/fl} mutants (B) at E10.5 stage. (C,D) Immunohistochemical analysis of the developing lens placode. Tcf711 protein is present in controls (C) and disappears in presumptive lens ectoderm of the AP2α-Cre;Tcf711^{fl/fl} mutants (D) at E9.5. (E-F') Tfap2α positive lens pit, present in controls (E,E') is completely missing in AP2α-Cre;Tcf711^{fl/fl} mutants (F,F') at E10.5. Dashed line marks the developing retina. ov-otic vesicle, ey-eye, np-nasal placode.

Conditional deletion of *Tcf711* in the lens placode causes severe defects in lens development

In order to delete *Tcf711* during early events of the lens placode development, we have crossed the *Tcf711* conditional knock-out mouse strain (EUCOMM) with Lens-Cre (Ashery-Padan et al., 2000). This Cre expressing mouse strain has been widely used in studies focused on early lens development, due to its ability to deliver recombination specifically in lens placode ectoderm from E9.0 onward (Ashery-Padan et al., 2000).

Histochemical staining on cryosections from the developing eye revealed that deletion of critical exons in *Tcf7l1* results in loss of Tcf7l1 protein expression (Fig. 17A',B'), along with reduction of the lens size in the Lens-Cre;*Tcf7l1*^{fl/fl} mutants, when comparing with the control embryos of the same developmental stage (E13.5) (Fig. 17A,B). Adult Lens-Cre;*Tcf7l1*^{fl/fl} animals were viable, but displayed severe microphthalmia. Sectioning and histochemical analysis at post-natal day 21 revealed severe reduction of the lens size (black arrowhead, Fig. 17D'), together with reduced or missing pupillary openings (black and white arrowhead, Fig. 17D') in the mutants (Fig. 17C-D').

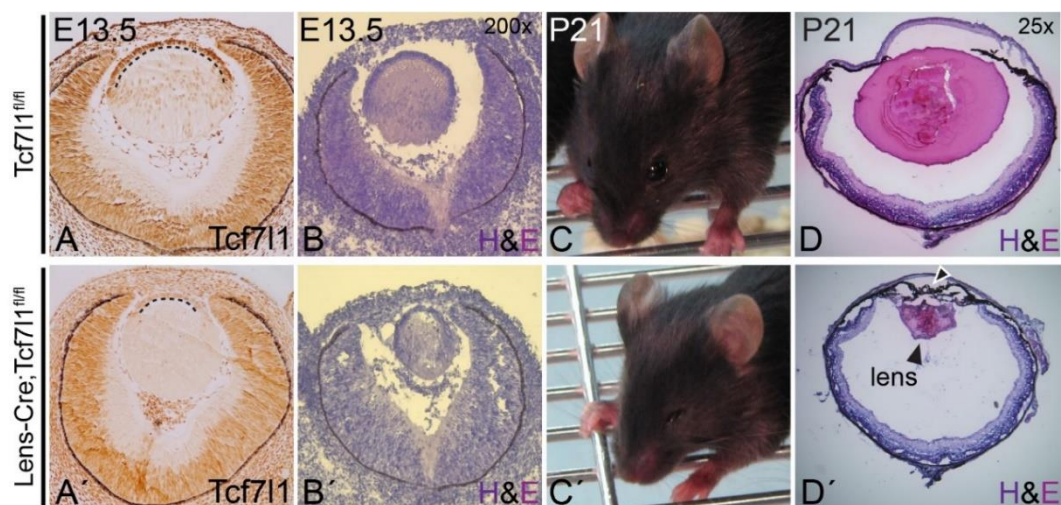


Figure 17: *Tcf7l1* is required for proper lens formation. (A,A') immunohistochemical staining of Tcf7l1 protein on cryosections from developing eyes of control and Lens-Cre;*Tcf7l1*^{fl/fl} mutant embryos at E13.5 stage. Note the reduction in the length of lens epithelium (dashed line). (B-D') Hematoxylin & eosin (H&E) staining revealed progressive reduction of the lens size in the mutants (B',D') when compared with corresponding controls from E13.5 to P21 stage (B,D). Macroscopically noticeable microphthalmia of Lens-Cre;*Tcf7l1*^{fl/fl} in pups at P21 stage (C') is not present in controls of a same stage (D).

Tcf7l1 is not required during early differentiation of the developing lens

It has been shown that aberrant activation of the Wnt/ β -catenin signaling pathway in the lens surface ectoderm arrests lens placode specification and completely disrupts eye development (Machon et al., 2010; Smith et al., 2005). However, when activation of the pathway occurs in later stages of the embryonic development (E10.5), lens develop, but display defects in differentiation of the lens epithelium or lens fiber cells. This has been shown either through stabilization of the β -catenin using MLR10-Cre (Martinez et al., 2009) or using transgenic mice expressing constitutively active form of *Lef1* (α A-CLEF) under the control of α A-crystallin promoter (Antosova et al., 2013).

To detect changes in the lens fiber cell differentiation, we performed immunohistochemical analysis on cryosections from developing eyes and compared the expression of differentiation markers in fiber cell of the *Lens-Cre;Tcf711^{fl/fl}* mutants and *Tcf711^{fl/fl}* controls at E13.5. Surprisingly, staining for Prox1 and C-Maf as well as γ -crystallin revealed no changes between mutant and control lenses (Fig. 18A-C'). We repeated this type of analysis, this time focusing on proteins that are involved in the maintenance of the lens epithelium. Staining of the sections, using antibodies against Pax6, FoxE3 and E-cadherin, also revealed no difference between mutant and control lenses at E13.5 (Fig. 18D-F').

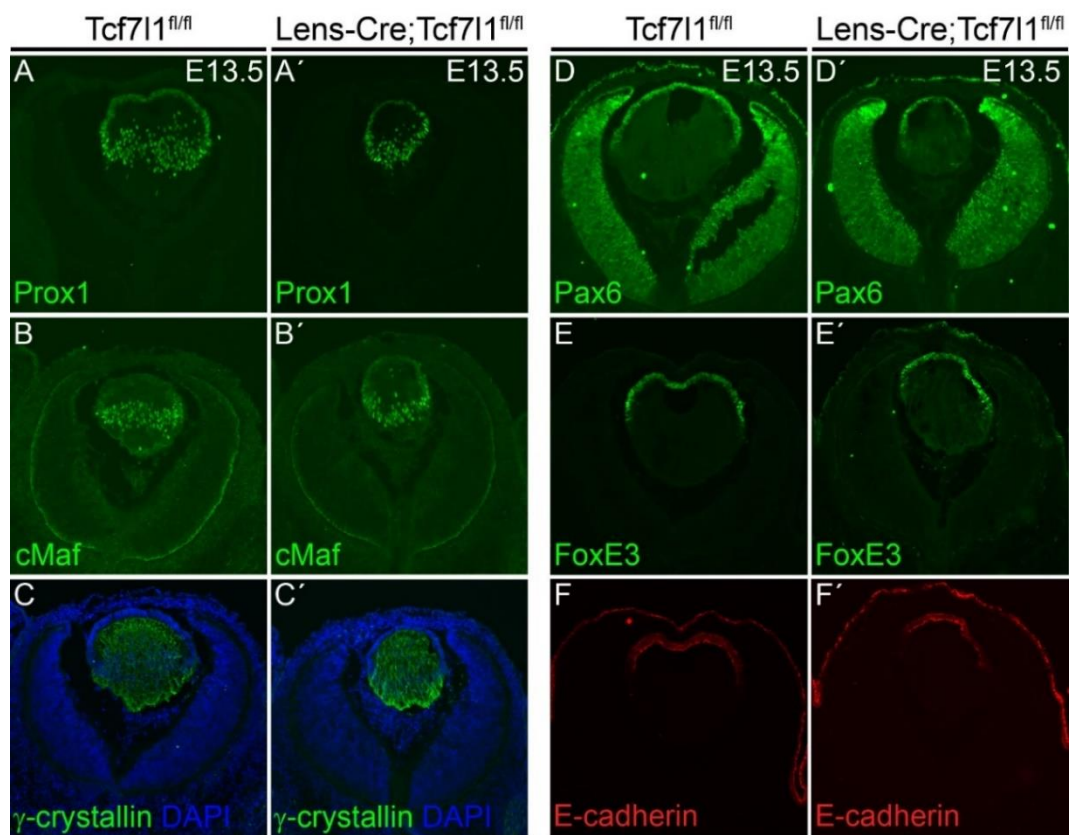


Figure 18: Deletion of *Tcf711* does not affect lens differentiation. (A-F') Immunohistochemical staining of cryosections from embryonic eyes at E13.5 stage revealed no changes between *Lens-Cre;Tcf711^{fl/fl}* mutants and controls, in regard to the expression of the early lens marker Prox1 (A,A'), markers of fiber cells cMaf (B,B') and γ -crystallin (C,C'), as well as of markers of lens epithelium, namely Pax6 (D,D'), FoxE3 (E,E'), and E-cadherin (F,F').

Absence of *Tcf7l1* results in the cell cycle misbalance and apoptosis of the fiber cells

Wnt/ β -catenin signaling pathway is known to regulate cell cycle progression (reviewed in Niehrs and Acebron (2012)). There were no changes in lens differentiation following *Tcf7l1* deletion, yet the size of the lens appeared to be smaller at E13.5, therefore we decided to evaluate putative changes in proliferation or cell death.

Quantification of the BrdU incorporation assay revealed no significant difference in the total amount of BrdU⁺ cells between the mutant and control lenses at E13.5 stage (Fig.19C). Surprisingly, we found statistically significant ($P<0,05$) increase in ectopic BrdU⁺ fiber cells in Lens-Cre;*Tcf7l1*^{fl/fl} mutants (arrows Fig. 19A'), that were not present in controls, since these cells are post-mitotic (Fig. 19A,B). To further confirm the presence of proliferating cells in the fiber cell compartment, we performed double immunohistochemistry using antibodies against PCNA and Pax6, markers of proliferating and epithelial cells, respectively (Fig. 19D-E'). Concordantly, we found aberrant PCNA⁺ fiber cells present in the mutants, when compared with controls (arrows Fig. 19D,D'). Quantification confirmed there is a significantly ($P<0,001$) higher number of the Pax6⁻/PCNA⁺ cells in the mutants than in controls at the E13.5 stage (Fig. 19E-F).

Disruption of the cell cycle often leads to cell death via apoptosis. Immunohistochemical analysis showed Caspase-3 staining among fiber cells (E-cadherin⁻) in the mutants but not in the controls at E13.5 (Fig. 19G,G'). More detailed quantification of the Caspase-3⁺ cells revealed a significant increase of the apoptosis in the lenses of Lens-Cre;*Tcf7l1*^{fl/fl} mutants. The highest number of the ectopic Caspase-3⁺ cells was observed in the mutants at E11.5 ($p<0.01$) and was still present (to lesser extent) at E13.5 stage ($p<0.05$) (Fig. 19G-I). Comparison of the total amount of cells (DAPI⁺) in mutant and controls, at E13.5 stage, revealed more than 30% decrease ($P<0,001$) of the cell numbers in the mutant lenses (Fig. 19J). The Pax6⁻ and E-cadherin⁻ population of fiber cells showed similar decrease in numbers of DAPI⁺ nuclei, suggesting that the loss of cells is equally spread among epithelial and fiber compartment (Fig. 19J). This data illustrate that *Tcf7l1* deletion in the lens placode will not allow lens epithelial cells to terminate their cell cycle progression during maturation into fiber cells, and are eventually driven to apoptosis.

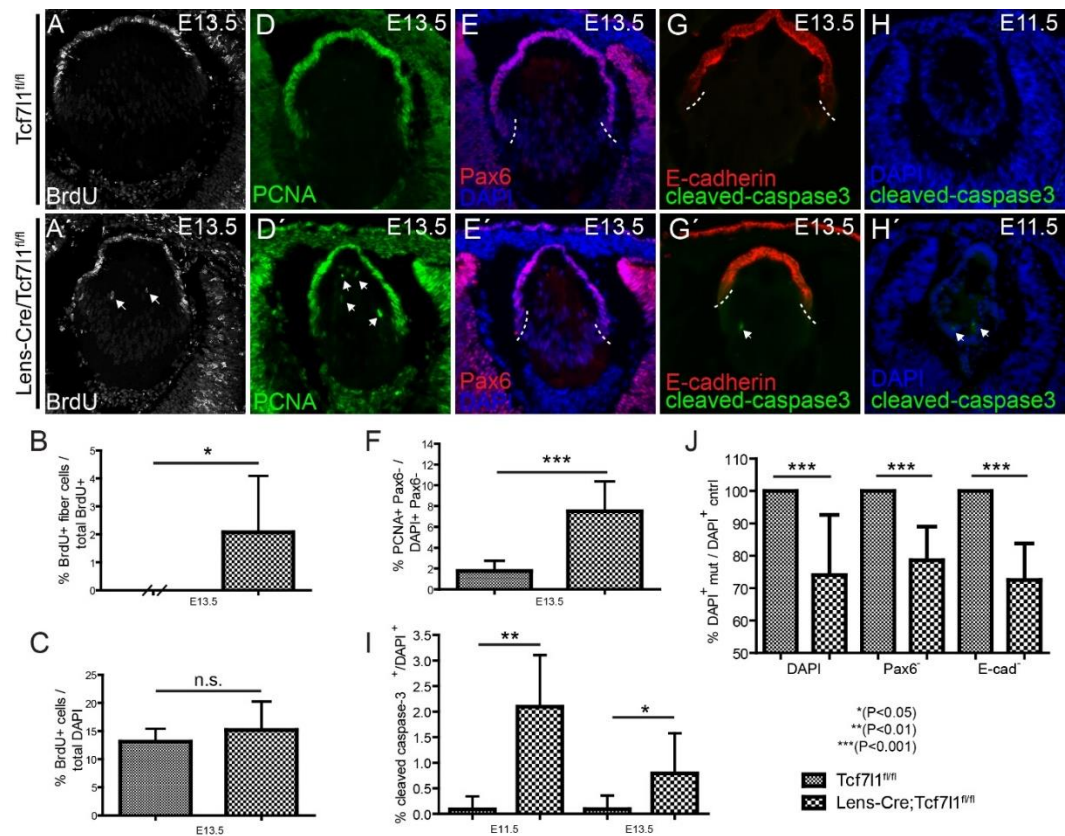


Figure 19: Absence of Tcf711 causes aberrant proliferation of fiber cells. (A, A') Confocal images of cryosections from E13.5 lenses after 1h BrdU pulse, stained with anti-BrdU antibody. Arrows in (A') indicate BrdU⁺ fiber cells in lenses of Lens-Cre;Tcf711^{fl/fl} mutants. (B, C) total ratio of BrdU⁺ nuclei per total nuclei at E13.5 was not significantly changed (n=7) (C). Significantly higher number of BrdU⁺ fiber cells in E13.5 mutant lenses in comparison with controls (B). (D-F) cryosections of control (D, E) and mutant (D', E'), stained with antibody against the marker of proliferation PCNA and the marker of epithelial cells Pax6. PCNA⁺ cells among the fiber cells (Pax6⁻) in Lens-Cre;Tcf711^{fl/fl} mutants are marked by arrows (E'). Significant increase of PCNA⁺ cells were observed in the mutants (p<0.001, T-test) when compared with controls (n_{mut}=16, n_{cntrl}=11) (F). (G-J) Immunohistochemical staining, using the marker of epithelial cells E-cadherin and the marker of apoptosis cleaved caspase-3, revealed apoptotic cells among the fiber cells of the Lens-Cre;Tcf711^{fl/fl} mutants (G', H') but not in the controls (G, H) at E11.5 and E13.5 stage. Quantification of the cleaved caspase 3 staining showed significant increase in apoptosis in the mutants at E11.5 (p<0.01, T-test) and E13.5 stage (p<0.05, T-test) (I). E13.5 mutant lenses are significantly hypo-cellular (p<0.001, T-test) (J). Nuclei were stained with DAPI.

Tcf7l1 is negative regulator of the *Cdkn1a*^{P21/Waf} expression during lens development

Regulation of the cell cycle progression is achieved through interaction of many proteins forming multiple feedback loops. In order to identify which particular genes might be responsible for the proliferation defects we observed in the lenses of Lens-Cre;*Tcf7l1*^{fl/fl} mutants, we employed differential gene expression analysis.

We have dissected 22 lenses from Lens-Cre;*Tcf7l1*^{fl/fl} mutants and 28 lenses from control animals at embryonic stage E16.5-17.0. We have divided them randomly into 3 mutant and 3 control groups (lenses?) and isolated the RNA. Extracted RNA was processed on Illumina MouseRef-8v2.0 Expression BeadChip and collected data were analyzed in R-environment, using Bioconductor packages. Among the 38 significantly ($p < 0.05$ & $|\log_{2}FC| \geq 1$) altered genes, 30 were upregulated and 8 downregulated (Fig. 20). The fact that more genes were up- rather than down-regulated, is in line with previous research, suggesting that *Tcf7l1* functions predominantly as a transcriptional repressor (Cole et al., 2008; Liu et al., 2005; Ombrato et al., 2012). One of the most upregulated genes (4.76 fold) was *cyclin dependent kinase inhibitor 1 a* (*Cdkn1a*), also known as p21^{Cip1/Waf}. At low levels, p21 promotes cell cycle progression; under stress conditions, its expression is increased in a p53-dependent manner, leading to cell cycle arrest in G1 phase (reviewed in Jung et al. (2010)).

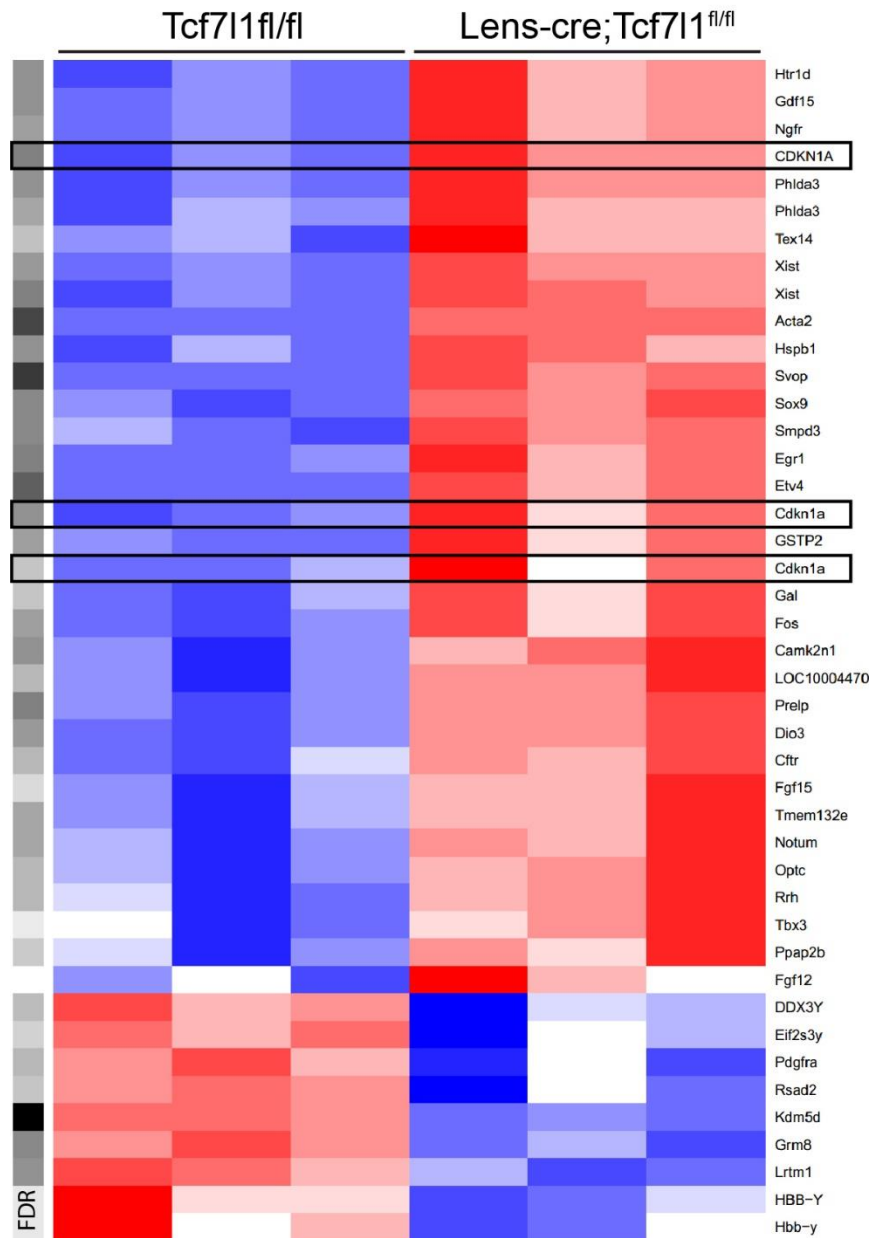


Figure 20: Heatmap showing patterns of differentially expressed genes in mutant and control, based on Z-score of probe intensity. RNA was isolated from dissected lenses of Lens-cre;Tcf7l1^{fl/fl} mutants and Tcf7l1^{fl/fl} controls at E16.5-17.0 stage. Analysis was performed on biological triplicates ($p < 0.05$ & $|\log FC| \geq 1$). Data from Illumina MouseRef-8v2.0 Expression BeadChip were analyzed in R-environment, using Bioconductor packages. Red represents genes upregulated and blue represents genes downregulated in the Tcf7l1^{fl/fl} x Lens-Cre;Tcf7l1^{fl/fl} lenses. FDR-False discovery rate

Immunohistochemical staining confirmed the p21 upregulation in eye sections of Lens-Cre;Tcf711^{fl/fl} mutants (arrows, Fig. 21B,D), while it was not detectable in the control lenses (Fig. 21A,C) at E11.5 and E13.5 stages. Furthermore, co-staining with E-cadherin, the marker of epithelial cells, revealed delay in formation of the lens vesicle in the mutant embryos, at embryonic stage E11.5 (Fig. 21A', B'). This is also manifested also by the presence of a lens stalk in Lens-Cre;Tcf711^{fl/fl} mutants (arrowhead Fig. 21D') not present in controls, at E13.5 (Fig. 21C').

It was shown recently, that, when crossed to certain genetic backgrounds, mice hemizygous for Lens-Cre transgene can develop various eye abnormalities, including smaller lens size (Dora et al., 2014). To exclude the possibility that phenotype observed in Lens-Cre;Tcf711^{fl/fl} mutants is caused by Lens-Cre transgene, we crossed our Tcf711^{fl/fl} strain with transgenic line LR-Cre. In this transgene, expression of the Cre-recombinase is driven by three copies of a lens-specific element derived from *Pax6* and starting its expression both in lens placode and retina, between the E9.0-9.5 stage (Kreslova et al., 2007). LR-Cre;Tcf711^{fl/fl} mutant mice also exhibit disrupted lens development, presence of the lens stalk and high number of p21⁺ cells at E13.5 (Fig. 21F,F'), when compared with LR-Cre;Tcf711^{fl/+} controls from the same stage (Fig. 21E,E'). Control crossing of Tcf711^{fl/fl} mouse strain with early retina specific Cre-recombinase expressing transgenic mouse strain Rx-Cre (Klimova et al., 2013) was performed to exclude possible contribution of the Tcf711 depletion in retina in the LR-Cre;Tcf711^{fl/fl} mutants. Histological analysis of the Rx-Cre;Tcf711^{fl/fl} mutants showed no obvious difference in lens and retina morphology between the mutant and control embryos at postnatal stage P0 (Fig. 21G,G').

Ultimately, we wanted to test the effects of *Tcf711* on p21 expression, using p21-Luc luciferase reporter (van de Wetering et al., 2002) in tissue cultures. In this construct, a 2.3 kb fragment of the P21^{CIP1/WAF1} promoter sequence was cloned into a luciferase reporter vector. We isolated MEFs from Ert2-Cre;Tcf711^{fl/fl} embryos. In this cell line, administration of the 4-hydroxitamoxifen (4-OHT) induces recombination, generating a Tcf711 KO cell line. We transiently transfected p21-Luc into Tcf711 KO MEFs, 3-fold increase in activity of the promoter was observed, however this activity was abolished by co-transfection of Tcf711 expressing plasmid (Fig. 21H), confirming that p21 is directly repressed by Tcf711.

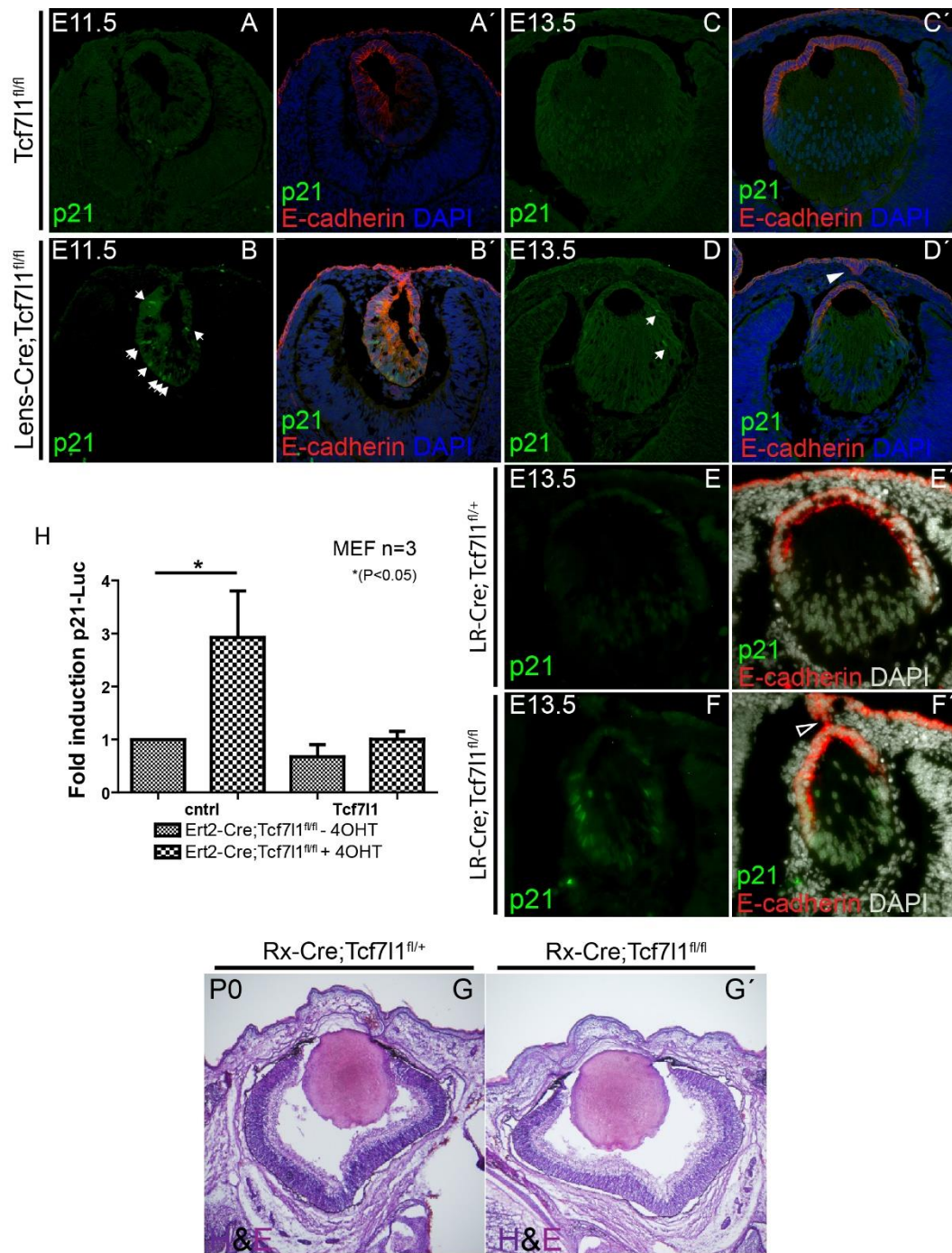


Figure 21: *Cdkn1a^{P21/Waf}* is negatively regulated by *Tcf711*. (A-D) immunohistological staining of p21 and E-cadherin proteins on eye cryosections from *Lens-Cre;Tcf711^{fl/fl}* mutants and controls at E11.5 and E13.5 stages. (E-F) immunohistological staining of p21 and E-cadherin proteins on eye cryosections from *LR-Cre;Tcf711^{fl/fl}* mutants and controls at E13.5 stage confirms the upregulation of p21 expression and delay in progression of lens development observed in *Lens-Cre;Tcf711^{fl/fl}* mutants. (G,G') Hematoxylin and eosin staining of the control and *Rx-Cre;Tcf711^{fl/fl}* mutants at P0 stage reveal no obvious difference in lens and retina development. (H) Transient transfection of the p21-Luc into mouse embryonic fibroblasts (MEFs) isolated from *Ert2-Cre;Tcf711^{fl/fl}* and treated with 4-hydroxitamoxifen (4-OHT) revealed 3 fold induction of the reporter ($p < 0.05$, $n = 3$), this activation was lost in the case of co-transfection with *Tcf711* expressing plasmid.

Discussion

How does the progressive activation of Wnt/ β -catenin pathway affect development of the anterior neural tissue, preplacodal region and neural crest?

Spatio-temporal regulation of Wnt/ β -catenin pathway activation, which is required for proper development of the prosencephalon, is secured by expression of several ANF specific negative regulators of the Wnt/ β -catenin signaling. Our data, together with evidence from others (Cole et al., 2008; Liu et al., 2005; Ombrato et al., 2012; Wu et al., 2012) characterize *Tcf711* as a Wnt/ β -catenin target gene repressor. Aberrant activation of the Wnt/ β -catenin pathway, due to *Tcf711* systemic deficiency, is considered the cause of strong A-P patterning defects both in zebrafish (Dorsky et al., 2003; Kim et al., 2000) and mouse (Merrill et al., 2004). In zebrafish, the *Tcf711a* loss-of-function in headless (*hdl*) mutants, as well as MO-mediated knock-down of *Tcf711a* and *Tcf711b* variants, result in expansion of the expression of the MHB markers *Pax2.1* and *Gbx1* anteriorly, accompanied by the loss of *Six3* and *Rx3* expression (Dorsky et al., 2003). The *Tcf711* mice mutants also displayed expansion of the midbrain marker *Engrailed*, joined with the downregulation of *Hesx1* expression (Merrill et al., 2004). Similarly, deletion of *Dkk1* (Mukhopadhyay et al., 2001), *Six3* (Lagutin et al., 2003), *Hesx1* (Andoniadou et al., 2007) and *ICAT* (Sato et al., 2004) in mouse is followed by the loss of anterior neural tissue, a fact that has been interpreted as a defect in A-P patterning induced by aberrant Wnt/ β -catenin signaling. We think that this is a rather generalized view and that, in the context of the ANF phenotypes, is only partially true. In *Xenopus*, low levels of ectopic Wnt/ β -catenin activation enrich the NC population without affecting A-P patterning, while high doses affect both (Wu et al., 2005). This might be also valid for mammals, as mice carrying ENU-induced activating point-mutations in *Lrp6* and β -catenin display a gradual loss of the prospective prosencephalon, depending on the strength of the Wnt/ β -catenin pathway overactivation, but do not manifest a shift of posterior markers towards the anterior part of the embryo (Fossat et al., 2011). Furthermore, compound deletion of one *Hesx1* allele and both alleles of *Tcf711* in mouse, using prosencephalon-specific *Hesx1*-Cre, results in the aberrant activation of Wnt/ β -catenin signaling, accompanied with loss of anterior neural tissue and no effect on the A-P patterning (Andoniadou et al., 2011). Similarly, we did not detect any changes in the expression of the MHB markers *Fgf8* or *Gbx2* in *AP2 α -Cre;Tcf711^{fl/fl}* mutants. Nevertheless, we did observed a gradual loss (depending on the strength of the phenotype) of the posterior prosencephalon marker *Tcf712* and the ANF markers *Six3*, *Fgf8* and *FoxG1*. This was

accompanied by the expansion of *Sox9*, *FoxD3* and *Sox10*-positive NC populations along the NPB anteriorly. We therefore conclude that the loss of Tcf711 mediated repression of Wnt target genes in the AP2 α -Cre;Tcf711^{fl/fl} mutants allows the gradient of Wnt ligands to influence cell fate in a wider region of the ANF than in controls, without having an effect on A-P patterning. This is not the case with AP2 α -Cre; β -cat^{Ex3fl/+} mutants, in which ectopic stabilization of β -catenin facilitates strong over-activation of Wnt/ β -catenin driven transcription, affecting both NC and A-P. Notably, we observed effects on the population of undifferentiated Sox9-positive NC cells in AP2 α -Cre; β -cat^{Ex3fl/+} mutants at E9.5 and earlier. In contrast, the imbalance in NC differentiation observed in Wnt1-Cre/ β -cat^{Ex3fl/+} mutants occurred one day later, at E10.5 (Lee et al., 2004). This merely reflects the earlier onset of Cre recombination in AP2 α -Cre (Macatee et al., 2003) than in the widely used Wnt1-Cre (Danielian et al., 1998; Lewis et al., 2013), rendering AP2 α -Cre a more suitable tool for studying early events of NC development. Our data provide solid evidence for earlier role of the Wnt/ β -catenin pathway in NC development in regard to previously published findings from the mouse model showing the requirement of the Wnt/ β -catenin pathway in NC maintenance and differentiation (Brault et al., 2001; Gay et al., 2015; Lee et al., 2004).

The effects of the Tcf711 deficiency in mice and zebrafish on NC development were not, until now, characterized in detail. Analogously to the NC expansion in AP2 α -Cre;Tcf711^{fl/fl} mutant mice, we observed ectopic expression of *FoxD3*, *Pax3* and *Sox9* mRNA along the entire anterior NPB, upon Tcf711a MO-mediated knock-down in zebrafish, implicating the conservation of Tcf711 function across vertebrate species. In accordance with this, MO-mediated knock-down of *Dkk1* in *Xenopus* is followed by the enrichment of NC population, marked by the expansion of *Snail2* mRNA expression towards the anterior portion of the embryo (Carmona-Fontaine, 2007). *Hesx1* mutant mice display expansion of Wnt target genes, as well as of the NC markers *Pax3* and *FoxD3* anteriorly (Andoniadou et al., 2007). Furthermore, loss of the Wnt inhibitor *Dkk1* has been shown to cause expansion of the NC mRNA marker *Sox10* (Carmona-Fontaine et al., 2007), being in agreement with the interpretation of the data presented here. Finally, mutual functional redundancy of these factors was demonstrated in zebrafish, where injection of either *Six3* or *Hesx1* mRNA rescued the *hdl* phenotype (induced by Tcf711a deletion) (Andoniadou et al., 2011; Lagutin et al., 2003).

Our analysis of the AP2 α -Cre;Tcf711^{fl/fl} mutants identify Tcf711 as a negative regulator of the NC population. Given the fact that NC are positively regulated by

Wnt/ β -catenin pathway in all studied vertebrates, other Tcf/Lefs should be responsible for activation of Wnt/ β -catenin targets in the NC. It is likely that *Lef1*, *Tcf7* and *Tcf712* are redundant in NC cells, since whole body double knock-outs of *Lef1/Tcf7* and *Tcf7/Tcf712* in mice do not display any obvious NC phenotype (Galceran et al., 1999; Gregorieff et al., 2004). Ectopic Sox9-positive cells in AP2 α -Cre; β -cat^{ΔEx3fl/+} mutants spatially overlap with the elevation of the BAT-gal reporter, *Lef1*, *Tcf7* but not *Tcf712* proteins, suggesting that *Lef1* and *Tcf7* are positively regulated by Wnt/ β -catenin signaling and probably participate in the expression of Wnt responsive NC specific genes. This is further supported by our microarray data showing more than 4 times increase in expression of *Lef1* in the NPB of the AP2 α -Cre;*Tcf711*^{fl/fl} mutants. *Sp5*, another well-defined Wnt target gene and transcriptional repressor (Fujimura et al., 2007), was strongly upregulated in AP2 α -Cre;*Tcf711*^{fl/fl} mutants spreading its expression across the entire ANF. Work in *Xenopus* has identified *Sp5* as a novel NC-specific inducer (Park et al., 2013). MO-mediated knock-down of *Sp5* leads to the upregulation of *Zic1*, making it a candidate target of *Sp5* repression. *Zic1* acts as a NC inducer only when expressed in appropriate balance with *Pax3*, another NC inducer (Hong and Saint-Jeannet, 2007; Park et al., 2013). *Pax3* has been recently identified as a direct target of Tcf/Lefs (Zhao et al., 2014), providing an additional link to the GRN driving NC induction. Aberrant induction of *Sp5*-mediated repression of *Zic1*, in combination with the ectopic expression of Wnt1 ligand which enhances the β -catenin/Tcf/Lef driven transcription of *Pax3*, might serve as an artificial positive feedback loop, further potentiating the effects on NC induction. Additionally, the aberrant Wnt/ β -catenin signaling present in AP2 α -Cre;*Tcf711*^{fl/fl} mutants might upregulate the expression of the transcription factor *Axud1*, a novel Wnt-dependent, positive regulator of NC specification (Simoës-Costa et al., 2015).

Analysis of the microarray data from the *Tcf711* mutant embryos at the 6-8s stage uncovered downregulation of PPR genes involved in specification and maintenance of the nasal and lens placodes, namely members of the Six and Eya families (more specifically *Six3-5*, *Eya2,3*), of the master regulator of eye development *Pax6* and of *Otx2*, which is also involved in the establishing the anterior character of the head. It has been shown that *Pax6* deficiency causes arrest of nasal, lens and adenohypophyseal placode development in mouse (Dellovade et al., 1998; Grindley et al., 1995; Hogan et al., 1986). Similar defects were described after *Six3* deletion in mouse, displaying anophthalmia and reduced nasal structures (Lagutin et al., 2003). Transcription factor *Six3* appears to be indispensable for *Pax6* expression during lens induction (Liu et al., 2006) forming in this way a core auto-regulatory

feedback loop of the PPR GRN. This loop is further maintained by *Pax6*-dependent expression of *Six3*, *Dach1*, and *Eya1* (Purcell et al., 2005). In nasal placode, *Pax6* expression is retained thanks to transcription factors *Six1* and *Six4*, whose absence results in arrest of the placodal development (Chen et al., 2009). Interestingly, transcription factor FoxG1, generally not implicated in the placode development, is also expressed in developing nasal placode and its deficiency leads to severe arrest of nasal placode development in mouse (Duggan et al., 2008). In the first part of results, we show complete loss of both *Six3* and *FoxG1* mRNA expression in the AP2 α -Cre;Tcf711^{fl/fl} mutants, thus we demonstrate requirement of *Tcf711* for the expression of the genes governing the development of anterior placodes. This was further confirmed by the fact that the Tcf711 “milder” mutants did not develop nasal and lens placodes. Recently published work (Gaston-Massuet et al., 2016) revealed requirement of the Tcf711-mediated control of Wnt/ β -catenin signaling activity during development of pituitary gland (also PPR derivative) in mouse, further backing our hypothesis. Notably, Gaston-Massuet et al. also managed to link two different point mutations *TCF7L1* to congenital hypopituitarism in humans.

Our data from mRNA *in situ* hybridization, showing expression of Tcf711 both in the anterior neuroectoderm and surrounding non-neural ectoderm of the early mouse neurula (1-5s), are in line with previous studies at pre-somitic stages (E7.5), where Tcf711 was detected in the anterior portion of all three germ layers (Merrill et al., 2004). This suggests that hampering of the Tcf711 function should affect only the most anterior part of the PPR. Concomitantly, the strong aberrant activation of the BAT-gal signal in the most anterior tip of the neural- and non-neural-ectoderm at 8s stage in the AP2 α -Cre;Tcf711^{fl/fl} mutants allows us to interpret the resulting phenotype as an effect of aberrantly activated Wnt/ β -catenin signaling in developing PPR. First part of the results describes aberrant expansion of the NC population on expansion of the ANF tissue in Tcf711 deficient embryos, induced by increased activity of the Wnt/ β -catenin pathway. The exact mechanism with which Wnt/ β -catenin pathway promotes NC fate is still under intensive investigation, but according to available data (described above), it appears that several NC specific genes are direct targets of Wnt/ β -catenin-dependent transcription. On the other hand, despite the few reported examples of genes negatively regulated by β -catenin:Tcf/Lef complex, reviewed in Hoverter and Waterman (2008), there is no evidence of Tcf/Lef interfering with transcription factors involved in the GRN of the anterior PPR. Similarly to the situation in ANF, it rather appears that anterior PPR is influenced by indirect effects of the ectopic Wnt/ β -catenin signaling pathway activation in the NPB. We believe that over-abundant signaling

from excessively formed NC cells, which is associated with reduction of the pool of PPR progenitor cells at the NPB, is the major cause of the multiple placodal phenotypes in AP2 α -Cre;Tcf711^{fl/fl}.

It is well known from zebrafish, *Xenopus* and chicken, that BMP (a member of TGF- β superfamily) and Wnt/ β -catenin signaling inhibit the placodal development, while medium activity of the BMP pathway and high activity of the Wnt/ β -catenin signaling is crucial for NC specification and maintenance during neurulation (Bhat et al., 2013; Kwon et al., 2010; Litsiou et al., 2005; Steventon et al., 2009). Under physiological conditions, secretion of these morphogens by migrating NC cells plays important role in restricting the spatial distribution of the placodes. This has been nicely demonstrated in chicken, where TGF- β 1, Activin- β A and Activin- β B secreted from migrating NC cells in the mesoderm induced Smad3-dependent inhibition of *Pax6* expression in periocular ectoderm, which was further potentiated by activation of the Wnt/ β -catenin signaling thanks to TGF- β -induced expression of Wnt2 ligand (Grocott et al., 2011). Studies in mouse confirmed the negative effect of nuclear β -catenin on *Pax6* expression, using Lens-Cre or LR-Cre driven stabilization of the β -catenin (β -cat^{Ex3fl/+} strain) (Kreslova et al., 2007; Smith et al., 2005). Decreased levels of the *Pax6* in presumptive lens ectoderm further potentiate the phenotype, as the expression of *Dkk1* and *Sfrp2* genes is dependent on transcriptional factor *Pax6* (Machon et al., 2010). The “placode suppressing loop”, initiated by ectopic Wnt/ β -catenin signaling, is in the AP2 α -Cre;Tcf711^{fl/fl} mutants potentiated to even higher

extent as the other negative regulators of the Wnt/ β -catenin pathway, e.g. Six3, Hesx1 and FoxG1, become downregulated after Tcf711 ablation.

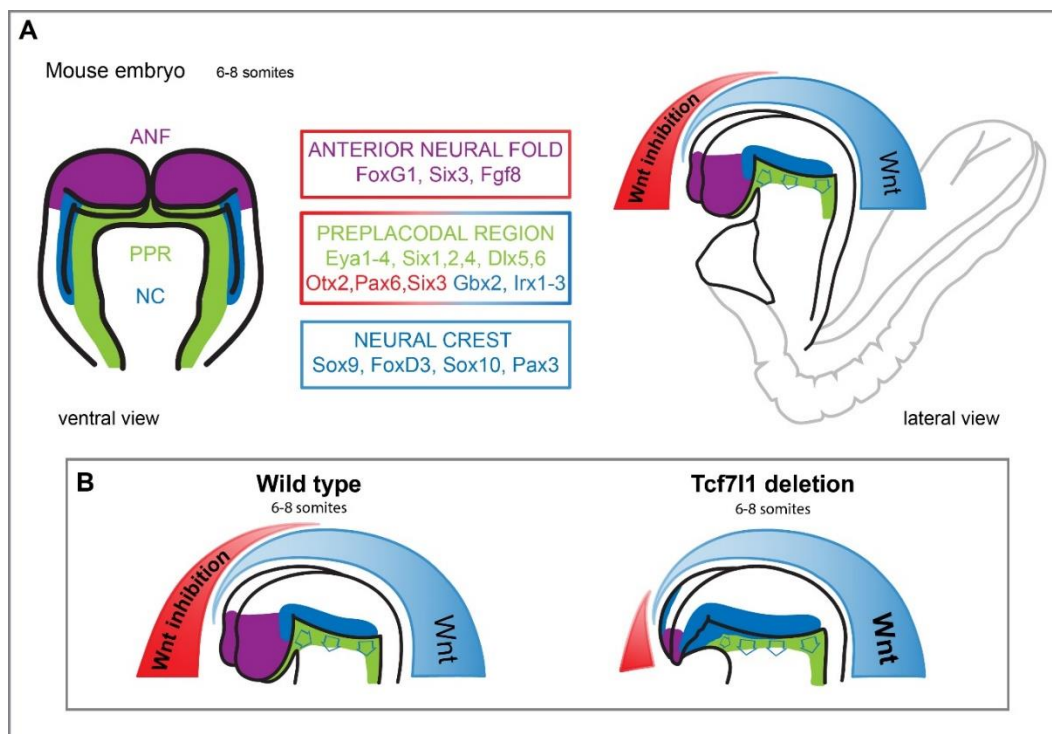


Figure 22: Schematic overview of the embryonic head ectoderm differentiation in relation to Wnt/ β -catenin signaling and Tcf711 deletion. (A) (shown previously as Fig. 5) Ventral view of the head region (left) and lateral view of the whole developing mouse embryo (right) at 6-8 somite stage. A→P gradient of the Wnt antagonists promotes differentiation of the most anterior ectoderm into *foxg1*, *six3*, *fgf8* expressing ANF and *otx2*, *pax6* and *six3* characteristic for the anterior PPR. While A←P gradient of the active Wnt/ β -catenin signaling induce formation of the *gbx2*, *irx1-3* positive posterior PPR and *pax3*, *sox9*, *foxd3* and *sox10* expressing NC. **(B)** Summary of the phenotypical changes resulting from the absence of Tcf711 in AP2 α -Cre;Tcf711^{fl/fl} mutants. These mutants display expansion of the *sox9*, *foxD3*, and *sox10* expressing NC population, accompanied with combined reduction in expression of the ANF specific genes *foxG1*, *six3*, *fgf8*, *zic1*, and *hesx1* and PPR specifiers *eya3*, *pax6*, *six3*, and *foxG1*, caused by overabundance of the Wnt/ β -catenin pathway activation in the anterior ectoderm. ANF-anterior neural fold, PPR-preplacodal region, NC- neural crest

Not surprisingly, deletion of *Tcf711* in lens placode, using either Lens-Cre expressed in presumptive lens ectoderm (Ashery-Padan et al., 2000) or LR-Cre delivering recombination in presumptive lens ectoderm and neuroectoderm of the developing retina (Kreslova et al., 2007), results in considerably milder lens phenotype than the one observed in AP2 α -Cre;Tcf711^{fl/fl}, supporting our hypothesis that the main reason behind the AP2 α -Cre;Tcf711^{fl/fl} phenotype is the ectopic signaling from aberrantly formed NC cells. It is necessary to mention that the onset of Cre-recombination in Lens-Cre and LR-Cre occurs approximately one day later than in AP2 α -Cre, however it should still be early enough, since ectopic stabilization of β -catenin, using the same Lens- and LR-Cre expressing lines, blocks expression of

Pax6 and completely disrupts lens placode development (Machon et al., 2010; Smith et al., 2005). The morphological defects of the Lens-Cre;Tcf711^{fl/fl} mutants share, to some extent, common features with the phenotype observed in the MLR10-Cre; β -catenin^{ex3/+} mutants (Martinez et al., 2009). In these mice, the onset of β -catenin stabilization is triggered one day later (E10.0) than in Lens-Cre; β -catenin^{ex3/+} mutants (Martinez et al., 2009; Smith et al., 2005; Zhao et al., 2004). In Lens-Cre;Tcf711^{fl/fl} mutants, apart from the fact that the lenses look less defective and with no changes in differentiation, an increase in BrDU staining and proliferation markers has been observed, as well as increase in apoptosis in fiber cells. Similarly, MLR10-Cre; β -catenin^{ex3/+} mutants display enhanced proliferation but to a much higher extent and in both epithelial and fiber cells, whereas apoptosis is also present, predominantly in fiber cells (Martinez et al., 2009). Martinez and colleagues also showed upregulation of cell cycle proteins connected with cell cycle progression, namely CyclinD1, p57 and phosphorylated-histone 3 (PH3). Levels of these proteins should be also analyzed in Lens-Cre;Tcf711^{fl/fl} mutants, especially since CyclinD1 has been reported to be a target of the Wnt/ β -catenin-dependent transcription factor c-Myc (Daksis et al., 1994). Another way of how Wnt/ β -catenin pathway induces proliferation through expression of the transcription factor c-Myc is that it represses p21^{Cip1/Waf} gene, presumably in cooperation with transcriptional repressors Sp1 and Sp3 (Gartel et al., 2001). Interestingly, p21^{Cip1/Waf} transcriptional activation is also induced in the presence of Tcf/Lef factors, but only of those isoforms that contains the C-clamp binding domain (Tcf7 and Tcf712) (Hoverter et al., 2012). This effect is probably β -catenin-independent, as the induction of the p21-Luc reporter occurs even when β -catenin insensitive forms (dnTcf7 and dnTcf712) were used (Hoverter et al., 2012; van de Wetering et al., 2002). Here, we report for the first time the Tcf/Lef-dependent negative regulation of p21^{Cip1/Waf} expression. The fact that Tcf711 on one hand does not have a C-clamp and on the other hand acts as a transcriptional repressor would not make it a good candidate for Tcf/Lef responsible for c-Myc expression in lens ectoderm. Therefore, the upregulation of p21, observed during early lens development in the mutants, might be simply attributed to p21 promoter de-repression caused by absence of the Tcf711. This is however an assumption that would require further experimental confirmation. Collectively, Wnt/ β -catenin driven regulation of p21^{Cip1/Waf} expression appears to be complex and context-dependent, as individual Tcf/Lefs display different potential to affect its transcription.

In summary, collective evidence point towards the fact that Tcf711 is one of the several inhibitors of Wnt/ β -catenin pathway in the anterior neural and non-neural

ectoderm, which, under physiological conditions, define a spatial border to the expansion of the NC. Similarity in the phenotypes following deficiency of individual Wnt antagonists signifies that the anterior NPB region is very close to a threshold of the NC inducing Wnt/ β -catenin activation. Therefore, from the evolutionary perspective, attenuation of the sensitivity to Wnt/ β -catenin signaling in the anterior ectoderm by fine-tuning of the expression levels of Wnt signaling inhibitors may represent a very sensitive tool that allows simultaneous modification of three prominent features of the vertebrates, the sensory placodes, the neural crest and the forebrain.

Conclusions

This thesis is focused on the involvement of Tcf711 and Wnt/ β -catenin signaling pathway during specification of the head ectoderm in mouse. The key conclusions are:

- Tcf711 is required as repressor of Wnt/ β -catenin-driven gene expression in the anterior head ectoderm.
- Tcf711 is a negative regulator of the neural crest.
- Conditional inactivation of Tcf711 in the neural plate border leads to Wnt/ β -catenin dependent expansion of the NC cell population.
- Evidence of the inductive capability of the Wnt/ β -catenin pathway on early NC development eliminates most of the ambiguity in the interpretation of previous findings about NC development in mouse and other vertebrate model organisms.
- Tcf711 proved to be indispensable for proper development of the ANF and PPR probably due to abnormal signaling from the aberrantly formed NC cells.
- Our data also provide a model, which explains the phenotypes previously acquired in mouse after de-repression of the Wnt/ β -catenin signaling pathway during early brain development.
- During lens induction Tcf711 is employed in control of proliferation and its absence leads to arrest in cell cycle progression and apoptosis.
- The balanced proliferation of the lens epithelial cells and fiber cells appears to be maintained by Tcf71-dependent negative regulation of p21^{Cip1/Waf} expression.

List of publications

Machon, O., Masek, J., Machonova, O., Krauss, S., and Kozmik, Z. (2015). Meis2 is essential for cranial and cardiac neural crest development. *BMC Dev Biol* **15**, 40.

Manuscript in revision:

Tcf711 protects the anterior neural fold from adopting the neural crest fate

Jan Mašek, Vladimír Kořínek, M. Mark Taketo, Ondřej Machoň, and Zbyněk Kozmik; submitted to the journal *Development*, currently under revision

References

- Aberle, H., Bauer, A., Stappert, J., Kispert, A., and Kemler, R.** (1997). beta-catenin is a target for the ubiquitin-proteasome pathway. *EMBO J* **16**, 3797-3804.
- Ahrens, K., and Schlosser, G.** (2005). Tissues and signals involved in the induction of placodal Six1 expression in *Xenopus laevis*. *Dev Biol* **288**, 40-59.
- Andoniadou, C.L., Signore, M., Sajedi, E., Gaston-Massuet, C., Kelberman, D., Burns, A.J., Itasaki, N., Dattani, M., and Martinez-Barbera, J.P.** (2007). Lack of the murine homeobox gene *Hesx1* leads to a posterior transformation of the anterior forebrain. *Development* **134**, 1499-1508.
- Andoniadou, C.L., Signore, M., Young, R.M., Gaston-Massuet, C., Wilson, S.W., Fuchs, E., and Martinez-Barbera, J.P.** (2011). HESX1- and TCF3-mediated repression of Wnt/beta-catenin targets is required for normal development of the anterior forebrain. *Development* **138**, 4931-4942.
- Antosova, B., Smolikova, J., Borkovcova, R., Strnad, H., Lachova, J., Machon, O., and Kozmik, Z.** (2013). Ectopic activation of Wnt/beta-catenin signaling in lens fiber cells results in cataract formation and aberrant fiber cell differentiation. *PLoS One* **8**, e78279.
- Arce, L., Yokoyama, N.N., and Waterman, M.L.** (2006). Diversity of LEF/TCF action in development and disease. *Oncogene* **25**, 7492-7504.
- Ashery-Padan, R., Marquardt, T., Zhou, X., and Gruss, P.** (2000). Pax6 activity in the lens primordium is required for lens formation and for correct placement of a single retina in the eye. *Genes Dev* **14**, 2701-2711.
- Bang, A.G., Papalopulu, N., Goulding, M.D., and Kintner, C.** (1999). Expression of Pax-3 in the lateral neural plate is dependent on a Wnt-mediated signal from posterior nonaxial mesoderm. *Dev Biol* **212**, 366-380.
- Barriga, E.H., Trainor, P.A., Bronner, M., and Mayor, R.** (2015). Animal models for studying neural crest development: is the mouse different? *Development* **142**, 1555-1560.
- Bernatik, O., Ganji, R.S., Dijksterhuis, J.P., Konik, P., Cervenka, I., Polonio, T., Krejci, P., Schulte, G., and Bryja, V.** (2011). Sequential activation and inactivation of Dishevelled in the Wnt/beta-catenin pathway by casein kinases. *J Biol Chem* **286**, 10396-10410.
- Bhat, N., Kwon, H.J., and Riley, B.B.** (2013). A gene network that coordinates preplacodal competence and neural crest specification in zebrafish. *Dev Biol* **373**, 107-117.
- Bilic, J., Huang, Y.L., Davidson, G., Zimmermann, T., Cruciat, C.M., Bienz, M., and Niehrs, C.** (2007). Wnt induces LRP6 signalosomes and promotes dishevelled-dependent LRP6 phosphorylation. *Science* **316**, 1619-1622.
- Blythe, S.A., Cha, S.W., Tadjuidje, E., Heasman, J., and Klein, P.S.** (2010). beta-Catenin primes organizer gene expression by recruiting a histone H3 arginine 8 methyltransferase, Prmt2. *Dev Cell* **19**, 220-231.
- Brack, A.S., Murphy-Seiler, F., Hanifi, J., Deka, J., Eyckerman, S., Keller, C., Aguet, M., and Rando, T.A.** (2009). BCL9 is an essential component of canonical Wnt signaling that mediates the differentiation of myogenic progenitors during muscle regeneration. *Dev Biol* **335**, 93-105.
- Brault, V., Moore, R., Kutsch, S., Ishibashi, M., Rowitch, D.H., McMahon, A.P., Sommer, L., Boussadia, O., and Kemler, R.** (2001). Inactivation of the beta-catenin gene by Wnt1-Cre-mediated deletion results in dramatic brain malformation and failure of craniofacial development. *Development* **128**, 1253-1264.
- Bryja, V., Bonilla, S., and Arenas, E.** (2006). Derivation of mouse embryonic stem cells. *Nat Protoc* **1**, 2082-2087.
- Burstyn-Cohen, T., Stanleigh, J., Sela-Donenfeld, D., and Kalcheim, C.** (2004). Canonical Wnt activity regulates trunk neural crest delamination linking BMP/noggin signaling with G1/S transition. *Development* **131**, 5327-5339.
- Cadigan, K.M., and Waterman, M.L.** (2012). TCF/LEFs and Wnt signaling in the nucleus. *Cold Spring Harb Perspect Biol* **4**.
- Carmona-Fontaine, C., Acuna, G., Ellwanger, K., Niehrs, C., and Mayor, R.** (2007). Neural crests are actively precluded from the anterior neural fold by a novel inhibitory mechanism dependent on Dickkopf1 secreted by the prechordal mesoderm. *Dev Biol* **309**, 208-221.
- Castrop, J., van Norren, K., and Clevers, H.** (1992). A gene family of HMG-box transcription factors with homology to TCF-1. *Nucleic Acids Res* **20**, 611.

- Cervenka, I., Wolf, J., Masek, J., Krejci, P., Wilcox, W.R., Kozubik, A., Schulte, G., Gutkind, J.S., and Bryja, V. (2011). Mitogen-activated protein kinases promote WNT/beta-catenin signaling via phosphorylation of LRP6. *Mol Cell Biol* **31**, 179-189.
- Chen, B., Kim, E.H., and Xu, P.X. (2009). Initiation of olfactory placode development and neurogenesis is blocked in mice lacking both Six1 and Six4. *Dev Biol* **326**, 75-85.
- Chen, J., Luo, Q., Yuan, Y., Huang, X., Cai, W., Li, C., Wei, T., Zhang, L., Yang, M., Liu, Q., et al. (2010). Pygo2 associates with MLL2 histone methyltransferase and GCN5 histone acetyltransferase complexes to augment Wnt target gene expression and breast cancer stem-like cell expansion. *Mol Cell Biol* **30**, 5621-5635.
- Cheung, M., Chaboissier, M.C., Mynett, A., Hirst, E., Schedl, A., and Briscoe, J. (2005). The transcriptional control of trunk neural crest induction, survival, and delamination. *Dev Cell* **8**, 179-192.
- Clevers, H., and Nusse, R. (2012). Wnt/beta-catenin signaling and disease. *Cell* **149**, 1192-1205.
- Cole, M.F., Johnstone, S.E., Newman, J.J., Kagey, M.H., and Young, R.A. (2008). Tcf3 is an integral component of the core regulatory circuitry of embryonic stem cells. *Genes Dev* **22**, 746-755.
- Cole, M.F., and Young, R.A. (2008). Mapping key features of transcriptional regulatory circuitry in embryonic stem cells. *Cold Spring Harb Symp Quant Biol* **73**, 183-193.
- Daksis, J.I., Lu, R.Y., Facchini, L.M., Marhin, W.W., and Penn, L.J. (1994). Myc induces cyclin D1 expression in the absence of de novo protein synthesis and links mitogen-stimulated signal transduction to the cell cycle. *Oncogene* **9**, 3635-3645.
- Danielian, P.S., Muccino, D., Rowitch, D.H., Michael, S.K., and McMahon, A.P. (1998). Modification of gene activity in mouse embryos in utero by a tamoxifen-inducible form of Cre recombinase. *Curr Biol* **8**, 1323-1326.
- Deka, J., Wiedemann, N., Anderle, P., Murphy-Seiler, F., Bultinck, J., Eyckerman, S., Stehle, J.C., Andre, S., Vilain, N., Zilian, O., et al. (2010). Bcl9/Bcl9l are critical for Wnt-mediated regulation of stem cell traits in colon epithelium and adenocarcinomas. *Cancer Res* **70**, 6619-6628.
- Dellovade, T.L., Pfaff, D.W., and Schwanzel-Fukuda, M. (1998). The gonadotropin-releasing hormone system does not develop in Small-Eye (Sey) mouse phenotype. *Brain Res Dev Brain Res* **107**, 233-240.
- Dora, N.J., Collinson, J.M., Hill, R.E., and West, J.D. (2014). Hemizygous Le-Cre transgenic mice have severe eye abnormalities on some genetic backgrounds in the absence of LoxP sites. *PLoS One* **9**, e109193.
- Dorsky, R.I., Itoh, M., Moon, R.T., and Chitnis, A. (2003). Two tcf3 genes cooperate to pattern the zebrafish brain. *Development* **130**, 1937-1947.
- Dottori, M., Gross, M.K., Labosky, P., and Goulding, M. (2001). The winged-helix transcription factor Foxd3 suppresses interneuron differentiation and promotes neural crest cell fate. *Development* **128**, 4127-4138.
- Duggan, C.D., DeMaria, S., Baudhuin, A., Stafford, D., and Ngai, J. (2008). Foxg1 is required for development of the vertebrate olfactory system. *J Neurosci* **28**, 5229-5239.
- Fossat, N., Jones, V., Garcia-Garcia, M.J., and Tam, P.P. (2012). Modulation of WNT signaling activity is key to the formation of the embryonic head. *Cell Cycle* **11**, 26-32.
- Fossat, N., Jones, V., Khoo, P.L., Bogani, D., Hardy, A., Steiner, K., Mukhopadhyay, M., Westphal, H., Nolan, P.M., Arkell, R., et al. (2011). Stringent requirement of a proper level of canonical WNT signalling activity for head formation in mouse embryo. *Development* **138**, 667-676.
- Fujimura, N., Vacik, T., Machon, O., Vlcek, C., Scalabrin, S., Speth, M., Diep, D., Krauss, S., and Kozmik, Z. (2007). Wnt-mediated down-regulation of Sp1 target genes by a transcriptional repressor Sp5. *J Biol Chem* **282**, 1225-1237.
- Galceran, J., Farinas, I., Depew, M.J., Clevers, H., and Grosschedl, R. (1999). Wnt3a^{-/-}-like phenotype and limb deficiency in Lef1^(-/-)Tcf1^(-/-) mice. *Genes Dev* **13**, 709-717.
- Garcia-Castro, M.I., Marcelle, C., and Bronner-Fraser, M. (2002). Ectodermal Wnt function as a neural crest inducer. *Science* **297**, 848-851.
- Garnett, A.T., Square, T.A., and Medeiros, D.M. (2012). BMP, Wnt and FGF signals are integrated through evolutionarily conserved enhancers to achieve robust expression of Pax3 and Zic genes at the zebrafish neural plate border. *Development* **139**, 4220-4231.
- Gartel, A.L., Ye, X., Goufman, E., Shianov, P., Hay, N., Najmabadi, F., and Tyner, A.L. (2001). Myc represses the p21(WAF1/CIP1) promoter and interacts with Sp1/Sp3. *Proc Natl Acad Sci U S A* **98**, 4510-4515.

- Gaston-Massuet, C., McCabe, M.J., Scagliotti, V., Young, R.M., Carreno, G., Gregory, L.C., Jayakody, S.A., Pozzi, S., Gualtieri, A., Basu, B., et al.** (2016). Transcription factor 7-like 1 is involved in hypothalamo-pituitary axis development in mice and humans. *Proc Natl Acad Sci U S A*.
- Gay, M.H., Valenta, T., Herr, P., Paratore-Hari, L., Basler, K., and Sommer, L.** (2015). Distinct adhesion-independent functions of beta-catenin control stage-specific sensory neurogenesis and proliferation. *BMC Biol* **13**, 24.
- Gregorieff, A., Grosschedl, R., and Clevers, H.** (2004). Hindgut defects and transformation of the gastro-intestinal tract in Tcf4(-)/Tcf1(-) embryos. *EMBO J* **23**, 1825-1833.
- Grindley, J.C., Davidson, D.R., and Hill, R.E.** (1995). The role of Pax-6 in eye and nasal development. *Development* **121**, 1433-1442.
- Grocott, T., Johnson, S., Bailey, A.P., and Streit, A.** (2011). Neural crest cells organize the eye via TGF-beta and canonical Wnt signalling. *Nat Commun* **2**, 265.
- Grocott, T., Tambalo, M., and Streit, A.** (2012). The peripheral sensory nervous system in the vertebrate head: a gene regulatory perspective. *Dev Biol* **370**, 3-23.
- Groves, A.K., and LaBonne, C.** (2014). Setting appropriate boundaries: fate, patterning and competence at the neural plate border. *Dev Biol* **389**, 2-12.
- Hanashima, C., Li, S.C., Shen, L., Lai, E., and Fishell, G.** (2004). Foxg1 suppresses early cortical cell fate. *Science* **303**, 56-59.
- Harada, N., Tamai, Y., Ishikawa, T., Sauer, B., Takaku, K., Oshima, M., and Taketo, M.M.** (1999). Intestinal polyposis in mice with a dominant stable mutation of the beta-catenin gene. *EMBO J* **18**, 5931-5942.
- Heeg-Truesdell, E., and LaBonne, C.** (2006). Neural induction in *Xenopus* requires inhibition of Wnt-beta-catenin signaling. *Dev Biol* **298**, 71-86.
- Hogan, B.L., Horsburgh, G., Cohen, J., Hetherington, C.M., Fisher, G., and Lyon, M.F.** (1986). Small eyes (Sey): a homozygous lethal mutation on chromosome 2 which affects the differentiation of both lens and nasal placodes in the mouse. *Journal of embryology and experimental morphology* **97**, 95-110.
- Holland, J.D., Klaus, A., Garratt, A.N., and Birchmeier, W.** (2013). Wnt signaling in stem and cancer stem cells. *Curr Opin Cell Biol* **25**, 254-264.
- Hong, C.S., and Saint-Jeannet, J.P.** (2007). The activity of Pax3 and Zic1 regulates three distinct cell fates at the neural plate border. *Mol Biol Cell* **18**, 2192-2202.
- Hoverter, N.P., Ting, J.H., Sundaresh, S., Baldi, P., and Waterman, M.L.** (2012). A WNT/p21 circuit directed by the C-clamp, a sequence-specific DNA binding domain in TCFs. *Mol Cell Biol* **32**, 3648-3662.
- Hoverter, N.P., and Waterman, M.L.** (2008). A Wnt-fall for gene regulation: repression. *Sci Signal* **1**, pe43.
- Hsu, S.C., Galceran, J., and Grosschedl, R.** (1998). Modulation of transcriptional regulation by LEF-1 in response to Wnt-1 signaling and association with beta-catenin. *Mol Cell Biol* **18**, 4807-4818.
- Ikeda, S., Kishida, S., Yamamoto, H., Murai, H., Koyama, S., and Kikuchi, A.** (1998). Axin, a negative regulator of the Wnt signaling pathway, forms a complex with GSK-3beta and beta-catenin and promotes GSK-3beta-dependent phosphorylation of beta-catenin. *EMBO J* **17**, 1371-1384.
- Ikeya, M., Lee, S.M., Johnson, J.E., McMahon, A.P., and Takada, S.** (1997). Wnt signalling required for expansion of neural crest and CNS progenitors. *Nature* **389**, 966-970.
- Janssens, S., Van Den Broek, O., Davenport, I.R., Akkers, R.C., Liu, F., Veenstra, G.J., Hoppler, S., Vleminckx, K., and Destree, O.** (2013). The Wnt signaling mediator tcf1 is required for expression of foxd3 during *Xenopus* gastrulation. *Int J Dev Biol* **57**, 49-54.
- Jung, Y.S., Qian, Y., and Chen, X.** (2010). Examination of the expanding pathways for the regulation of p21 expression and activity. *Cell Signal* **22**, 1003-1012.
- Kawano, Y., and Kypta, R.** (2003). Secreted antagonists of the Wnt signalling pathway. *J Cell Sci* **116**, 2627-2634.
- Kiecker, C., and Niehrs, C.** (2001). A morphogen gradient of Wnt/beta-catenin signalling regulates anteroposterior neural patterning in *Xenopus*. *Development* **128**, 4189-4201.
- Kim, C.H., Oda, T., Itoh, M., Jiang, D., Artinger, K.B., Chandrasekharappa, S.C., Driever, W., and Chitnis, A.B.** (2000). Repressor activity of Headless/Tcf3 is essential for vertebrate head formation. *Nature* **407**, 913-916.
- Kim, S.E., Huang, H., Zhao, M., Zhang, X., Zhang, A., Semonov, M.V., MacDonald, B.T., Zhang, X., Garcia Abreu, J., Peng, L., et al.** (2013). Wnt stabilization of beta-catenin reveals principles for morphogen receptor-scaffold assemblies. *Science* **340**, 867-870.

- Kioussi, C., Briata, P., Baek, S.H., Rose, D.W., Hamblet, N.S., Herman, T., Ohgi, K.A., Lin, C., Gleiberman, A., Wang, J., *et al.* (2002). Identification of a Wnt/Dvl/beta-Catenin --> Pitx2 pathway mediating cell-type-specific proliferation during development. *Cell* **111**, 673-685.
- Kitagawa, M., Hatakeyama, S., Shirane, M., Matsumoto, M., Ishida, N., Hattori, K., Nakamichi, I., Kikuchi, A., Nakayama, K., and Nakayama, K. (1999). An F-box protein, FWD1, mediates ubiquitin-dependent proteolysis of beta-catenin. *EMBO J* **18**, 2401-2410.
- Kleber, M., Lee, H.Y., Wurdak, H., Buchstaller, J., Riccomagno, M.M., Ittner, L.M., Suter, U., Epstein, D.J., and Sommer, L. (2005). Neural crest stem cell maintenance by combinatorial Wnt and BMP signaling. *J Cell Biol* **169**, 309-320.
- Klimova, L., Lachova, J., Machon, O., Sedlacek, R., and Kozmik, Z. (2013). Generation of mRx-Cre transgenic mouse line for efficient conditional gene deletion in early retinal progenitors. *PLoS One* **8**, e63029.
- Korinek, V., Barker, N., Morin, P.J., van Wichen, D., de Weger, R., Kinzler, K.W., Vogelstein, B., and Clevers, H. (1997). Constitutive transcriptional activation by a beta-catenin-Tcf complex in APC^{-/-} colon carcinoma. *Science* **275**, 1784-1787.
- Korinek, V., Barker, N., Willert, K., Molenaar, M., Roose, J., Wagenaar, G., Markman, M., Lamers, W., Destree, O., and Clevers, H. (1998). Two members of the Tcf family implicated in Wnt/beta-catenin signaling during embryogenesis in the mouse. *Mol Cell Biol* **18**, 1248-1256.
- Kramps, T., Peter, O., Brunner, E., Nellen, D., Froesch, B., Chatterjee, S., Murone, M., Zullig, S., and Basler, K. (2002). Wnt/wingless signaling requires BCL9/legless-mediated recruitment of pygopus to the nuclear beta-catenin-TCF complex. *Cell* **109**, 47-60.
- Kratochwil, K., Galceran, J., Tontsch, S., Roth, W., and Grosschedl, R. (2002). FGf4, a direct target of LEF1 and Wnt signaling, can rescue the arrest of tooth organogenesis in Lef1^(-/-) mice. *Genes Dev* **16**, 3173-3185.
- Krausova, M., and Korinek, V. (2013). Wnt signaling in adult intestinal stem cells and cancer. *Cell Signal* **26**, 570-579.
- Kreslova, J., Machon, O., Ruzickova, J., Lachova, J., Wawrousek, E.F., Kemler, R., Krauss, S., Piatigorsky, J., and Kozmik, Z. (2007). Abnormal lens morphogenesis and ectopic lens formation in the absence of beta-catenin function. *Genesis* **45**, 157-168.
- Kwon, H.J., Bhat, N., Sweet, E.M., Cornell, R.A., and Riley, B.B. (2010). Identification of early requirements for preplacodal ectoderm and sensory organ development. *PLoS Genet* **6**, e1001133.
- Lagutin, O.V., Zhu, C.C., Kobayashi, D., Topczewski, J., Shimamura, K., Puelles, L., Russell, H.R., McKinnon, P.J., Solnica-Krezel, L., and Oliver, G. (2003). Six3 repression of Wnt signaling in the anterior neuroectoderm is essential for vertebrate forebrain development. *Genes Dev* **17**, 368-379.
- Lee, H.Y., Kleber, M., Hari, L., Brault, V., Suter, U., Taketo, M.M., Kemler, R., and Sommer, L. (2004). Instructive role of Wnt/beta-catenin in sensory fate specification in neural crest stem cells. *Science* **303**, 1020-1023.
- Lewis, A.E., Vasudevan, H.N., O'Neill, A.K., Soriano, P., and Bush, J.O. (2013). The widely used Wnt1-Cre transgene causes developmental phenotypes by ectopic activation of Wnt signaling. *Dev Biol* **379**, 229-234.
- Li, B., Kuriyama, S., Moreno, M., and Mayor, R. (2009). The posteriorizing gene Gbx2 is a direct target of Wnt signalling and the earliest factor in neural crest induction. *Development* **136**, 3267-3278.
- Litsiou, A., Hanson, S., and Streit, A. (2005). A balance of FGF, BMP and WNT signalling positions the future placode territory in the head. *Development* **132**, 4051-4062.
- Liu, F., van den Broek, O., Destree, O., and Hoppler, S. (2005). Distinct roles for Xenopus Tcf/Lef genes in mediating specific responses to Wnt/beta-catenin signalling in mesoderm development. *Development* **132**, 5375-5385.
- Liu, J.A., Wu, M.H., Yan, C.H., Chau, B.K., So, H., Ng, A., Chan, A., Cheah, K.S., Briscoe, J., and Cheung, M. (2013). Phosphorylation of Sox9 is required for neural crest delamination and is regulated downstream of BMP and canonical Wnt signaling. *Proc Natl Acad Sci U S A* **110**, 2882-2887.
- Liu, W., Lagutin, O.V., Mende, M., Streit, A., and Oliver, G. (2006). Six3 activation of Pax6 expression is essential for mammalian lens induction and specification. *EMBO J* **25**, 5383-5395.
- Luo, W., Peterson, A., Garcia, B.A., Coombs, G., Kofahl, B., Heinrich, R., Shabanowitz, J., Hunt, D.F., Yost, H.J., and Virshup, D.M. (2007). Protein phosphatase 1 regulates assembly and function of the beta-catenin degradation complex. *EMBO J* **26**, 1511-1521.

- Macatee, T.L., Hammond, B.P., Arenkiel, B.R., Francis, L., Frank, D.U., and Moon, A.M.** (2003). Ablation of specific expression domains reveals discrete functions of ectoderm- and endoderm-derived FGF8 during cardiovascular and pharyngeal development. *Development* **130**, 6361-6374.
- Machon, O., Kreslova, J., Ruzickova, J., Vacik, T., Klimova, L., Fujimura, N., Lachova, J., and Kozmik, Z.** (2010). Lens morphogenesis is dependent on Pax6-mediated inhibition of the canonical Wnt/beta-catenin signaling in the lens surface ectoderm. *Genesis* **48**, 86-95.
- Mao, B., Wu, W., Li, Y., Hoppe, D., Stanek, P., Glinka, A., and Niehrs, C.** (2001). LDL-receptor-related protein 6 is a receptor for Dickkopf proteins. *Nature* **411**, 321-325.
- Maretto, S., Cordenonsi, M., Dupont, S., Braghetta, P., Broccoli, V., Hassan, A.B., Volpin, D., Bressan, G.M., and Piccolo, S.** (2003). Mapping Wnt/beta-catenin signaling during mouse development and in colorectal tumors. *Proc Natl Acad Sci U S A* **100**, 3299-3304.
- Martinez, G., Wijesinghe, M., Turner, K., Abud, H.E., Taketo, M.M., Noda, T., Robinson, M.L., and de longh, R.U.** (2009). Conditional mutations of beta-catenin and APC reveal roles for canonical Wnt signaling in lens differentiation. *Invest Ophthalmol Vis Sci* **50**, 4794-4806.
- McMahon, A.P., and Bradley, A.** (1990). The Wnt-1 (int-1) proto-oncogene is required for development of a large region of the mouse brain. *Cell* **62**, 1073-1085.
- Merrill, B.J., Pasolli, H.A., Polak, L., Rendl, M., Garcia-Garcia, M.J., Anderson, K.V., and Fuchs, E.** (2004). Tcf3: a transcriptional regulator of axis induction in the early embryo. *Development* **131**, 263-274.
- Meyers, E.N., Lewandoski, M., and Martin, G.R.** (1998). An Fgf8 mutant allelic series generated by Cre- and Flp-mediated recombination. *Nat Genet* **18**, 136-141.
- Monaghan, A.P., Kioschis, P., Wu, W., Zuniga, A., Bock, D., Poustka, A., Delius, H., and Niehrs, C.** (1999). Dickkopf genes are co-ordinately expressed in mesodermal lineages. *Mech Dev* **87**, 45-56.
- Mosimann, C., Hausmann, G., and Basler, K.** (2009). Beta-catenin hits chromatin: regulation of Wnt target gene activation. *Nat Rev Mol Cell Biol* **10**, 276-286.
- Mukhopadhyay, M., Shtrom, S., Rodriguez-Esteban, C., Chen, L., Tsukui, T., Gomer, L., Dorward, D.W., Glinka, A., Grinberg, A., Huang, S.P., et al.** (2001). Dickkopf1 is required for embryonic head induction and limb morphogenesis in the mouse. *Dev Cell* **1**, 423-434.
- Nguyen, H., Merrill, B.J., Polak, L., Nikolova, M., Rendl, M., Shaver, T.M., Pasolli, H.A., and Fuchs, E.** (2009). Tcf3 and Tcf4 are essential for long-term homeostasis of skin epithelia. *Nat Genet* **41**, 1068-1075.
- Niehrs, C., and Acebron, S.P.** (2012). Mitotic and mitogenic Wnt signalling. *EMBO J* **31**, 2705-2713.
- Nusse, R., and Varmus, H.E.** (1982). Many tumors induced by the mouse mammary tumor virus contain a provirus integrated in the same region of the host genome. *Cell* **31**, 99-109.
- Ohyama, T., Mohamed, O.A., Taketo, M.M., Dufort, D., and Groves, A.K.** (2006). Wnt signals mediate a fate decision between otic placode and epidermis. *Development* **133**, 865-875.
- Ombrato, L., Lluís, F., and Cosma, M.P.** (2012). Regulation of self-renewal and reprogramming by TCF factors. *Cell Cycle* **11**, 39-47.
- Park, D.S., Seo, J.H., Hong, M., Bang, W., Han, J.K., and Choi, S.C.** (2013). Role of Sp5 as an essential early regulator of neural crest specification in xenopus. *Dev Dyn* **242**, 1382-1394.
- Parker, D.S., Jemison, J., and Cadigan, K.M.** (2002). Pygopus, a nuclear PHD-finger protein required for Wingless signaling in Drosophila. *Development* **129**, 2565-2576.
- Parker, D.S., Ni, Y.Y., Chang, J.L., Li, J., and Cadigan, K.M.** (2008). Wingless signaling induces widespread chromatin remodeling of target loci. *Mol Cell Biol* **28**, 1815-1828.
- Pereira, L., Yi, F., and Merrill, B.J.** (2006). Repression of Nanog gene transcription by Tcf3 limits embryonic stem cell self-renewal. *Mol Cell Biol* **26**, 7479-7491.
- Petersen, C.P., and Reddien, P.W.** (2009). Wnt signaling and the polarity of the primary body axis. *Cell* **139**, 1056-1068.
- Pieper, M., Ahrens, K., Rink, E., Peter, A., and Schlosser, G.** (2012). Differential distribution of competence for panplacodal and neural crest induction to non-neural and neural ectoderm. *Development* **139**, 1175-1187.
- Popperl, H., Schmidt, C., Wilson, V., Hume, C.R., Dodd, J., Krumlauf, R., and Beddington, R.S.** (1997). Misexpression of Cwnt8C in the mouse induces an ectopic embryonic axis and causes a truncation of the anterior neuroectoderm. *Development* **124**, 2997-3005.
- Purcell, P., Oliver, G., Mardon, G., Donner, A.L., and Maas, R.L.** (2005). Pax6-dependence of Six3, Eya1 and Dach1 expression during lens and nasal placode induction. *Gene Expr Patterns* **6**, 110-118.

- Reya, T., O'Riordan, M., Okamura, R., Devaney, E., Willert, K., Nusse, R., and Grosschedl, R. (2000). Wnt signaling regulates B lymphocyte proliferation through a LEF-1 dependent mechanism. *Immunity* **13**, 15-24.
- Rodriguez, C.I., Buchholz, F., Galloway, J., Sequerra, R., Kasper, J., Ayala, R., Stewart, A.F., and Dymecki, S.M. (2000). High-efficiency deleter mice show that FLPe is an alternative to Cre-loxP. *Nat Genet* **25**, 139-140.
- Roose, J., and Clevers, H. (1999). TCF transcription factors: molecular switches in carcinogenesis. *Biochim Biophys Acta* **1424**, M23-37.
- Roose, J., Molenaar, M., Peterson, J., Hurenkamp, J., Brantjes, H., Moerer, P., van de Wetering, M., Destree, O., and Clevers, H. (1998). The Xenopus Wnt effector XTcf-3 interacts with Groucho-related transcriptional repressors. *Nature* **395**, 608-612.
- Rubinfeld, R.S., and Martin, N.F. (1993). Meibomian gland function and giant papillary conjunctivitis. *American journal of ophthalmology* **115**, 120-121.
- Saint-Jeannet, J.P., He, X., Varmus, H.E., and Dawid, I.B. (1997). Regulation of dorsal fate in the neuraxis by Wnt-1 and Wnt-3a. *Proc Natl Acad Sci U S A* **94**, 13713-13718.
- Saint-Jeannet, J.P., and Moody, S.A. (2014). Establishing the pre-placodal region and breaking it into placodes with distinct identities. *Dev Biol* **389**, 13-27.
- Sakai, D., Tanaka, Y., Endo, Y., Osumi, N., Okamoto, H., and Wakamatsu, Y. (2005). Regulation of Slug transcription in embryonic ectoderm by beta-catenin-Lef/Tcf and BMP-Smad signaling. *Dev Growth Differ* **47**, 471-482.
- Sandell, L.L., Butler Tjaden, N.E., Barlow, A.J., and Trainor, P.A. (2014). Cochleovestibular nerve development is integrated with migratory neural crest cells. *Dev Biol* **385**, 200-210.
- Satoh, K., Kasai, M., Ishida, T., Tago, K., Ohwada, S., Hasegawa, Y., Senda, T., Takada, S., Nada, S., Nakamura, T., et al. (2004). Anteriorization of neural fate by inhibitor of beta-catenin and T cell factor (ICAT), a negative regulator of Wnt signaling. *Proc Natl Acad Sci U S A* **101**, 8017-8021.
- Schlosser, G., and Ahrens, K. (2004). Molecular anatomy of placode development in *Xenopus laevis*. *Dev Biol* **271**, 439-466.
- Schwab, K.R., Patterson, L.T., Hartman, H.A., Song, N., Lang, R.A., Lin, X., and Potter, S.S. (2007). Pygo1 and Pygo2 roles in Wnt signaling in mammalian kidney development. *BMC Biol* **5**, 15.
- Schweizer, L., and Varmus, H. (2003). Wnt/Wingless signaling through beta-catenin requires the function of both LRP/Arrow and frizzled classes of receptors. *BMC Cell Biol* **4**, 4.
- Semenov, M.V., Tamai, K., Brott, B.K., Kuhl, M., Sokol, S., and He, X. (2001). Head inducer Dickkopf-1 is a ligand for Wnt coreceptor LRP6. *Curr Biol* **11**, 951-961.
- Shimizu, T., Bae, Y.K., Muraoka, O., and Hibi, M. (2005). Interaction of Wnt and caudal-related genes in zebrafish posterior body formation. *Dev Biol* **279**, 125-141.
- Shy, B.R., Wu, C.I., Khramtsova, G.F., Zhang, J.Y., Olopade, O.I., Goss, K.H., and Merrill, B.J. (2013). Regulation of Tcf7l1 DNA binding and protein stability as principal mechanisms of Wnt/beta-catenin signaling. *Cell Rep* **4**, 1-9.
- Siegfried, E., Wilder, E.L., and Perrimon, N. (1994). Components of wingless signalling in *Drosophila*. *Nature* **367**, 76-80.
- Sierra, J., Yoshida, T., Joazeiro, C.A., and Jones, K.A. (2006). The APC tumor suppressor counteracts beta-catenin activation and H3K4 methylation at Wnt target genes. *Genes Dev* **20**, 586-600.
- Simoës-Costa, M., and Bronner, M.E. (2015). Establishing neural crest identity: a gene regulatory recipe. *Development* **142**, 242-257.
- Simoës-Costa, M., Stone, M., and Bronner, M.E. (2015). Axud1 Integrates Wnt Signaling and Transcriptional Inputs to Drive Neural Crest Formation. *Dev Cell* **34**, 544-554.
- Smith, A.N., Miller, L.A., Song, N., Taketo, M.M., and Lang, R.A. (2005). The duality of beta-catenin function: a requirement in lens morphogenesis and signaling suppression of lens fate in periocular ectoderm. *Dev Biol* **285**, 477-489.
- Srivastava, M., Begovic, E., Chapman, J., Putnam, N.H., Hellsten, U., Kawashima, T., Kuo, A., Mitros, T., Salamov, A., Carpenter, M.L., et al. (2008). The Trichoplax genome and the nature of placozoans. *Nature* **454**, 955-960.
- Steventon, B., Araya, C., Linker, C., Kuriyama, S., and Mayor, R. (2009). Differential requirements of BMP and Wnt signalling during gastrulation and neurulation define two steps in neural crest induction. *Development* **136**, 771-779.
- Steventon, B., Mayor, R., and Streit, A. (2012). Mutual repression between Gbx2 and Otx2 in sensory placodes reveals a general mechanism for ectodermal patterning. *Dev Biol* **367**, 55-65.

- Tago, K., Nakamura, T., Nishita, M., Hyodo, J., Nagai, S., Murata, Y., Adachi, S., Ohwada, S., Morishita, Y., Shibuya, H., et al.** (2000). Inhibition of Wnt signaling by ICAT, a novel beta-catenin-interacting protein. *Genes Dev* **14**, 1741-1749.
- Tam, W.L., Lim, C.Y., Han, J., Zhang, J., Ang, Y.S., Ng, H.H., Yang, H., and Lim, B.** (2008). T-cell factor 3 regulates embryonic stem cell pluripotency and self-renewal by the transcriptional control of multiple lineage pathways. *Stem Cells* **26**, 2019-2031.
- Taneyhill, L.A., and Bronner-Fraser, M.** (2005). Dynamic alterations in gene expression after Wnt-mediated induction of avian neural crest. *Mol Biol Cell* **16**, 5283-5293.
- Tang, W., Dodge, M., Gundapaneni, D., Michnoff, C., Roth, M., and Lum, L.** (2008). A genome-wide RNAi screen for Wnt/beta-catenin pathway components identifies unexpected roles for TCF transcription factors in cancer. *Proc Natl Acad Sci U S A* **105**, 9697-9702.
- Teo, J.L., and Kahn, M.** (2010). The Wnt signaling pathway in cellular proliferation and differentiation: A tale of two coactivators. *Adv Drug Deliv Rev* **62**, 1149-1155.
- Thomas, K.R., and Capecchi, M.R.** (1990). Targeted disruption of the murine int-1 proto-oncogene resulting in severe abnormalities in midbrain and cerebellar development. *Nature* **346**, 847-850.
- Thompson, B., Townsley, F., Rosin-Arbesfeld, R., Musisi, H., and Bienz, M.** (2002). A new nuclear component of the Wnt signalling pathway. *Nat Cell Biol* **4**, 367-373.
- Travis, A., Amsterdam, A., Belanger, C., and Grosschedl, R.** (1991). LEF-1, a gene encoding a lymphoid-specific protein with an HMG domain, regulates T-cell receptor alpha enhancer function [corrected]. *Genes Dev* **5**, 880-894.
- Vallin, J., Thuret, R., Giacomello, E., Faraldo, M.M., Thiery, J.P., and Broders, F.** (2001). Cloning and characterization of three *Xenopus* slug promoters reveal direct regulation by Lef/beta-catenin signaling. *J Biol Chem* **276**, 30350-30358.
- van de Wetering, M., Cavallo, R., Dooijes, D., van Beest, M., van Es, J., Loureiro, J., Ypma, A., Hursh, D., Jones, T., Bejsovec, A., et al.** (1997). Armadillo coactivates transcription driven by the product of the *Drosophila* segment polarity gene dTCF. *Cell* **88**, 789-799.
- van de Wetering, M., Oosterwegel, M., Dooijes, D., and Clevers, H.** (1991). Identification and cloning of TCF-1, a T lymphocyte-specific transcription factor containing a sequence-specific HMG box. *EMBO J* **10**, 123-132.
- van de Wetering, M., Sancho, E., Verweij, C., de Lau, W., Oving, I., Hurlstone, A., van der Horn, K., Batlle, E., Coudreuse, D., Haramis, A.P., et al.** (2002). The beta-catenin/TCF-4 complex imposes a crypt progenitor phenotype on colorectal cancer cells. *Cell* **111**, 241-250.
- Wu, C.I., Hoffman, J.A., Shy, B.R., Ford, E.M., Fuchs, E., Nguyen, H., and Merrill, B.J.** (2012). Function of Wnt/beta-catenin in counteracting Tcf3 repression through the Tcf3-beta-catenin interaction. *Development* **139**, 2118-2129.
- Wu, J., Yang, J., and Klein, P.S.** (2005). Neural crest induction by the canonical Wnt pathway can be dissociated from anterior-posterior neural patterning in *Xenopus*. *Dev Biol* **279**, 220-232.
- Yi, F., Pereira, L., and Merrill, B.J.** (2008). Tcf3 functions as a steady-state limiter of transcriptional programs of mouse embryonic stem cell self-renewal. *Stem Cells* **26**, 1951-1960.
- Zhao, H., Yang, Y., Rizo, C.M., Overbeek, P.A., and Robinson, M.L.** (2004). Insertion of a Pax6 consensus binding site into the alphaA-crystallin promoter acts as a lens epithelial cell enhancer in transgenic mice. *Invest Ophthalmol Vis Sci* **45**, 1930-1939.
- Zhao, T., Gan, Q., Stokes, A., Lassiter, R.N., Wang, Y., Chan, J., Han, J.X., Pleasure, D.E., Epstein, J.A., and Zhou, C.J.** (2014). beta-catenin regulates Pax3 and Cdx2 for caudal neural tube closure and elongation. *Development* **141**, 148-157.

Appendix

Machon et al. *BMC Developmental Biology* (2015) 15:40
DOI 10.1186/s12861-015-0093-6



RESEARCH ARTICLE

Open Access

Meis2 is essential for cranial and cardiac neural crest development



Ondrej Machon^{1*}, Jan Masek¹, Olga Machonova¹, Stefan Krauss² and Zbynek Kozmik¹

Abstract

Background: TALE-class homeodomain transcription factors Meis and Pbx play important roles in formation of the embryonic brain, eye, heart, cartilage or hematopoiesis. Loss-of-function studies of Pbx1, 2 and 3 and Meis1 documented specific functions in embryogenesis, however, functional studies of Meis2 in mouse are still missing. We have generated a conditional allele of Meis2 in mice and shown that systemic inactivation of the Meis2 gene results in lethality by the embryonic day 14 that is accompanied with hemorrhaging.

Results: We show that neural crest cells express Meis2 and Meis2-deficient embryos display defects in tissues that are derived from the neural crest, such as an abnormal heart outflow tract with the persistent truncus arteriosus and abnormal cranial nerves. The importance of Meis2 for neural crest cells is further confirmed by means of conditional inactivation of Meis2 using crest-specific AP2 α -IRES-Cre mouse. Conditional mutants display perturbed development of the craniofacial skeleton with severe anomalies in cranial bones and cartilages, heart and cranial nerve abnormalities.

Conclusions: Meis2-null mice are embryonic lethal. Our results reveal a critical role of Meis2 during cranial and cardiac neural crest cells development in mouse.

Keywords: Meis2, Neural crest, Persistent truncus arteriosus, Craniofacial skeleton, Cranial nerves

Background

Neural crest cells (NCC) represent a multi-potent embryonic cell population that generates a very diverse range of cell types including cranial nerves, neurons and glia of the peripheral nervous system, enteric neurons, melanocytes, cranial bones and cartilages [1, 2]. The first NCC appear at the neurula stage in the neural plate border region. As the neural tube closes in mouse, NCC delaminate from the regions of neural plate border and ectomesenchyme after epithelial-to-mesenchymal transition (EMT) and migrate to various developing organs. The very broad differentiation potential of NCC provides a complex model of cell type specification and migration and the gene regulatory network determining the spatio-temporal control of NCC diversification has been extensively studied. For instance, the NCC population is specified by the set of transcription factors Sox9, Sox10, FoxD3, Snai2 together with Msx1, Pax3/7 or Zic1 in the

neural plate border [3]. These effector genes are regulated by coordinated action of signaling pathways such as Wnt, Bmp and Fgf from the adjacent paraxial mesoderm and non-neural ectoderm [2, 4]. The differentiation potential of NCC is spatially determined by their position along the rostrocaudal axis. In a simplified view, cranial NCC coming from mesencephalic and rhombencephalic regions generate head bones, cartilages, cranial nerves and selected connective tissues [5, 6]. Vagal NCC from the area of somites 1-7 are destined to the enteric nervous system. Cardiac NCC (somites 1-4) are involved in septation of the cardiac outflow tract [7] and trunk NCC form sensory and sympathetic ganglia. The current debate, however, favors the scenario proposing that originally multi-potent NCC stem cells are exposed to different environmental cues along the rostrocaudal axis that spatiotemporally restrict their differentiation potential [1, 8].

Meis proteins are transcription factors that are orthologous to the *Drosophila* homothorax (Hth) protein. They contain a TALE (three-amino-acid loop extension) sub-class of the homeodomain that binds to DNA. In

* Correspondence: machon@img.cas.cz

¹Institute of Molecular Genetics, The Czech Academy of Sciences, 14200 Praha, Czech Republic
Full list of author information is available at the end of the article



© 2015 Machon et al. **Open Access** This article is distributed under the terms of the Creative Commons Attribution 4.0 International License (<http://creativecommons.org/licenses/by/4.0/>), which permits unrestricted use, distribution, and reproduction in any medium, provided you give appropriate credit to the original author(s) and the source, provide a link to the Creative Commons license, and indicate if changes were made. The Creative Commons Public Domain Dedication waiver (<http://creativecommons.org/publicdomain/zero/1.0/>) applies to the data made available in this article, unless otherwise stated.

humans and mice, three homologues Meis1, Meis2 and Meis3 have been identified [9] and it has been shown that they directly bind to Pbx proteins [10–12]. The Meis/Pbx protein complex binds to DNA through respective Meis- and Pbx-consensus binding sites thereby regulating transcription. The Meis/Pbx complex plays important roles during development of several organs including limbs [13, 14], heart [15, 16], lens [17], pancreas [18] and hindbrain [19–22]. Hox genes are among the target genes of Meis-Pbx control via modulation of histone acetylation indicating recruitment of Hox proteins as cofactors of Meis-Pbx complex [23, 24].

Mice lacking Meis1 display liver hypoplasia, hemorrhage, impaired erythropoiesis and eye defects, and die by the embryonic day (E) 14.5 [25, 26]. Although a substantial amount of data have been reported on the role of Meis1 in organogenesis, hematopoiesis and leukemia induction, the function of the other homologs, Meis2 and Meis3, is much less clear. Chicken Meis2 has a specific role in determining cell fate in the midbrain-hindbrain boundary by controlling the expression of *Otx2* [22] and it also affects proliferation of retinal progenitor cells [27]. Several recent reports in various model systems indicated that Meis2 may play a role in neural crest cells. Meis2 was identified as one of the key transcription factors in the gene regulatory network driving differentiation of human embryonic stem cells towards cardiovascular cell types, and this was further confirmed by knock-down experiments in zebrafish [16]. Morpholino-based screens in zebrafish revealed the importance of Meis1 and Meis2 factors during craniofacial development [28]. Moreover, gene expression analysis of EMT in endocardial cushions identified Meis2 among enriched genes [29]. In this context it is very interesting that some human disorders displaying cleft palate and heart developmental defects have been linked to mutations in the Meis2 locus [30–33]. Nonetheless, a clear picture of the Meis2 function based on a genetic mouse model is still missing.

In the present study, we examined the role of Meis2 during embryogenesis by generating conditional knock-out mice. We studied morphological defects after either zygotic inactivation of the Meis2 allele or NCC-specific conditional knock-out using AP2 α -IRES-Cre. We conclude that hemorrhaging most probably causes embryonic lethality. Further, many embryonic defects in the tissues derived from neural crest in systemic Meis2-nulls were recapitulated upon conditional deletion of Meis2 in NCC suggesting an indispensable role of Meis2 in NCC.

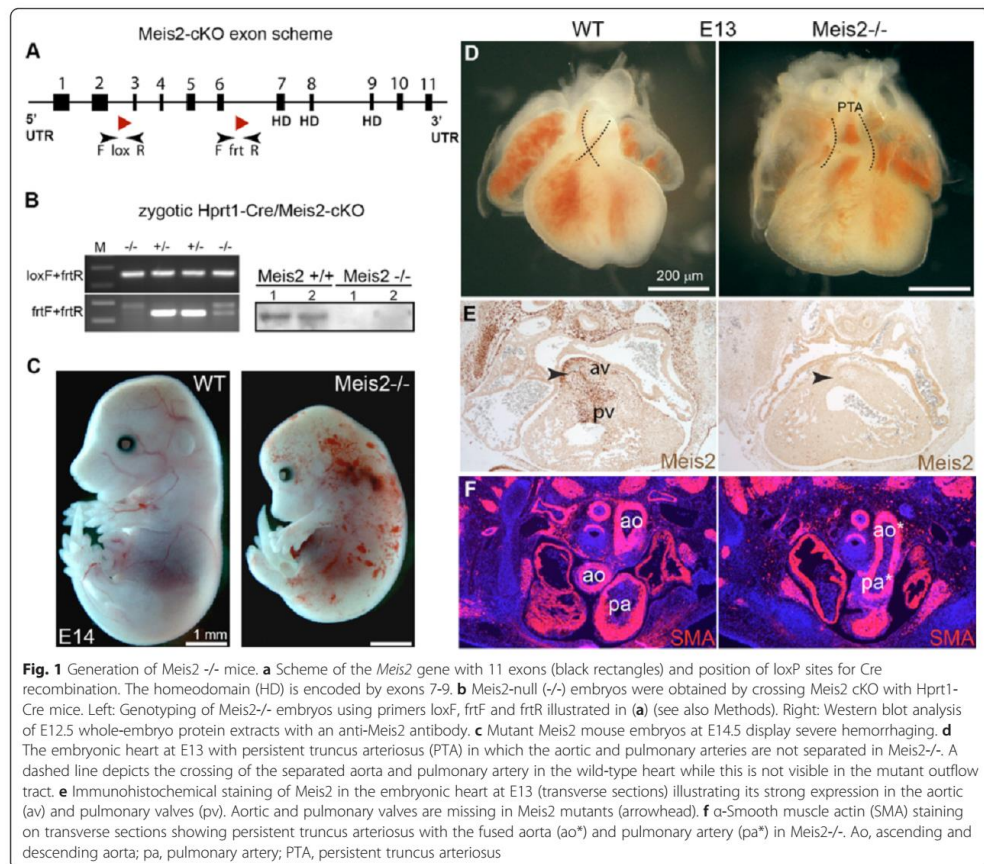
Results

Meis2^{-/-} embryos are lethal and display hemorrhaging

A conditional mutant allele of the *Meis2* gene (Meis2 cKO) was created by inserting LoxP sites in the introns

2 and 6 that flank exons 3 and 6 in the *Meis2* gene (Fig. 1a). To generate mutant mice lacking functional Meis2 in the whole organism, Meis2 cKO were at first crossed with the Hprt1-Cre mice (Jax Mice and Services) that exert a zygotic expression of Cre recombinase facilitating gene excision in all tissues. The first generation mice, which were heterozygous for the Meis2 gene (Meis2^{+/-}), were intercrossed to obtain Meis2-null (Meis2^{-/-}) animals. Animals were genotyped using primers flanking loxP sites as depicted in Fig. 1a. The loss of exons 3–6 in Meis2^{-/-} embryos was tested by PCR (Fig. 1a, left). The absence of Meis2 protein was verified using Western blot analysis of protein extracts from E12.5 embryos (Fig. 1b, right). Meis2^{-/-} mice displayed embryonic lethality between E13.5–E14.5 and suffered from hemorrhaging (Fig. 1c). The size of mutant embryos was smaller at E14.5 as mutant embryos stopped growing approximately at E13.5 when hemorrhaging became prominent. Although the severity of this phenotype varied among Meis2^{-/-} (n = 29 litters, 51 mutants), all mutants displayed bleeding and a small liver size (Additional file 1: Figure S1B).

A detailed inspection of internal organs in mutant embryos revealed that the liver was the most impaired organ with a destructed cellular organization in large regions (Additional file 1: Figure S1C–D). These impaired regions contained almost no erythrocytes labelled with Ter119 but many apoptotic cells as shown by TUNEL assay (Additional file 1: Figure S1E–F). Surprisingly, Meis2 was not found to be expressed in the fetal liver while Meis1 was readily detectable (Additional file 1: Figure S1A). Based on this we suggest that the observed cell death in the liver is a consequence of strong hemorrhaging in the whole embryo that leads to anemia and apoptosis primarily in the liver and may be a cause of the embryonic lethality. Having observed anemia in Meis2^{-/-} embryos we further pursued the possibility that Meis2 may influence embryonic hematopoiesis similarly to Meis1 that controls proliferation of hematopoietic stem cells in the fetal liver and is also essential for megakaryocyte viability [25, 26, 34]. We therefore mapped the expression of Meis2 and Meis1 in the area of the aorta-gonad-mesonephros (AGM), the site of origin of embryonic hematopoietic stem cells. As shown in Additional file 1: Figure S2B, neither Meis2 nor Meis1 were observed in endothelial cells labelled with CD31 but both proteins were abundant in the mesenchyme surrounding the endothelial wall of the dorsal aorta. We further found that circulating hematopoietic progenitors labeled with anti-Runx1 antibody did not express Meis2 (Additional file 1: Figure S2C). Finally, we carried out erythroblast cultures derived from the fetal liver and found no differences in the growth and differentiation of liver erythroid progenitors between Meis2^{-/-} and



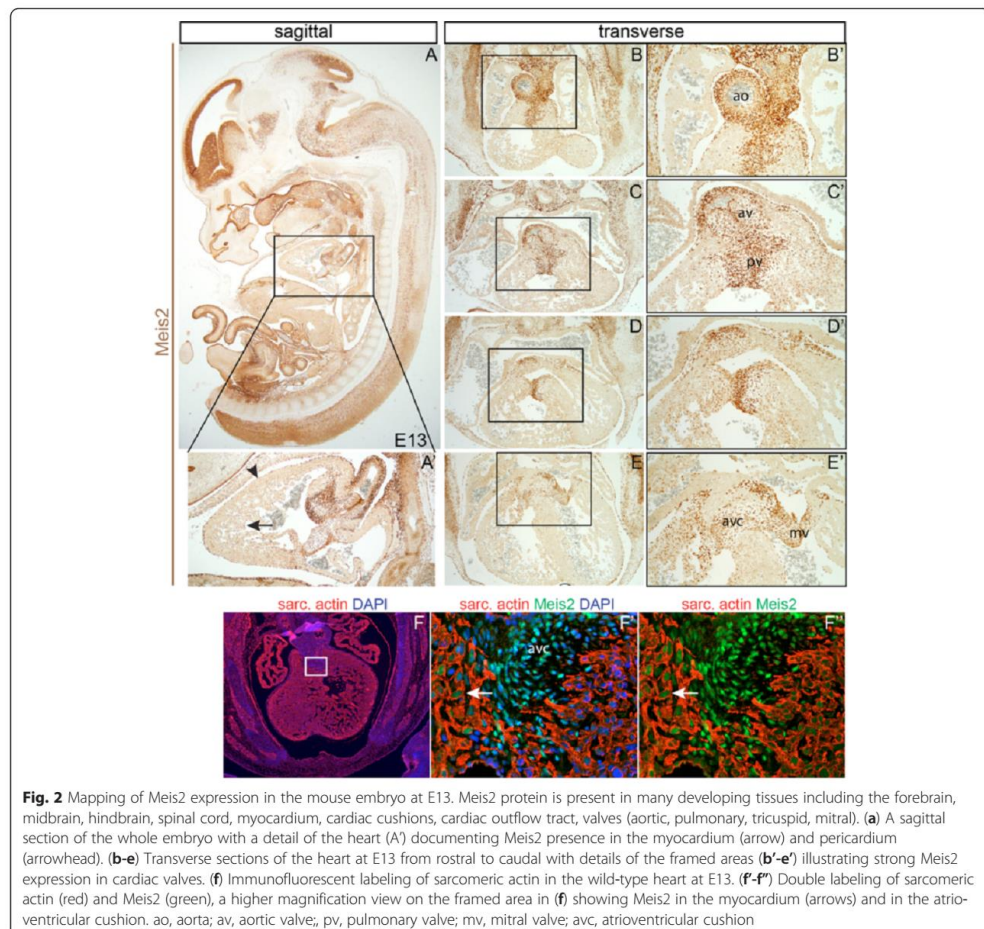
controls (data not shown). As *Meis2*, in our hands, was not detected in hematopoietic progenitors neither in the AGM nor in the fetal liver, we hypothesize that the anemia in the mutants originates from extensive bleeding or defective circulation rather than defects in hematopoiesis.

The lack of *Meis2* results in fetal heart malformation

In the heart of *Meis2*^{-/-} embryos at E12.5, we observed incomplete septation of the outflow tract that normally separates the aorta from the pulmonary artery. This defect is known as persistent truncus arteriosus (PTA) and was observed in all analyzed mutants ($n = 8$ litters, 14 mutants) (Fig. 1d). To correlate the observed defects with the expression of *Meis2*, we carried out immunohistochemistry on sections of embryonic heart at E13 using anti-*Meis2* antibody. As shown in Fig. 1e, a

remarkably strong presence of *Meis2* was observed in the aortic and pulmonary valves. Strikingly, these valves were lost in the *Meis2*^{-/-} heart (arrowheads). To visualize the PTA in the *Meis2*^{-/-} outflow tract, we used antibody against α -smooth muscle actin (SMA). Stained heart sections confirmed the PTA but SMA appeared normally expressed in the mutant heart (Fig. 1f).

Widespread expression of *Meis2* was observed in the developing embryo including the central nervous system, in the upper and lower jaw and in the lumen of the intestinal tract (Fig. 2a). Specifically in the heart, *Meis2* protein was detected in the myocardium (arrow) and pericardium (arrowhead) (Fig. 2a) in which *Meis2*-positive cells also expressed sarcomeric actin (Fig. 2f-f', arrows). Remarkably strong expression of *Meis2* was found in the valves (aortic, pulmonary, tricuspid and mitral) as well as in the atrioventricular cushion (Fig. 2b-f').

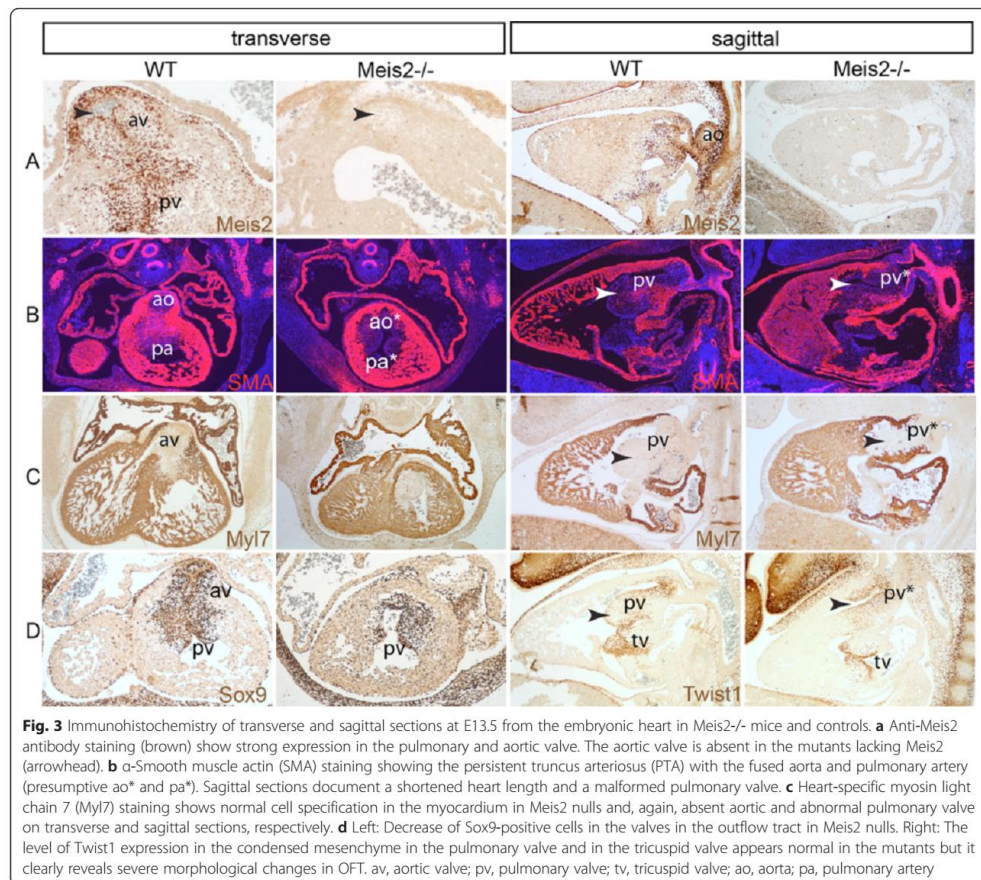


To document heart defects in *Meis2*^{-/-} embryos in detail, we performed immunofluorescence on transverse and sagittal sections from embryos at E12.5 using antibodies against Meis2, α -smooth muscle actin (SMA) and heart-specific myosin Myl7. Figure 3a-c illustrates that the aortic and pulmonary arteries were not separated (ao*, pa*, pv* in Fig. 3b) and the aortic valve was absent (arrowhead in Fig. 3a). These regions strongly expressed Meis2 in the controls and the signal was lost in the mutants (Fig. 3a). Both the aortico-pulmonary spiral septum and the aortic and pulmonary valves are formed from cardiac neural crest cells [7] which can be visualized by anti-Sox9 and anti-Twist1 antibody [35]. In *Meis2*^{-/-} embryonic hearts, we observed less Sox9-

positive cells in the outflow valves. The number of Twist1-positive cells was not significantly changed though its expression level was reduced and the organization of these cells was altered compared to controls (Fig. 3d). Clear morphological defects in the septation of the truncus arteriosus and in the outflow valves (arrowheads) strongly suggest that the defective outflow tract in *Meis2* nulls arises from impaired cardiac neural crest cells.

Neural crest cells express high levels of Meis2

Based on the heart abnormalities of potential neural crest origin, we decided to map the expression of Meis2 at the embryonic stages that are critical for generation and migration of NCC. At E8.5 before the neural tube

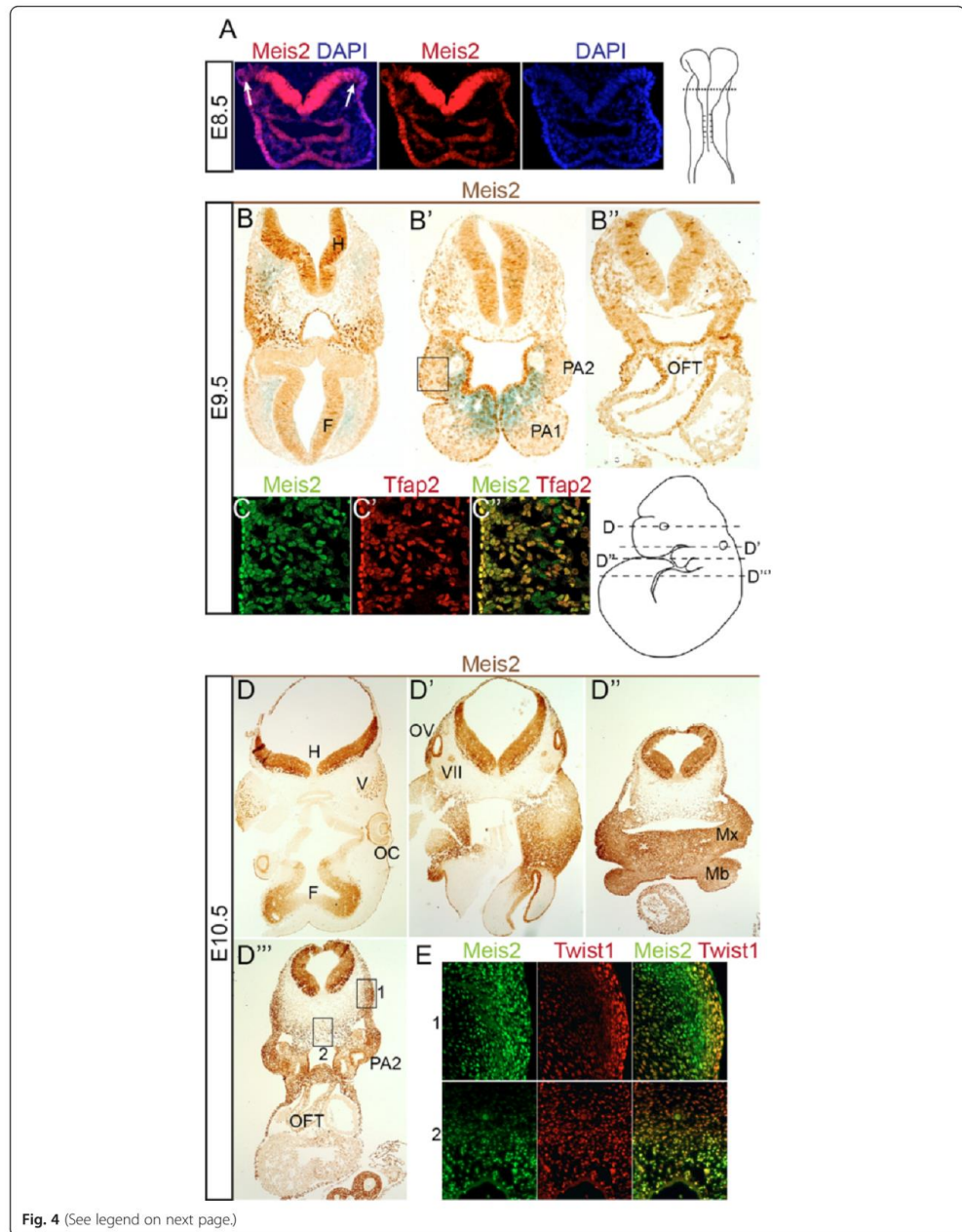


closure, abundant *Meis2* expression was noticed in the neural plate that weakened towards the plate border from which the premigratory NCC delaminate (Fig. 4a). At E9.5, the *Meis2* protein was found in the neuroepithelium of the hindbrain (Fig. 4b-b'') in which the signal became diminished towards the roof plate. *Meis2* was also seen in migrating cells in the mesenchyme lateral to the hindbrain and in the pharyngeal arches 1-2 (PA1 and PA2) (Fig. 4b') and in the outflow tract (OFT) (Fig. 4B''). Many of these cells especially in the PA co-express *Tfap2*, a marker of NCC [36, 37] (Fig. 4c-c'' and Additional file 1: Figure S3C-D''). At E10.5, *Meis2* protein was detected in the developing tissues that are derived from NCC, such as the trigeminal and facial nerve ganglions, in the the otic vesicle and its surrounding mesenchyme, in the maxillary and mandibular component of the PA1, in the cardiac outflow tract cushion and in the

PA2 (Fig. 4d-d'' and Additional file 1: Figure S3A-B''). The expression pattern revealed by our immunohistochemistry thus corresponds to *in situ* hybridization of *Meis2* mRNA reported by Cecconi and co-workers [38]. Apart from the neuroectoderm, many of *Meis2*-positive cells displayed a mesenchymal character as revealed by co-staining with the anti-*Twist1* antibody (Fig. 2E and Additional file 1: Figure S3E).

Conditional deletion of *Meis2* in neural crest cells leads to a defective heart outflow tract

Because some developmental defects in *Meis2* nulls may arise from affected NCC, we aimed to verify this assumption by means of conditional inactivation of *Meis2*. We employed AP2 α -IRES-Cre (AP2 α -Cre) transgenic mouse in which Cre recombinase was inserted into the *Tfap2* (AP2 α) gene enabling loxP recombination specifically



(See figure on previous page.)

Fig. 4 Meis2 is expressed in migrating NCC. **(a)** Meis2 expression in the neural plate stage at E8.5 becomes weak towards the neural plate border (arrows). Right: schematic embryo at E8.5 with a depicted section plane (dashed). **(b-b'')** Sections from rostral (**b'**) to caudal (**b''**) of wild-type embryos at E9.5 revealing Meis2 in pharyngeal arches (PA), hindbrain (H) and in the cardiac outflow tract (OFT). **(c-c'')** Immunofluorescent double-labeling of Meis2 (green) and Tfpap2 (red) in the region approximately depicted by a black rectangle in A'. **(d-d'')** Transverse sections from rostral to caudal at E10.5 with immunostained Meis2. Sections levels correspond to the illustrated cartoon. Meis2 was detected in the hindbrain (H), forebrain (F), optic cup (OC), trigeminal nerve ganglion (V), otic vesicle (OV), facial nerve ganglion (VII), maxillary (Mx) and mandibular (Mb) process of PA1, in PA2 and outflow tract (OFT). **(e)** Immunofluorescence of Meis2 (green) and Twist1 (red) shows their co-expression in two areas labelled with rectangles in D''. Upper panels (1) belong to the lateral zone (1) and lower panels (2) to the midline area (2)

in NCC [39]. Conditional mutants AP2 α -Cre/Meis2 cKO survived the critical stage E14, at which systemic Meis2 nulls die, but they were lethal around the time of birth. This cKO approach also allowed us to analyze older embryos. To perform lineage tracing experiments and examine migratory routes of NCC, conditional mutants AP2 α -Cre/Meis2 cKO were crossed to ROSA26 reporter mice [40]. This allele allows detection of Cre-mediated recombination using β -galactosidase enzymatic assay and tracing of all cells derived from AP2 α -Cre positive NCC. Figure 5a-a' illustrates lineage tracing of NCC in normal and AP2 α -Cre/Meis2 cKO embryos. 75 % of mutants (n = 8 litters, 8 mutants) displayed aberrant distribution of β -galactosidase-positive cells along the neural tube (arrow in 5A'), and all mutants had abnormalities in the PA2, which appeared thinner and misshaped, (arrowheads in 5A-A') and also all mutants had smaller otic vesicles (asterisks). Sectioning of AP2 α -Cre/Meis2 cKO/ROSA26 E10.5 embryos revealed poor colonization of the OFT by cardiac NCC (arrows in 5B-B'). Conditional deletion of Meis2 effectively erased the Meis2 protein in the regions of the AP2 α -Cre activity, however, many surrounding cells still express normal levels of Meis2 (arrows in Fig. 5c-c'). Next we studied the OFT defects at later stages using immunohistochemistry on cryosections from AP2 α -Cre/Meis2 cKO/ROSA26 embryos. At E11, anti-Sox9 antibody labelled all β -galactosidase-positive cells in the OFT and we observed a lower density and disorganization of double-labelled cells in conditional mutants (Fig. 5d-d'). 90 % of mutants had malformed OFT valves at E12 (n = 5 litters, 9 mutants) (such as av in Fig. 5e-e'). However, the septation of the truncus arteriosus appeared normal in conditional mutants as the aorta and pulmonary arteries were normally separated (Fig. 5f-f'), which was never seen in systemic nulls all displaying the PTA. Of note, we detected still high levels of Meis2 in non-recombined cells, including the smooth muscle of artery walls and in the vicinity of valves, which may provide explanation for less severe defects in conditional mutants compared to systemic ones. Finally, Fig. 5g-g' shows an example of valve malformation at E14 known as double outlet right ventricle (DORV) labelled with anti-Sox9. In summary, tissue-specific deletion of Meis2 using AP2 α -Cre resulted in various valve defects in the heart outflow tract documenting its critical role in cardiac NCC.

Meis2 affects cranial nerve development

As Meis2 expression is abundant in the head region, we next explored other NCC derivatives such as cranial nerves. Formation of their neuronal projections in Meis2 $^{-/-}$ embryos was followed using whole-mount immunostaining of neurofilaments with the 2H3 antibody. As seen in Fig. 6a-b', the trigeminal (cranial nerve V), facial (VII) and vestibulocochlear (acoustic) nerves (VIII) were severely impaired in Meis2 nulls at E10.5 (asterisks in Fig. 6b'). An analogous analysis was performed in AP2 α -Cre/Meis2 cKO. We again crossed conditional mutants with ROSA26 reporters to map the activity of Cre. β -galactosidase signal in AP2 α -Cre/ROSA26 controls was seen in trigeminal ganglions, the lens, the pericardial mesenchyme and the surface ectoderm. A similar spatial pattern in this head region was found in the mutants AP2 α -Cre/Meis2 cKO/ROSA26 and the size of the trigeminal ganglion V was smaller and misshapen (Fig. 6c'). 2H3 neurofilament staining showed that the cranial nerves VII and VIII were damaged in conditional mutants (asterisks in Fig. 6d') but the trigeminal nerve V again less affected than in Meis2 $^{-/-}$ (n = 3 litters, 3 mutants). Thus, the phenotype in cranial nerves appeared weaker in conditional mutants in comparison with systemic ones. We further noticed that the cornea and eyelids were not developed properly (Fig. 6e-e') (similarly in Meis2 $^{-/-}$ embryos at E13.5, not shown). The cornea was much thinner (arrow) while eye lids (el) did not grow and close over the eye bulbs. The cornea was reported to originate from NCC [41–43] as also indicated by our lineage tracing data showing AP2 α -Cre activity in the pericardial mesenchyme (Fig. 6c). In summary, tissue-specific deletion of Meis2 in NCC and the surface ectoderm resulted in malformed cranial nerves, the cornea and eyelids.

Development of cranial cartilage is perturbed in Meis2-null embryos

Next, we examined the development of the craniofacial skeleton that is derived from NCC. Mapping of AP2 α -Cre/ROSA26 showed complete recombination in PA1 and otic vesicle at E10 and this was further verified at E13 on sagittal view in which recombined cells resided in jaws and the nasal cartilage (Fig. 7a). Immunostaining

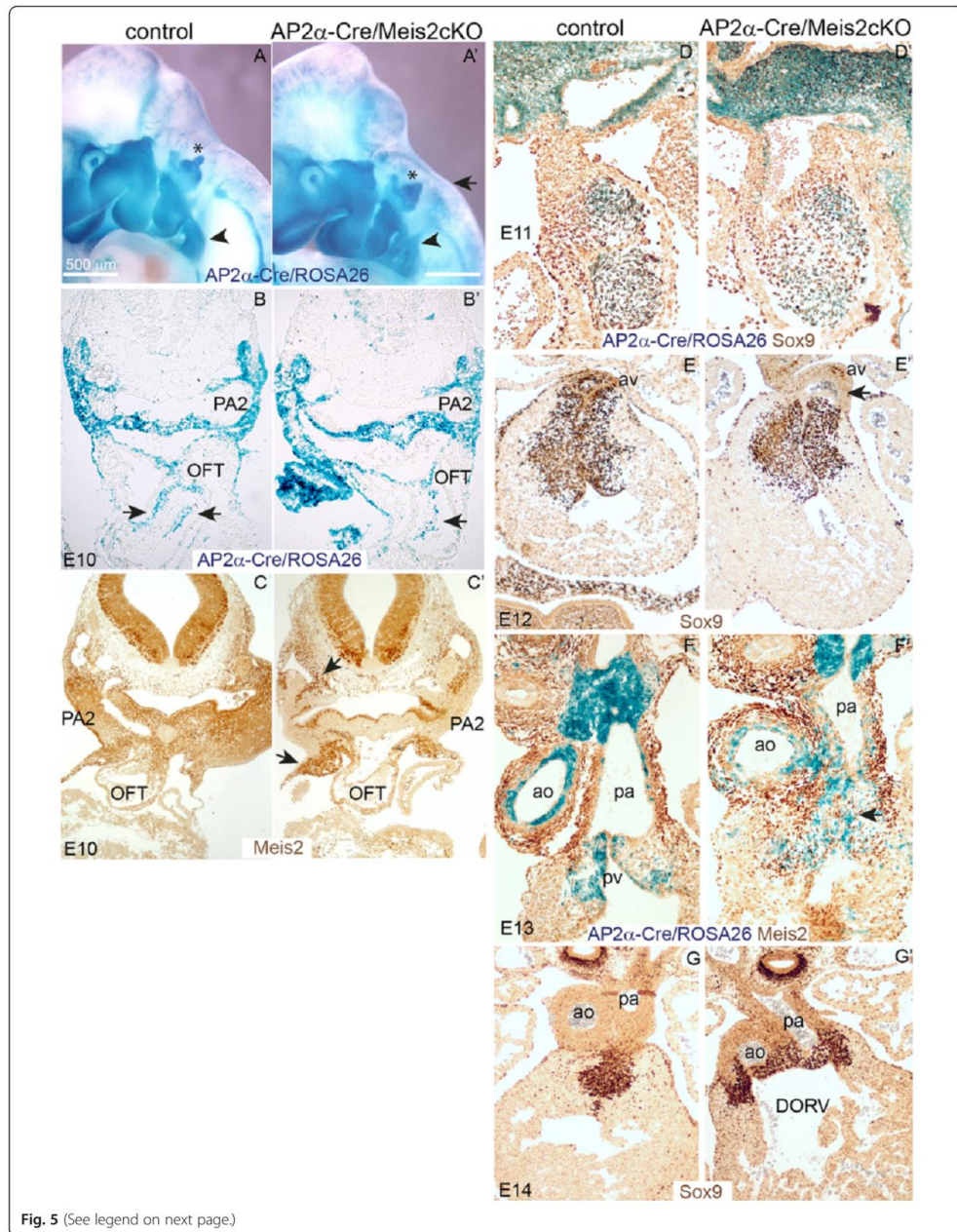


Fig. 5 (See legend on next page.)

(See figure on previous page.)

Fig. 5 Heart defects upon conditional inactivation of Meis2 in NCC. **(a-a')** Lineage tracing of NCC in AP2 α -Cre /Meis2 cKO/ROSA26 embryos at E10.5 **(a')** and controls **(a)**. **(b-b')** Sections of embryos shown in **(a)** at the level of PA2 and OFT, compare position and number of β -galactosidase-positive cells in the control and the mutant cKO (arrows in B'). **(c-c')** Immunohistochemical staining of Meis2 in cKO **(c')** shows the areas of its deletion. **(d-d')** Cryosections of the OFT from AP2 α -Cre /Meis2 cKO/ROSA26 stained for β -galactosidase and Sox9, note cells disorganization in cKO **(d')**. **(e-e')** Paraffin-embedded sections of E12 heart stained with anti-Sox9 defective aortic valve in cKO **(e')**. **(f-f')** Meis2 and β -galactosidase double-labeling of E13 OFT shows a number of Meis2-positive cells in cKO **(f')** that are excluded from Cre recombined areas. The pulmonary valve does not develop properly. **(g-g')** anti-Sox9 immunohistochemical labeling of severed valves in cKO at E14 **(g')**. Ao, aorta; av, aortic valve; OFT, outflow tract; PA2, pharyngeal arch 2; pa, pulmonary artery, DORV, double outlet right ventricle

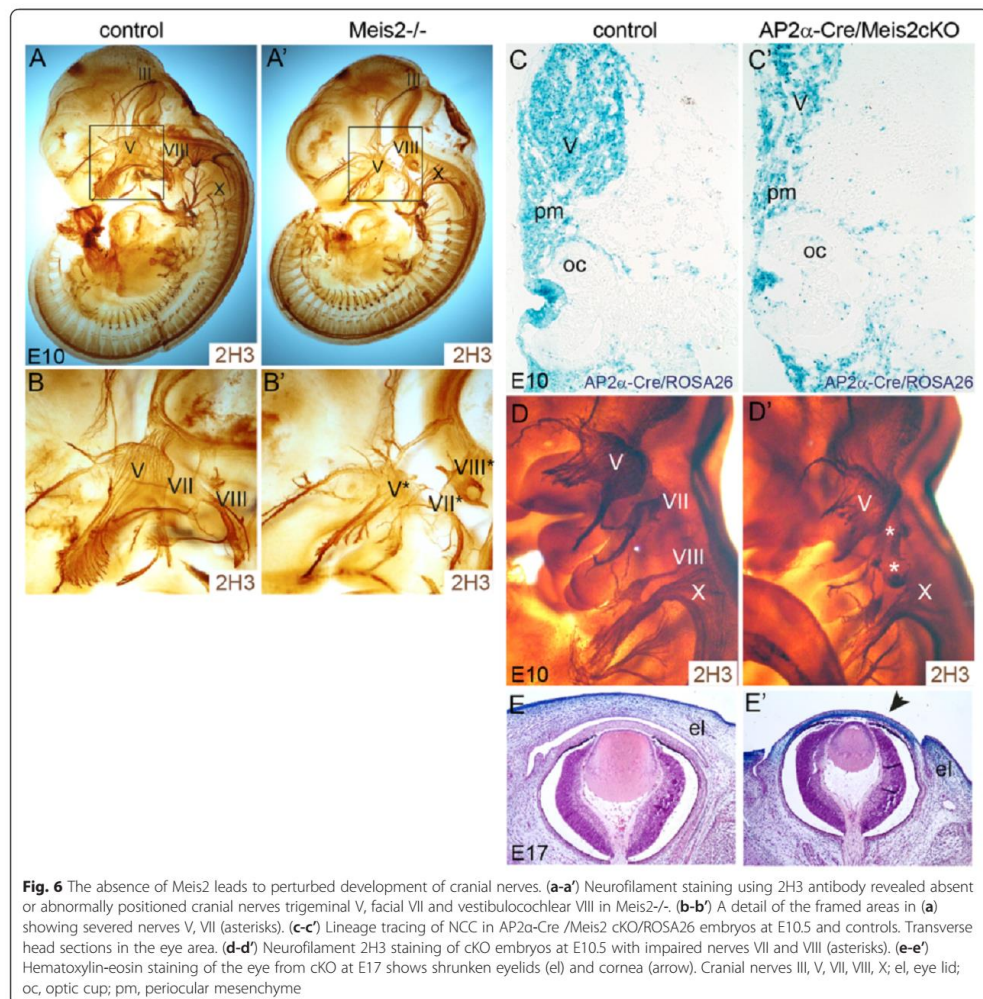
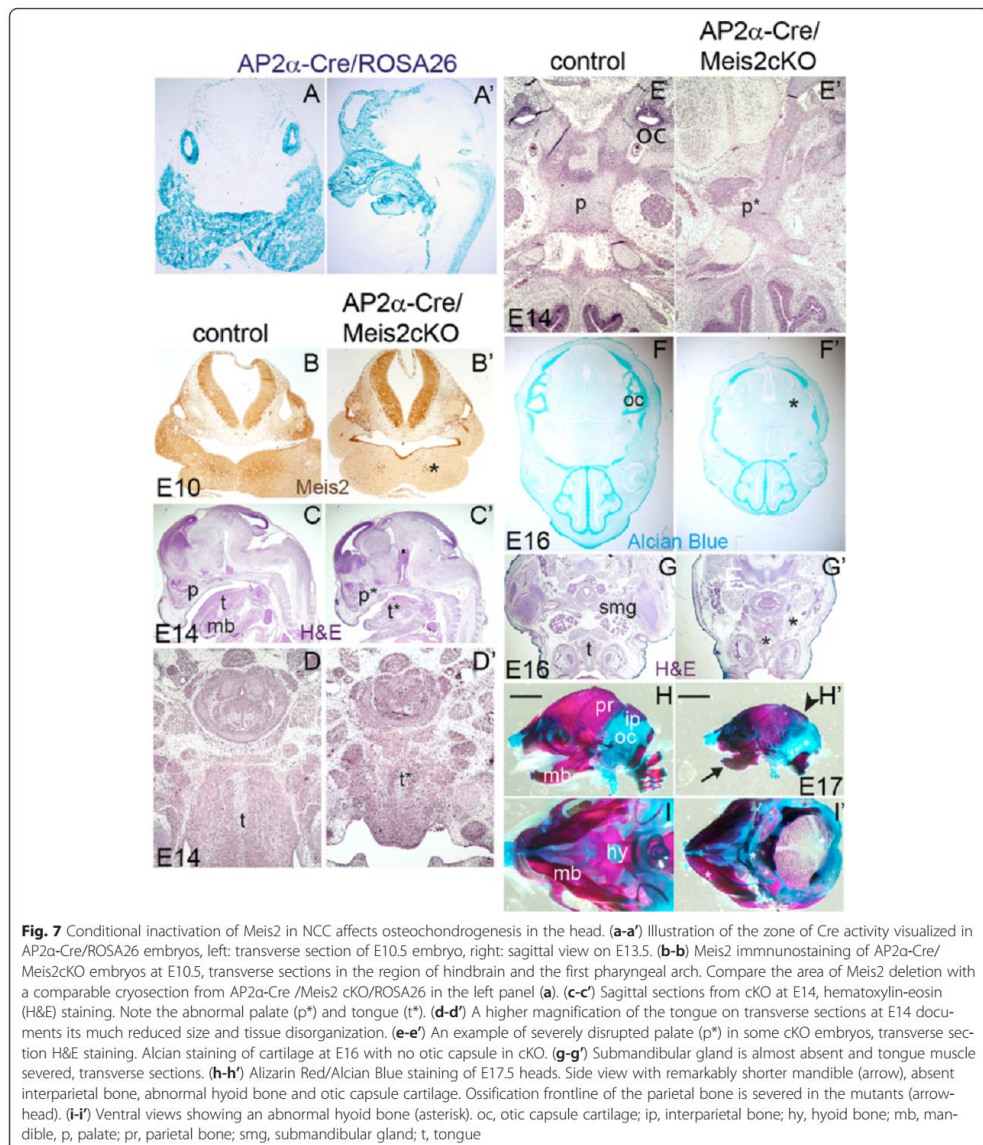


Fig. 6 The absence of Meis2 leads to perturbed development of cranial nerves. **(a-a')** Neurofilament staining using 2H3 antibody revealed absent or abnormally positioned cranial nerves trigeminal V, facial VII and vestibulocochlear VIII in Meis2 $^{-/-}$. **(b-b')** A detail of the framed areas in **(a)** showing severed nerves V, VII (asterisks). **(c-c')** Lineage tracing of NCC in AP2 α -Cre /Meis2 cKO/ROSA26 embryos at E10.5 and controls. Transverse head sections in the eye area. **(d-d')** Neurofilament 2H3 staining of cKO embryos at E10.5 with impaired nerves VII and VIII (asterisks). **(e-e')** Hematoxylin-eosin staining of the eye from cKO at E17 shows shrunken eyelids (el) and cornea (arrow). Cranial nerves III, V, VII, VIII, X; el, eye lid; oc, optic cup; pm, periocular mesenchyme



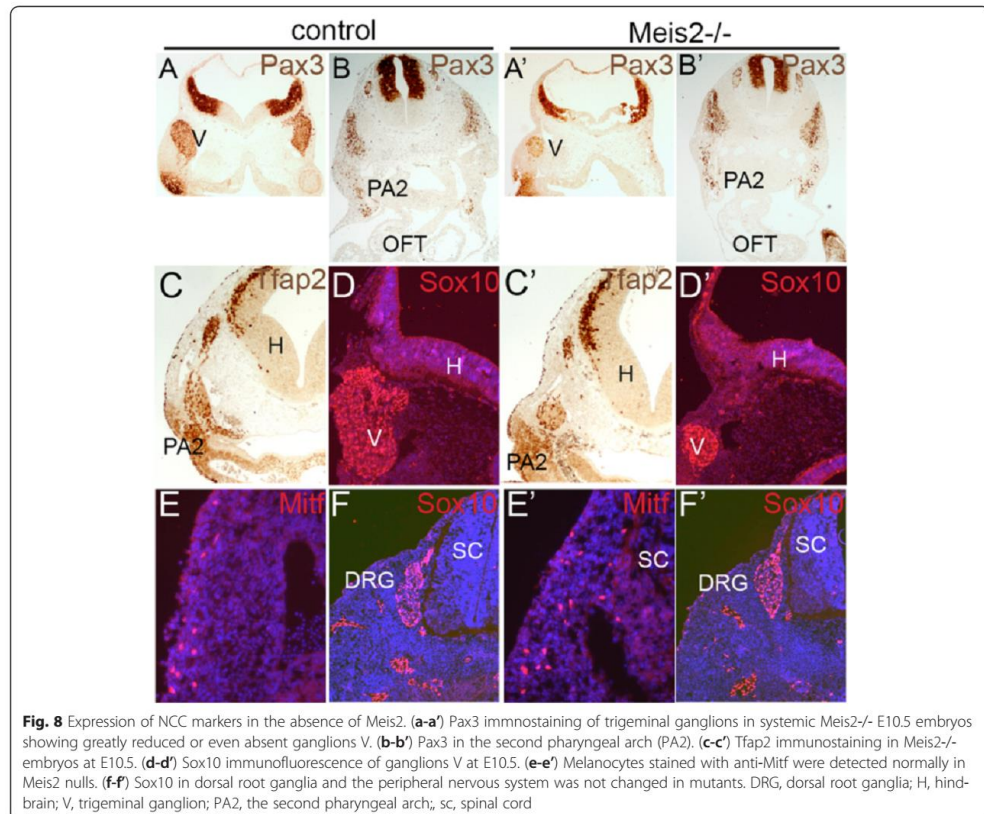
of the Meis2 protein confirmed efficient deletion in AP2α-Cre/Meis2 cKO in the regions of Cre recombination (asterisk in Fig. 7b; compare with the panel 7a). We found abnormal palate (p) and tongue (t) in sagittal sections of E14 conditional mutants (Fig. 7c-c'). The size

of tongue was greatly reduced and muscle fibers looked disorganized, as shown in a detailed view on transverse sections (Fig. 7d-d'). In 33 % of mutants (n = 6 litters, 4 mutants), severely malformed developing cartilage were observed in the palate (asterisk in Fig. 7e'), 67 % of

mutants also displayed abnormal palates though less severe. Further, the otic capsule cartilage was absent as shown by Alcian staining at E16 (asterisk in Fig. 7f'). Submandibular gland (smg) was missing in 33 % mutants and 66 % had much smaller smg (Fig. 7g-g') (n = 6 litters, 4 and 8 mutants, respectively). We carried out whole-mount Alcian Blue/Alizarin red staining at E17.5 that confirmed our observations from tissue sections: The mandibular bone was poorly developed and its length was much shorter in the mutants (black arrow in Fig. 7h'). The interparietal bone and the cartilage of the otic capsule were absent and the boundary of ossification of the parietal bone was abnormal (arrowhead in Fig. 7h'). The hyoid bone was severely malformed (asterisk in Fig. 7i'). These defects clearly document that Meis2 is essential for the head bones and cartilages that originate from cranial NCC.

Meis2 does not affect proliferation and expression of main determinants of NCC

Migrating NCC are exposed to a number of environmental factors that can alter their properties including fate restriction or proliferation. In order to class Meis2 into the gene regulatory network determining NCC development we first examined the levels of expression of well-known genes specifying NCC. Trigeminal ganglions stained with anti-Pax3 were found reduced in size or completely missing in Meis2^{-/-} embryos at E10 (Fig. 8a-a'). Conditional mutants showed normal levels of Pax3 and a normal size of ganglions V (not shown). Pax3 was reported to control colonization of the OFT by cardiac NCC [44] and the promoter of Pax3 is directly controlled by Pbx1 [45]. As Pbx1^{-/-} embryos display similar heart defects as Meis2^{-/-} embryos [15], we checked the expression of Pax3 in the OFT and PA2 of our mutants.



However, we found no change in Pax3-positive cells in PA2, moreover, Pax3 was not detected in the OFT even in wild-type controls (Fig. 8b-b'). Next we assayed the level of expression of Tfap2, Sox10 and Mitf, a marker of melanocyte precursors. As shown in Fig. 8c-f, their expression was not found to be changed in the absence of Meis2.

We also analyzed the number and spatial distribution of migrating NCC using anti-Sox9 antibody at E10.5. Sox9-positive NCC are abundant in the embryonic head mesenchyme and pharyngeal arches, however, their quantification did not reveal significant changes between controls and mutants (Additional file 1: Figure S4A). Further, we examined cell proliferation using antibodies against PCNA and PH3 on head sections. Again, quantification of all proliferating cells (all PCNA+ or PH3+) or proliferating NCC (Sox9+/PCNA+ or PH3+) did not differ between controls and mutants (Additional file 1: Figure S4B-D). Finally, apoptosis, as measured by anti-Cas3 immunohistochemistry at E10.5, was not significantly altered in the mutants (Additional file 1: Figure S4E). In summary, Meis2 absence did not result in dramatic changes in cell proliferation and viability at E10.5.

Systemic Meis2 mutants show aberrant position of FoxD3 and Sox9

As the defects in NCC derivatives in the absence of Meis2 were not caused most probably by insufficient cell proliferation or changed expression of main NCC

specifiers we performed whole-mount in situ hybridization to map the position of migrating NCC. At first, E9.5 embryos from Meis2^{-/-} embryos and control littermates were stained with riboprobes for *FoxD3* and *Sox9* mRNA [46, 47]. As shown in Fig. 9A-B, both *FoxD3* and *Sox9* were expressed in Meis2^{-/-} embryos at the levels that were comparable to control littermates, indicating again that the overall differentiation program of NCC was not affected. Interestingly, we observed an aberrant position of FoxD3-positive cranial NCC in Meis2 nulls (arrows in Fig. 9a-a'). Expression of *FoxD3* mRNA in the trigeminal ganglion confirmed its abnormality as also seen in Fig. 6b'. *Sox9* mRNA revealed that otic vesicles were consistently smaller in mutants (arrow in Fig. 9b'). Next, we carried out the same analysis in E9.5 embryos from conditional mutants AP2α-Cre/Meis2 cKO. However, the levels and distribution *FoxD3* and *Sox9* transcripts were not altered in conditional mutants (n = 5 litters, 8 mutants) (Fig. 9c-d'). Thus, the changes in the expression pattern of NCC specifying genes Sox9 and FoxD3 were found to be more profound in systemic Meis2 mutants compared to conditional ones which may explain their stronger phenotypic defects.

Discussion

In this study, we showed that the transcription factor Meis2 is abundant in NCC and it is essential for their function. The embryonic lethal phenotypes of mutant

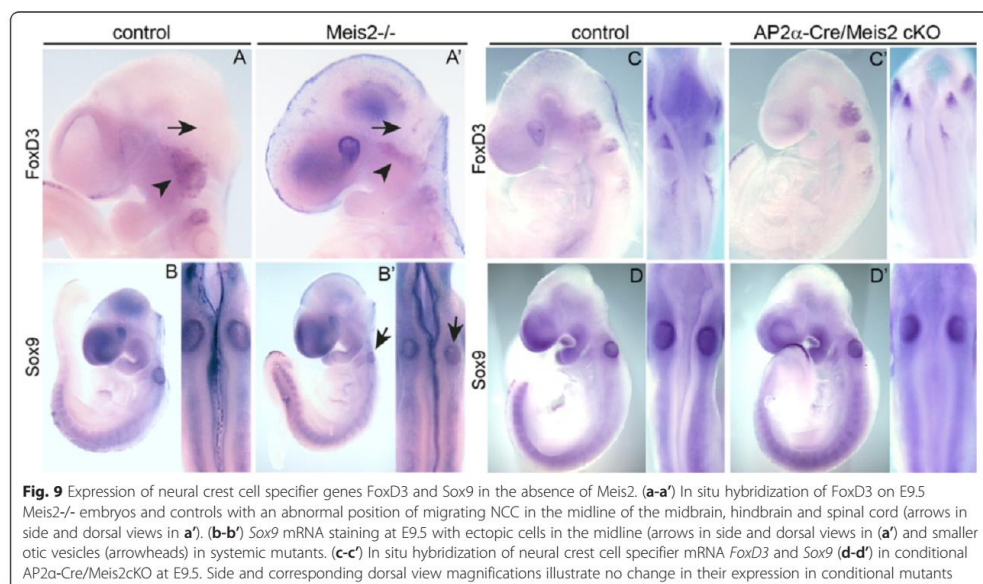


Fig. 9 Expression of neural crest cell specifier genes FoxD3 and Sox9 in the absence of Meis2. **(a-a')** In situ hybridization of FoxD3 on E9.5 Meis2^{-/-} embryos and controls with an abnormal position of migrating NCC in the midline of the midbrain, hindbrain and spinal cord (arrows in side and dorsal views in **a'**). **(b-b')** Sox9 mRNA staining at E9.5 with ectopic cells in the midline (arrows in side and dorsal views in **a'**) and smaller otic vesicles (arrowheads) in systemic mutants. **(c-c')** In situ hybridization of neural crest cell specifier mRNA FoxD3 and Sox9 **(d-d')** in conditional AP2α-Cre/Meis2cKO at E9.5. Side and corresponding dorsal view magnifications illustrate no change in their expression in conditional mutants

mouse embryos of Meis2 and its paralogue Meis1 are similar in the timing of death and in strong hemorrhaging. Meis1 is expressed hematopoietic stem cells in the fetal liver, the primary organ of hematopoiesis at E13. Various assays showed defects in erythropoiesis providing explanation for anemia in Meis1 mutants [25, 26]. In contrast, we did not detect Meis2 in the fetal liver and in hematopoietic progenitors in the dorsal aorta. We therefore speculate that hemorrhaging in Meis2^{-/-} embryos caused destructive changes primarily in the fetal liver that is highly sensitive to low oxygen. Impaired function of the liver may lead to failure in erythropoiesis and thus bleeding rather than defects in hematopoiesis in Meis2 mutants may cause lethality. Despite 83 % sequence identity of Meis1 and Meis2 and the almost identical homeodomain, they acquired different functions during evolution probably due to distinct expression patterns.

Stankunas and colleagues [15, 45] showed that various combinations of mutant alleles of Pbx1/2/3 or Meis1 exhibit cardiac anomalies in the outflow tract or in the septation of ventricles implying that cardiac NCC require transcriptional control by combinatory Meis/Pbx complexes. Along this line, zebrafish Meis2 genes influence development of heart and cranial skeleton [16, 28]. The data presented here extend our knowledge about the role of Meis/Pbx complexes controlling the fate of NCC. Apart from the previously proposed function in cardiac neural crest, we suggest that a similar transcriptional control network takes place in cranial NCC including chondrogenic and neuronal lineages. Our data represent the first loss-of-function study of Meis2 in mouse and may in fact serve as a disease model for certain human developmental disorders. Intriguingly, several reports describe patients with Meis2 mutations who display disorders such as the cleft palate, septal defects in the heart or intellectual disabilities [30–33].

Pax3 is expressed in the neural plate border and plays an important role in cardiac NCC as documented by conditional knock-out studies in mouse [44]. A specific Pbx1/Meis1 complex has been reported to directly regulate Pax3 in premigratory NCC in rhombomeres, in which cardiac NCC originate, linking Pbx1-Pax3 regulatory hierarchy with the OFT defects in Pbx1^{-/-} embryos [45]. We did not see reduced Pax3 expression in Meis2^{-/-} at E10.5 although Pax3-positive trigeminal ganglions were shrunken in systemic mutants. Nor could we detect Pax3 in the wild-type OFT at E10.5. It is possible that Meis2 and Pax3 are co-expressed in earlier NCC in which these factors may cooperate during NCC differentiation.

Our experiments utilizing conditional mutants AP2 α -Cre/Meis2 cKO confirm defects in tissues derived from cardiac and cranial NCC such as the OFT or craniofacial

cartilage. However, the phenotypes in cKO appeared in some cases weaker than in systemic mutants. PTA, for instance, was never found in conditional mutants while all systemic mutants displayed defective septation of the OFT. It is important to note that we still found a substantial amount of Meis2 protein after conditional deletion in the areas that are in close vicinity of AP2 α -Cre targeted regions (mapped in the ROSA26 reporter) in which we observed effective inactivation. Standby Meis2-positive cells may be involved in forming the truncus septum. Although AP2 α -Cre mouse is the earliest driver for NCC [44], we cannot exclude the possibility that a minor NCC population forms before AP2 α -Cre mediated recombination and thus it is not targeted. Another possibility is that neighboring non-NCC cells expressing Meis2 participate in the truncus septation. In this context it is interesting to note that systemic Pax3 KO display the PTA while Wnt1-Cre or AP2 α -Cre cKOs of Pax3 show valve defects but normal separation of aorta and pulmonary arteries [44]. Moreover, the PTA defects were also seen in systemic Pbx1-3 mutants; the data from Pbx cKOs are not available [15, 45]. The fact that the truncus septation may partially originate from non-NCC population is supported by the report of Bai and colleagues [48] who observed PTA in Mef2c-Cre/Bmp4/7, a Cre driver not normally used for NCC targeting.

Altered proliferation, apoptosis or significant changes in expression of transcription factors determining NCC (Sox9, Sox10, Tfp2, Pax3, Mitf) were not detected between critical stages E10.5-E11.5 in our hands. Meis2 may influence late phases of NCC differentiation (including cell proliferation and viability) that is required for proper formation of the OFT or for differentiation of osteochondral progenitors.

We hypothesize that Meis2 absence may be compensated by Meis1 which may rescue some defects during earlier phases of NCC development. Meis2 deficiency is thus reflected in the areas and stages in which the Meis2 function is unique, e.g. during craniofacial development. Meis proteins may diversify in their expression pattern after the initial NCC specification and acquire unique function, for instance, during formation of the OFT and cartilage. In order to test this hypothesis it will be necessary to generate and analyze Meis1 and Meis2 conditional double mutants that may reveal potentially earlier role of Meis factors during NCC development.

Even though we did not see a major difference in Sox9 expression in early embryos, anomalies in the craniofacial skeleton of Wnt1-Cre/Sox9 cKO [47] and our AP2 α -Cre/Meis2 cKO are similar in the mandible, tongue, the otic capsule and the hyoid bone. This suggests that Sox9 and Meis2 cooperate in a similar differentiation process during chondrogenesis. It remains to

be elucidated what genes are direct targets of Meis factors. Altogether, our loss-of-function studies show that Meis2 transcription is an important player in the gene regulatory network determining differentiation of cardiac and cranial NCC.

Methods

Generation of Meis2 null mice

The LoxP recognition elements for the Cre recombinase were inserted in the introns 2 and 6 of the *Meis2* gene at the Gene Targeting & Transgenic Facility, University of Connecticut, USA. Transgenic mice termed Meis2 cKO were created by standard techniques using homologous recombination in mouse embryonic stem cells (129SvEv-Tac/C57BL/6 J F1) also at the Gene Targeting & Transgenic Facility. A neomycin selection cassette was removed using FLP-FRT recombination. Meis2 cKO were crossed to Hprt-Cre mice (strain 129S1/Sv-Hprt^{tm1(cre)Mnn}/J, stock 004302, The Jackson Laboratory) with the zygotic activity of the Cre recombinase to obtain animals that were heterozygous for Meis2 (Meis2^{+/-}) in the mixed genetic background. Primers for genotyping Meis2^{+/-} alleles: Mrg1-lox-F (forward) GAGGGGACAGTGGGTAAACA, Mrg1-rit-R (reverse) TCAGACCCAGGAATTTGAGG, a PCR product of 256 bp. Wild-type allele: Mrg1-rit-F GCAAGGGTGCTGAGGTTAAA and Mrg1-rit-R TCA GACCCAGGAATTTGAGG, a PCR product 235 bp. (Fig. 1a). Alternatively, Mrg1-lox-F GAGGGGACAGTGGTAAACA, Mrg1-lox-R GCGTTGCAGCTCACAGA AT, a PCR product of 142 bp.

All procedures involving experimental animals were approved by the Institutional Committee for Animal Care and Use (permission #PP-071/2011). This work did not include human subjects.

Immunohistochemistry

Embryos were fixed in 4 % paraformaldehyde overnight at 4 °C. 8–10 µm cryosections or 5-µm (paraffin-embedded) sections were permeabilized in 0.1 % Triton X-100 in PBS (PBT). After blocking sections were incubated overnight in a primary antibody (1 % BSA in PBT), washed with PBS and incubated with a fluorescent secondary for 1 h. Nuclei were visualized by DAPI (4,6-diamidino-2-phenylindol, 0.1 µg ml⁻¹, Roche). Primary antibodies: anti-Meis2 and anti-Meis1 (a gift from Dr. Buchberg), anti-Myl7 (1:250, Santa Cruz), smooth muscle actin (SMA) (1:1000, Sigma), Sox10, Twist1 (all Santa Cruz Biotech), 2H3 (neurofilaments), 3B5 (Tfap2a) and Pax3 (all DSHB), anti-alpha sarcomeric actin clone 5C5, anti-alpha smooth muscle actin clone 1A4 (both Sigma), anti-Myl7 (H60) (Santa Cruz Biotech), Mitf (a gift from Dr. H. Arnheiter), anti-Ter119 (BD Pharmingen). Secondary antibodies: anti-mouse (-rat, -rabbit) Alexa Fluor488 or 594 (Life Technologies). Biotinylated-

anti-mouse, -anti-rabbit, -anti-rat (Vector Laboratories), Vectastain ABC Elite kit and ImmPACT DAB substrate (all Vector Laboratories). Images were acquired in Leica MZ APO stereomicroscope with DC200 camera or Olympus SZX9 with DP72 camera. Fluorescence images were acquired in Zeiss Axioskop 2 microscope with objectives Ph3 Plan-Neofluar 40x/1.3 oil or Ph1 Plan-Neofluar 10x/0.3 and confocal Leica SP5. Bright-field light images were acquired in Nikon Diaphot 300 with objectives 4x/0.1 and 10x/0.25.

Scale2 protocol

Dissected embryonic hearts were fixed overnight in 4 % PFA, washed in PBS and transferred into ScaleA2 reagent (4 M urea, 10 % glycerol, 0.1 % triton X-100) as described in [49]. After two hours at RT hearts were photographed.

Alcian blue/Alizarin red staining

Embryos at E16.5–17.5 were dissected and scalded in hot water (65–70 °C, 2 min). They were dehydrated in 95 % ethanol for 48–72 h, changing solution every 12 h. After Alcian blue (Sigma) staining for 12 h, they were rinsed twice in ethanol and kept overnight. After clearing in 1 % KOH for 2 h and they were stained with Alizarin red (Sigma) for 5 h. Further clearing in 2 % KOH was carried out overnight, then in Glycerol (25 %) and 2 % KOH (75 %) for 8 h and Glycerol (50 %) and 2 % KOH (50 %) for 48 h. Tissue sections were rehydrated and stained in 0.04 % Alcian solution for 10 min. Pictures were obtained using binocular microscope Olympus SYX9 and camera Olympus DP72.

Whole-mount in situ hybridization

Riboprobes: Mouse *Foxd3* was cloned into pGEM-T-easy vector (Promega) using primers F-GGACCGCAA GAGTTCGCGGA, R-TCCGGAGCTCCCGTGTGCTGTT and antisense mRNA was transcribed with T7 polymerase. Mouse *Sox9* gene was cloned into pGEM-T-easy using primers F-GAGCACTCTGGGCAATCTCAG, R-CTCAGGGTCTGGTGAGCTGTG and antisense mRNA was transcribed with T7 polymerase. Whole-mount in situ hybridization was performed using standard protocols.

Conclusions

We present a pioneering functional description of Meis2, a member of TALE-class homeodomain transcription factors, which is strongly expressed in cranial neural crest cells. We generated a conditional allele of the Meis2 gene. Using systemic and neural crest-specific inactivation of Meis2, we provide evidence that Meis2 is an important player in the regulatory network controlling cranial and cardiac neural crest cells.

Additional file

Additional file 1: Figures S1-S4. Fetal liver in Meis2^{-/-} at E13.5 contains less erythrocytes and loses cell viability. **Figure S2.** Meis2 is abundant in the mesenchyme of the aorta-gonadomesonephros (AGM). **Figure S3.** Meis2 is strongly expressed in migrating NCC and in mesenchymal cells at E10.5. **Figure S4.** Proliferation and cell death of migrating NCC appears normal in Meis2^{-/-} mutants. (PDF 1406 kb)

Abbreviations

ao: aorta; ckO: conditional knock-out; DORV: double outlet right ventricle; MO: morpholino; NCC: neural crest cells; OFT: outflow tract; pa: Pulmonary artery; PTA: persistent truncus arteriosus; EMT: epithelial-mesenchymal transition.

Competing interests

The authors declare no competing financial and non-financial interests.

Authors' contributions

OM designed and performed experiments, interpreted data and wrote the manuscript. JM commented on the manuscript and performed experiments. OM performed experiments. SK, ZK interpreted data and commented on the manuscript. All authors have read and approved the manuscript.

Acknowledgments

The work was supported by the Norwegian Research Council (grant #174938) (OM, SK) and the Grant Agency of the Czech Republic (P305/12/2042) (OM, JM) and LK11214 (OM, JM) from the Ministry of Education, Youth and Sports of the Czech Republic. We are grateful to A. Buchberg (Thomas Jefferson University, Philadelphia, USA) for anti-Meis2.

Author details

¹Institute of Molecular Genetics, The Czech Academy of Sciences, 14200 Praha, Czech Republic. ²Unit for Cell Signaling, Oslo University Hospital, N-0349 Oslo, Norway.

Received: 11 August 2015 Accepted: 3 November 2015

Published online: 06 November 2015

References

- Bronner ME, LeDouarin NM. Development and evolution of the neural crest: an overview. *Dev Biol.* 2012;366(1):2–9.
- Dupin E, Sommer L. Neural crest progenitors and stem cells: from early development to adulthood. *Dev Biol.* 2012;366(1):83–95.
- Sauka-Spengler T, Bronner-Fraser M. A gene regulatory network orchestrates neural crest formation. *Nat Rev Mol Cell Biol.* 2008;9(7):557–68.
- Stuhlmiller TJ, Garcia-Castro ML. Current perspectives of the signaling pathways directing neural crest induction. *Cell Mol Life Sci.* 2012;69(22):3715–37.
- Minoux M, Rijli FM. Molecular mechanisms of cranial neural crest cell migration and patterning in craniofacial development. *Development.* 2010;137(16):2605–21.
- Santagati F, Rijli FM. Cranial neural crest and the building of the vertebrate head. *Nat Rev Neurosci.* 2003;4(10):806–18.
- Kirby ML, Hutson MR. Factors controlling cardiac neural crest cell migration. *Cell Adh Migr.* 2010;4(4):609–21.
- Lee RT, Nagai H, Nakaya Y, Sheng G, Trainor PA, Weston JA, et al. Cell delamination in the mesencephalic neural fold and its implication for the origin of ectomesenchyme. *Development.* 2013;140(24):4890–902.
- Nakamura T, Jenkins NA, Copeland NG. Identification of a new family of Pbx-related homeobox genes. *Oncogene.* 1996;13(10):2235–42.
- Jacobs Y, Schnabel CA, Cleary ML. Trimeric association of Hox and TALE homeodomain proteins mediates Hoxb2 hindbrain enhancer activity. *Mol Cell Biol.* 1999;19(7):5134–42.
- Shanmugam K, Green NC, Rambaldi I, Saragovi HU, Featherstone MS. Pbx and Meis as non-DNA-binding partners in trimeric complexes with HOX proteins. *Mol Cell Biol.* 1999;19(11):7577–88.
- Knoepfler PS, Bergstrom DA, Uetsuki T, Dac-Korytko I, Sun YH, Wright WE, et al. A conserved motif N-terminal to the DNA-binding domains of myogenic bHLH transcription factors mediates cooperative DNA binding with pbx-Meis1/Prep1. *Nucleic Acids Res.* 1999;27(18):3752–61.
- Mercader N, Leonardo E, Azpiazu N, Serrano A, Morata G, Martinez C, et al. Conserved regulation of proximodistal limb axis development by Meis1/Hth. *Nature.* 1999;402(6760):425–29.
- Capdevila J, Tsukui T, Rodriguez EC, Zappavigna V, Izpisua Belmonte JC. Control of vertebrate limb outgrowth by the proximal factor Meis2 and distal antagonism of BMPs by Gremlin. *Mol Cell.* 1999;4(5):839–49.
- Stankunas K, Shang C, Twu KY, Kao SC, Jenkins NA, Copeland NG, et al. Pbx/Meis deficiencies demonstrate multigenetic origins of congenital heart disease. *Circ Res.* 2008;103(7):702–09.
- Paige SL, Thomas S, Stoick-Cooper CL, Wang H, Maves L, Sandstrom R, et al. A temporal chromatin signature in human embryonic stem cells identifies regulators of cardiac development. *Cell.* 2012;151(1):221–32.
- Zhang X, Friedman A, Heaney S, Purcell P, Maas RL. Meis homeoproteins directly regulate Pax6 during vertebrate lens morphogenesis. *Genes Dev.* 2002;16(16):2097–107.
- Zhang X, Rowan S, Yue Y, Heaney S, Pan Y, Brendolan A, et al. Pax6 is regulated by Meis and Pbx homeoproteins during pancreatic development. *Dev Biol.* 2006;300(2):748–57.
- Choe SK, Vlachakis N, Sagerstrom CG. Meis family proteins are required for hindbrain development in the zebrafish. *Development.* 2002;129(3):585–95.
- Vlachakis N, Choe SK, Sagerstrom CG. Meis3 synergizes with Pbx4 and Hoxb1b in promoting hindbrain fates in the zebrafish. *Development.* 2001;128(8):1299–312.
- Waskiewicz AJ, Rikhof HA, Hernandez RE, Moens CB. Zebrafish Meis functions to stabilize Pbx proteins and regulate hindbrain patterning. *Development.* 2001;128(21):4139–51.
- Agoston Z, Schulte D. Meis2 competes with the Groucho co-repressor Tle4 for binding to Obx2 and specifies tectal fate without induction of a secondary midbrain-hindbrain boundary organizer. *Development.* 2009;136(19):3311–22.
- Choe SK, Lu P, Nakamura M, Lee J, Sagerstrom CG. Meis cofactors control HDAC and CBP accessibility at Hox-regulated promoters during zebrafish embryogenesis. *Dev Cell.* 2009;17(4):561–67.
- Ladam F, Sagerstrom CG. Hox regulation of transcription: more complex(es). *Dev Dyn.* 2014;243(1):4–15.
- Azcoitia V, Aracil M, Martinez A, Torres M. The homeodomain protein Meis1 is essential for definitive hematopoiesis and vascular patterning in the mouse embryo. *Dev Biol.* 2005;280(2):307–20.
- Hisa T, Spence SE, Rachel RA, Fujita M, Nakamura T, Ward JM, et al. Hematopoietic, angiogenic and eye defects in Meis1 mutant animals. *EMBO J.* 2004;23(2):450–59.
- Heine P, Dohle E, Bumsted-O'Brien K, Engelkamp D, Schulte D. Evidence for an evolutionary conserved role of homothorax/Meis1/2 during vertebrate retina development. *Development.* 2008;135(5):805–11.
- Melvin VS, Feng W, Hernandez-Lagunas L, Artinger KB, Williams T. A morpholino-based screen to identify novel genes involved in craniofacial morphogenesis. *Dev Dyn.* 2013;242(7):817–31.
- DeLaughter DM, Christodoulou DC, Robinson JY, Seidman CE, Baldwin HS, Seidman JG, et al. Spatial transcriptional profile of the chick and mouse endocardial cushions identify novel regulators of endocardial EMT in vitro. *J Mol Cell Cardiol.* 2013;59:196–204.
- Erdogan F, Ullmann R, Chen W, Schubert M, Adolph S, Hultschig C, et al. Characterization of a 5.3 Mb deletion in 15q14 by comparative genomic hybridization using a whole genome "tiling path" BAC array in a girl with heart defect, cleft palate, and developmental delay. *Am J Med Genet A.* 2007;143(2):172–78.
- Johansson S, Berland S, Gradek GA, Bongers E, de LN, Pfundt R, et al. Haploinsufficiency of MEIS2 is associated with orofacial clefting and learning disability. *Am J Med Genet A.* 2014;164A(7):1622–6.
- Crowley MA, Conlin LK, Zackai EH, Deardorff MA, Thiel BD, Spinner NB. Further evidence for the possible role of MEIS2 in the development of cleft palate and cardiac septum. *Am J Med Genet A.* 2010;152A(5):1326–27.
- Louw JJ, Coveleyn A, Jia Y, Hens G, Gewillig M, Devriendt K. MEIS2 involvement in cardiac development, cleft palate, and intellectual disability. *Am J Med Genet A.* 2015;167A(5):1142–6.
- Cai M, Langer EM, Gill JG, Satpathy AT, Albring JC, KC W, et al. Dual actions of Meis1 inhibit erythroid progenitor development and sustain general hematopoietic cell proliferation. *Blood.* 2012;120(2):335–46.

35. Rinon A, Lazar S, Marshall H, Buchmann-Moller S, Neufeld A, Elhanany-Tamir H, et al. Cranial neural crest cells regulate head muscle patterning and differentiation during vertebrate embryogenesis. *Development*. 2007;134(17):3065–75.
36. Schorle H, Meier P, Buchert M, Jaenisch R, Mitchell PJ. Transcription factor AP-2 essential for cranial closure and craniofacial development. *Nature*. 1996;381(6579):235–38.
37. Zhang J, Hagopian-Donaldson S, Serbedzija G, Elsemore J, Plehn-Dujowich D, McMahon AP, et al. Neural tube, skeletal and body wall defects in mice lacking transcription factor AP-2. *Nature*. 1996;381(6579):238–41.
38. Ceconi F, Proetzl G, varez-Bolado G, Jay D, Gruss P. Expression of Meis2, a Knotted-related murine homeobox gene, indicates a role in the differentiation of the forebrain and the somitic mesoderm. *Dev Dyn*. 1997;210(2):184–90.
39. Macatee TL, Hammond BP, Arenkiel BR, Francis L, Frank DU, Moon AM. Ablation of specific expression domains reveals discrete functions of ectoderm- and endoderm-derived FGF8 during cardiovascular and pharyngeal development. *Development*. 2003;130(25):6361–74.
40. Soriano P. Generalized lacZ expression with the ROSA26 Cre reporter strain. *Nat Genet*. 1999;21(1):70–1.
41. Hatou S, Yoshida S, Higa K, Miyashita H, Inagaki E, Okano H, et al. Functional corneal endothellium derived from corneal stroma stem cells of neural crest origin by retinoic acid and Wnt/beta-catenin signaling. *Stem Cells Dev*. 2013;22(5):828–39.
42. Yoshida S, Shimmura S, Nagoshi N, Fukuda K, Matsuzaki Y, Okano H, et al. Isolation of multipotent neural crest-derived stem cells from the adult mouse cornea. *Stem Cells*. 2006;24(12):2714–22.
43. Ittner LM, Wurdak H, Schwerdtfeger K, Kunz T, Ille F, Leveen P, et al. Compound developmental eye disorders following inactivation of TGFbeta signaling in neural-crest stem cells. *J Biol*. 2005;4(3):11.
44. Olaopa M, Zhou HM, Snider P, Wang J, Schwartz RJ, Moon AM, et al. Pax3 is essential for normal cardiac neural crest morphogenesis but is not required during migration nor outflow tract septation. *Dev Biol*. 2011;356(2):308–22.
45. Chang CP, Stankunas K, Shang C, Kao SC, Twu KY, Cleary ML. Pbx1 functions in distinct regulatory networks to pattern the great arteries and cardiac outflow tract. *Development*. 2008;135(21):3577–86.
46. Mundell NA, Labosky PA. Neural crest stem cell multipotency requires Foxd3 to maintain neural potential and repress mesenchymal fates. *Development*. 2011;138(4):641–52.
47. Mori-Akiyama Y, Akiyama H, Rowitch DH, de CB. Sox9 is required for determination of the chondrogenic cell lineage in the cranial neural crest. *Proc Natl Acad Sci U S A*. 2003;100(16):9360–65.
48. Bai Y, Wang J, Morikawa Y, Bonilla-Claudio M, Klysisik E, Martin JF. Bmp signaling represses Vegfa to promote outflow tract cushion development. *Development*. 2013;140(16):3395–402.
49. Hama H, Kurokawa H, Kawano H, Ando R, Shimogori T, Noda H, et al. Scale: a chemical approach for fluorescence imaging and reconstruction of transparent mouse brain. *Nat Neurosci*. 2011;14(11):1481–88.

Submit your next manuscript to BioMed Central and take full advantage of:

- Convenient online submission
- Thorough peer review
- No space constraints or color figure charges
- Immediate publication on acceptance
- Inclusion in PubMed, CAS, Scopus and Google Scholar
- Research which is freely available for redistribution

Submit your manuscript at
www.biomedcentral.com/submit



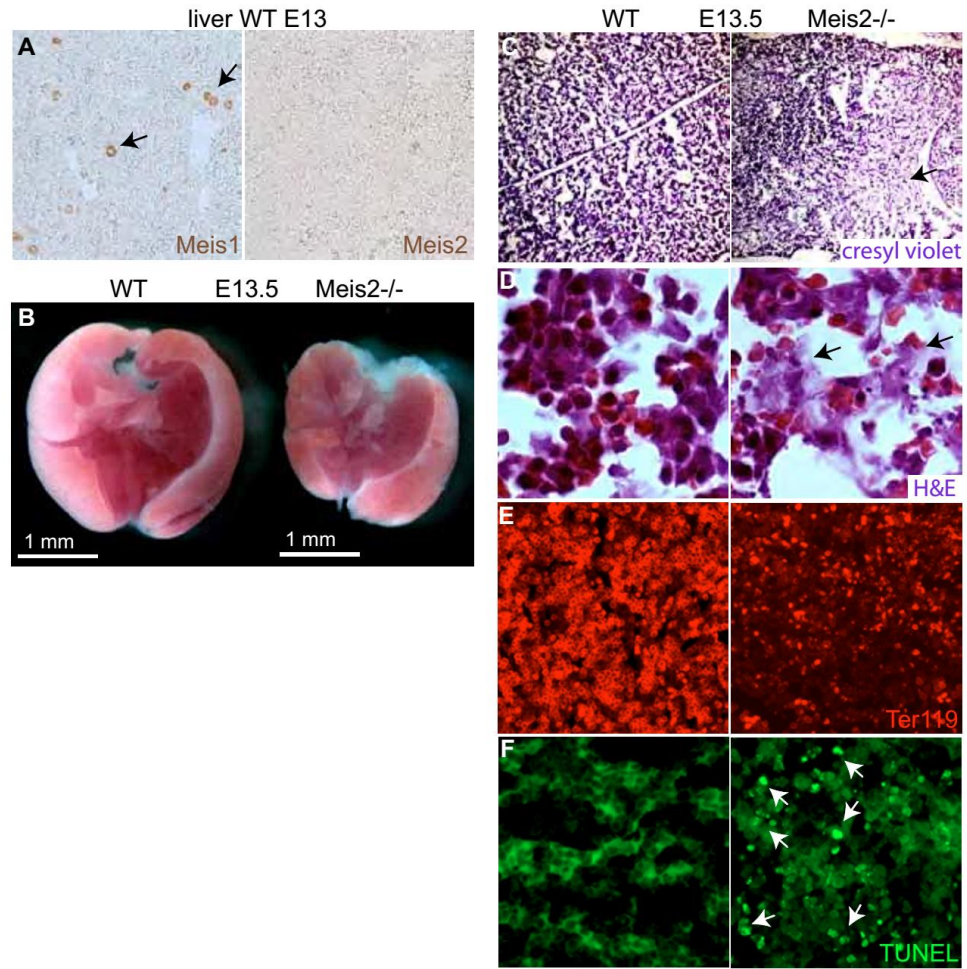


Fig. S1

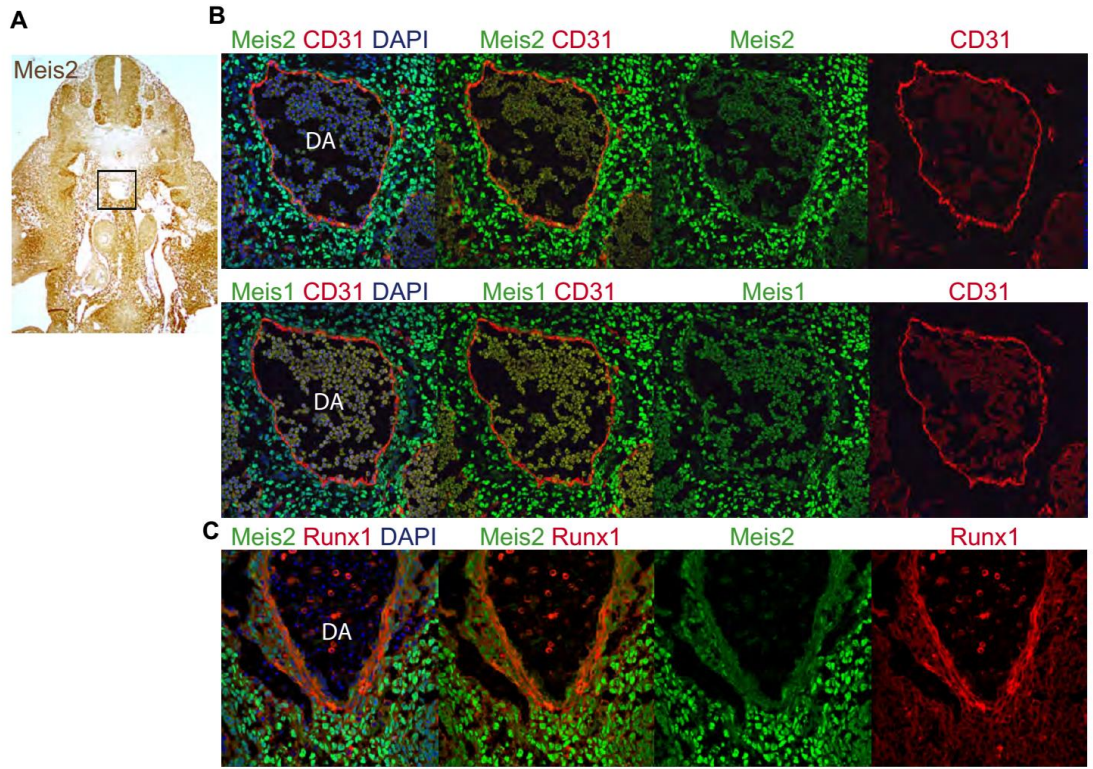


Fig. S2

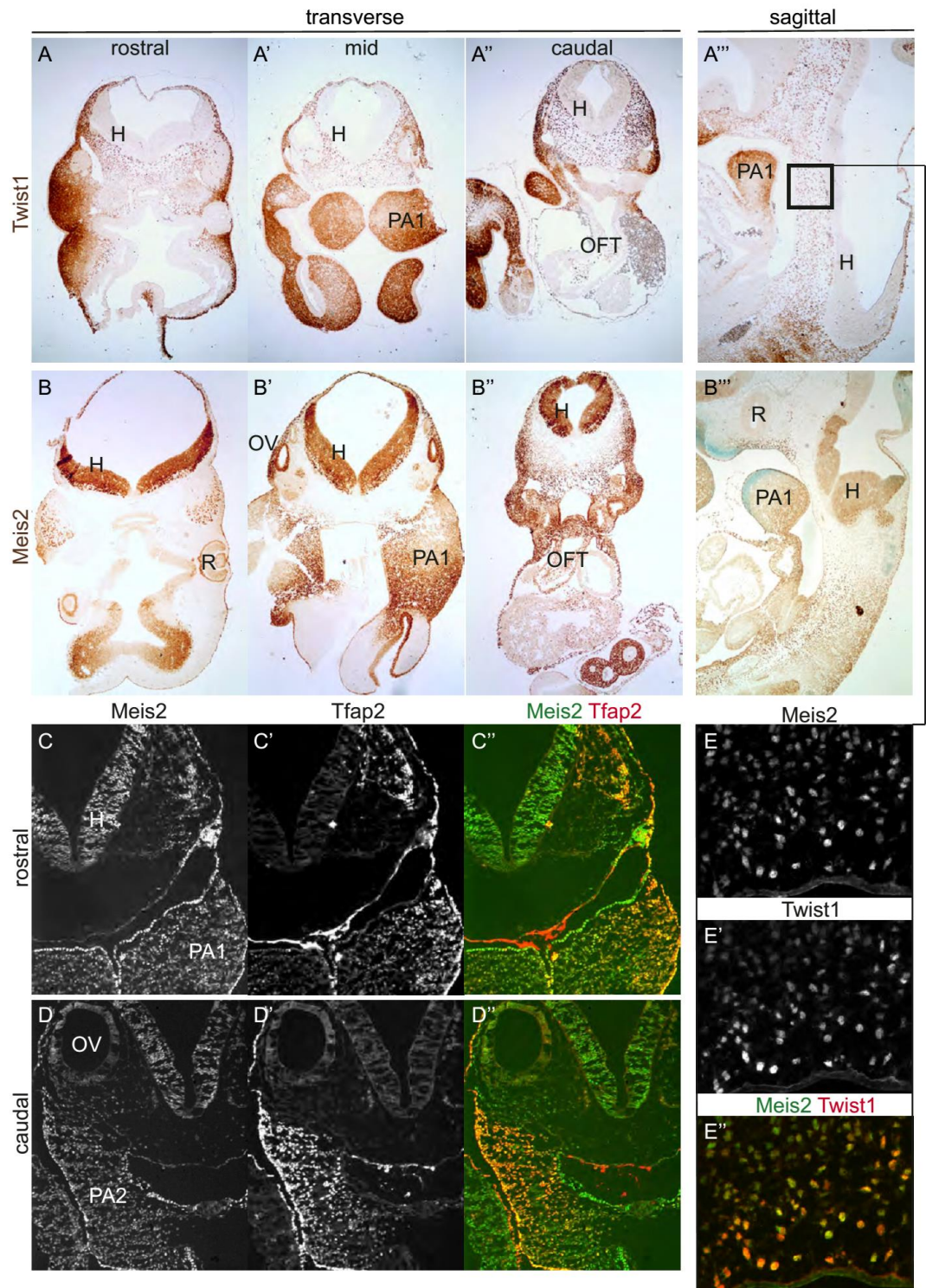


Fig. S3

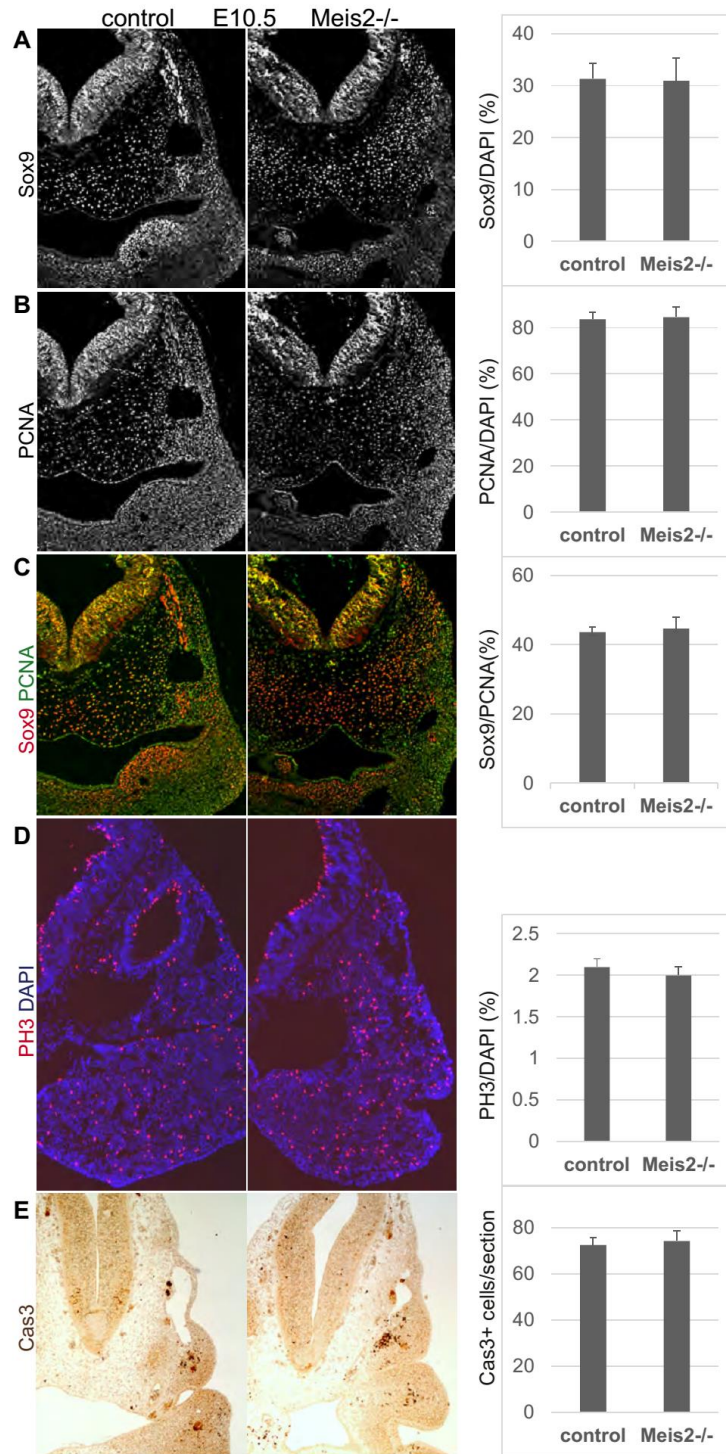


Fig. S4

Figure S1. Fetal liver in Meis2^{-/-} at E13.5 contains less erythrocytes and loses cell viability. (A) Meis2 is not expressed in the fetal liver in contrast to Meis1 that is readily detected by immunohistochemistry. (B) Comparison of the liver size in controls and Meis2^{-/-}. (C-D) Some regions in the mutant liver show disrupted cellular network and cell viability as revealed by cresyl violet and hematoxylin/eosin staining at a higher magnification. (E) Erythrocyte immunofluorescence using anti-Ter119 on liver sections at E13. (F) Apoptosis assay on liver sections using Cell Death Detection kit (Roche).

Figure S2. Meis2 is abundant in the mesenchyme of the aorta-gonad-mesonephros (AGM). (A) An overview of Meis2 immunohistochemistry in the trunk of mouse embryo at E10.5. (B) Immunofluorescent double-labeling of Meis2 or Meis1 and CD31 in AGM in which both proteins are absent in the endothelial wall (CD31+) of the dorsal aorta (DA) but strongly expressed in the surrounding mesenchyme. (C) Immunofluorescent double-labeling of Meis2 and Runx1 in the dorsal aorta at the AGM region showing no expression of Meis2 in circulating hemopoietic stem cells.

Figure S3. Meis2 is strongly expressed in migrating NCC and in mesenchymal cells at E10.5. (A-A'') Rostral to caudal transverse sections at a low-power magnification show the presence of Twist1 in mesenchymal cells around the otic vesicle, in PA1-PA2 and in the aortic sac. (A''') Sagittal view on E10.5 embryo stained for Twist1. (B-B'') Rostral to caudal transverse sections at a low-power magnification show Meis2 expression at E10.5 in mesenchymal cells, neuroectoderm, otic vesicle, PA1-PA2 and heart, (B''') sagittal view on Meis2 pattern. (C-D)

Immunofluorescent double-labeling of Meis2 and Tfp2 in a rostral region with PA1 (C-C') and in a caudal region with otic vesicle (D-D'') demonstrating a high number of NCC co-expressing both proteins. **(E-E'')** Immunofluorescent double-labeling of Meis2 and Twist1 in the region depicted by rectangle in (A'''). F, forebrain; H, hindbrain; OFT, outflow tract; OV, otic vesicle; PA1-2, pharyngeal arches; R, retina.

Figure S4. Proliferation and cell death of migrating NCC appears normal in Meis2^{-/-} mutants. **(A-C)** Sox9 and PCNA alone and double labeling (C) of transverse sections in the region of the otic vesicle in Meis2^{-/-} E10.5 embryos. Corresponding quantifications (as the percentage relative to all DAPI cells on a section) are shown to the right. **(D)** PH3 immunofluorescence and its counting with no significant difference in proliferating cells in the mutants. **(E)** Quantification of apoptosis assayed as the number of Cas3-positive cells after immunostaining of embryonic sections at E10.5 (brown). Bars represent the average from three experiment with standard deviations.

Mašek et al.

1 **Tcf711 protects the anterior neural fold from adopting the neural crest fate**

2 **Jan Mašek¹, Vladimír Kořínek¹, M. Mark Taketo², Ondřej Machoň^{1*}, Zbyněk Kozmik¹**

3 ¹Institute of Molecular Genetics, Academy of Science of the Czech Republic, Prague,
4 Czech Republic

5 ²Department of Pharmacology, Graduate School of Medicine, Kyoto University, Japan

6

7

8

9

10

11

12

13

14

15

16

17 **Keywords:** Tcf/Lef; Wnt signaling; neural crest; forebrain

18

19 *Corresponding author at: Institute of Molecular Genetics, Academy of Science of the
20 Czech Republic, Videnska 1083, Praha 4, 142 20, Czech Republic

21 E-mail: machon@img.cas.cz

22

23

24 **Summary statement**

25 Tcf711 mediated repression of the Wnt/ β -catenin pathway at the anterior neural tissue,
26 protects the cell identity of the prospective prosencephalon from conversion to the neural
27 crest.

Mašek et al.

28 **Abstract**

29 The neural crest (NC) is crucial for evolutionary diversification of vertebrates. NC cells are
30 induced at the neural plate border (NPB) by a coordinated action of several signaling
31 pathways including Wnt/ β -catenin. NC cells are normally generated in posterior NPB,
32 whereas the anterior neural fold is devoid of NC cells. Using the mouse model, we show
33 here that active repression of Wnt/ β -catenin signaling is required for maintenance of
34 neuroepithelial identity in the anterior neural fold and for inhibition of NC induction.
35 Conditional inactivation of Tcf711, a transcriptional repressor of Wnt target genes, leads to
36 aberrant activation of Wnt/ β -catenin signaling in the anterior neuroectoderm and its
37 conversion into the NC. This reduces the developing prosencephalon without affecting
38 the anterior-posterior neural character. Thus, Tcf711 defines the border between the NC
39 and the prospective forebrain via restriction of the Wnt/ β -catenin signaling gradient.

40 **Introduction**

41 Neural crest (NC) cells are vertebrate-specific, multipotent, highly migratory cells
42 originating from the ectoderm of the neural plate border (NPB). NC cells possess the
43 ability to differentiate into a wide range of cell types including the bone and cartilage of
44 the skull, sensory neurons, outflow tract of the heart, enteric ganglia and pigment cells.
45 During embryogenesis, a combination of gene expression driven by Wnt, FGF and BMP
46 pathways determine the future characteristics of the head ectoderm, transforming it either
47 into placodes, neural plate, epidermis or NC cells (Garnett et al., 2012; Groves and
48 LaBonne, 2014; Litsiou et al., 2005; Simoes-Costa and Bronner, 2015; Steventon et al.,
49 2009). Wnt/ β -catenin signaling represents one of the most extensively studied signaling
50 cascade. Binding of secreted Wnt proteins to their Frizzled receptors and their Lrp5/6 co-
51 receptors initiates a complex cascade of intracellular events leading to the stabilization of
52 β -catenin. Stabilized β -catenin accumulates in the cytoplasm and enters the nucleus
53 where it binds to the Tcf/Lef family of transcription factors, thereby regulating the
54 expression of Wnt target genes (Clevers and Nusse, 2012;
55 <http://web.stanford.edu/group/nusselab/cgi-bin/wnt/>).

Mašek et al.

56 Four Tcf/Lef genes have been identified in vertebrates; *Lef1* (alias *Lef1*) (Travis et
57 al., 1991), *Tcf7* (alias *Tcf1*) (van de Wetering et al., 1991), *Tcf711* and *Tcf712* (alias *Tcf3*
58 and *Tcf4*) (Castrop et al., 1992). Tcf/Lefs share several characteristic protein features,
59 such as the N-terminal β -catenin binding motif, GRG motifs for binding of Groucho/TLE
60 co-repressors, and the HMG box containing the DNA binding domain. *Tcf7* and *Tcf712*
61 also contain a C-clamp, a second DNA binding motif that further modulates gene target
62 specificity (Cadigan and Waterman, 2012). Distinct expression patterns of individual
63 Tcf/Lefs and their unequal capability to activate/repress Wnt target genes, represent the
64 ultimate regulation step of the Wnt/ β -catenin signaling pathway. *Tcf711*, expressed in the
65 anterior ectoderm at E7.5 and in the anterior neural fold (ANF) at E8.5 of the developing
66 mouse embryo (Korinek et al., 1998; Merrill et al., 2004), is the least potent activator but
67 the strongest repressor from the whole family (Cole et al., 2008; Liu et al., 2005; Ombrato
68 et al., 2012). *Tcf711*-deficient mice, that display duplicated axis and a severely reduced
69 anterior part of the embryo, die shortly after gastrulation (Merrill et al., 2004). *Tcf711*
70 inactivation appears to allow Wnt/ β -catenin signaling to spread towards the anterior
71 neural fold in both zebrafish and mouse. This leads to a deficiency in expression of the
72 ANF specific genes accompanied with severe defects in head formation (Andoniadou et
73 al., 2011; Dorsky et al., 2003; Kim et al., 2000). All these data have been interpreted in a
74 manner consistent with the repression of Wnt signaling in the ANF being required for A-P
75 axis determination of the neural tube.

76 Experiments in *Xenopus*, zebrafish and chicken have shown a requirement for
77 Wnt/ β -catenin signaling from the earliest steps of neural crest development - at first
78 during gastrulation, when Wnt/ β -catenin signaling drives the expression of the NC
79 specifier genes *Pax3* (Bang et al., 1999; Garnett et al., 2012; Taneyhill and Bronner-
80 Fraser, 2005; Zhao et al., 2014), *FoxD3* (Janssens et al., 2013) and *Gbx2* (Li et al.,
81 2009), later during NC maintenance (Kleber et al., 2005; Steventon et al., 2009) and the
82 epithelial-to-mesenchymal transition (EMT), via triggering the *Slug* gene expression
83 (Burstyn-Cohen et al., 2004; Sakai et al., 2005; Vallin et al., 2001). Compared to non-
84 mammalian experimental models, a clear picture about the role of Wnt/ β -catenin
85 signaling in early NC cell populations in mammals is absent. This is partly caused by a
86 lack of appropriate Cre drivers for the early pre-migratory NC lineage. The widely used

3

Mašek et al.

87 Wnt1-Cre mouse targets the NC population after its induction and specification (Danielian
88 et al., 1998; Lewis et al., 2013). Depletion of β -catenin using Wnt1-Cre leads to
89 malformations of the craniofacial structures, accompanied with a deficiency in sensory
90 neurons (Brault et al., 2001; Gay et al., 2015). Similar phenotypic changes have been
91 observed in compound Wnt1/Wnt3a mutants that also show impaired formation of
92 sensory neurons, and defects in several bones and cartilage derived from the NC (Ikeya
93 et al., 1997). Ectopic Wnt1-Cre driven expression of stabilized β -catenin (β -cat^{Ex3fl/+})
94 results in excessive differentiation of NC progenitors into NeuroD and Brn3a-positive
95 sensory neurons, thus limiting NC multipotency (Lee et al., 2004). Collectively, these data
96 confirm the requirement of Wnt/ β -catenin signaling in NC maintenance and differentiation
97 however, they do not clarify the role of Wnts in NC induction and specification. The
98 apparent inconsistency may be explained in two ways; either the signaling pathway
99 network governing NC induction, and specification differs between mouse and other
100 species (Barriga et al., 2015) or, more probably, the Wnt1-Cre driver targets the already
101 specified NC, thus not allowing the investigation of the earlier events of NC development.

102 The aim of our work was to investigate the role of Wnt/ β -catenin signaling in the
103 early development of the mammalian NC. We used a Cre-line derived from a NC inducer
104 gene, Tfp2 α (Ap2 α -Cre) (Macatee et al., 2003), in order to achieve conditional deletion
105 of Tcf711 in the earliest possible steps of the NC development. Conditional inactivation of
106 Tcf711 leads to trans- differentiation of ANF into NC cells accompanied with a loss of
107 anterior neural markers. Our data suggest that Tcf711, acting as a Wnt/ β -catenin
108 repressor, is required to maintain the anterior neural character by restricting the
109 expansion of the Wnt-induced NC cells.

110 RESULTS

111 AP2 α -Cre mediated deletion of Tcf711 during mouse NC specification results in 112 exencephaly.

113 Tcf711 is detected in the developing mouse ectoderm prior to gastrulation, and
114 later at E7.5, and it is expressed in the anterior ectoderm and mesoderm (Korinek et al.,
115 1998; Merrill et al., 2004). We characterized the expression of *Tcf711* during neurulation,

Mašek et al.

116 using whole mount *in situ* hybridization. *Tcf711* mRNA was detected in the anterior neural
117 plate at the 1 somite pair (s) stage, being further restricted to the ANF region and along
118 the anterior NPB with the progress of neurulation 3-4s (Fig. 1A). We next wanted to relate
119 the expression pattern of *Tcf711* to that of known NC-specific genes and the area of
120 Wnt/ β -catenin signaling. *Tfap2a* is one of the key genes involved in the NC induction,
121 while *FoxD3*, *Sox9*, *Sox10* have been linked with the NC specification (Groves and
122 LaBonne, 2014; Simoes-Costa and Bronner, 2015). During neurulation, the Tfap2a
123 protein is continuously expressed along the whole NPB (Fig. 1B). First *Sox9* and *FoxD3*
124 transcripts were detected in the neural plate as early as at the 1-2s stage, at 3-4s were
125 expressed robustly in two stripes along the anterior neural plate border (Figs 1C, S1A).
126 The onset of *Sox10* mRNA was detected later (4-5s) and slightly more caudally, in a very
127 similar pattern as the expression of *Sox9* (Fig. S1B). To map the activity of the Wnt/ β -
128 catenin pathway, we used the BAT-gal reporter mice (Maretto et al., 2003). The BAT-gal
129 signal, detected by immunostaining, spread from the 2-3s stage across the prospective
130 mesencephalon and metencephalon, but not reaching the ANF at the 4-5s stage (Fig.
131 1D). In conclusion, *Tcf711* expression in the ANF is reciprocal to that of *Sox9*, *FoxD3*,
132 *Sox10* and BAT-gal, that resides in the caudal areas of the neural plate, but it overlaps
133 with Tfap2a, lining the whole NPB.

134 In order to study the function of Tcf711 during NC induction and specification, we
135 inactivated Tcf711 by crossing Tcf711 conditional knock-out mice (EUCOMM) with AP2 α -
136 IRESCre (AP2 α -Cre) transgenics (Macatee et al., 2003). Tracing of the AP2 α -Cre-driven
137 recombination using the Rosa26^{EYFPfl/+} reporter strain revealed the first EYFP-positive
138 cells scattered throughout the embryo at E7.0 (Fig. 1E). The EYFP signal became
139 focused along the entire NPB at the 4s stage with the highest levels detected rostrally, in
140 the neural- and non-neural ectoderm of the ANF at the 5s stage. AP2 α -Cre most probably
141 mediates the recombination in the entire NC population as demonstrated by complete co-
142 localization of double immunofluorescence of EYFP-positive cells and Sox10-positive NC
143 cells in AP2 α -Cre;Rosa26^{EYFPfl/+} embryos at the 10s stage. At E10.5, the EYFP signal
144 was present in NC derivatives (brachial arches, dorsal root ganglia and sensory neurons),
145 the head ectoderm, lens placodes, and in the anterior telencephalon (Fig. 1E, Fig. S1C).

Mašek et al.

146 In AP2 α -Cre;Tcf711^{fl/fl} mutants, *Tcf711* mRNA was completely lost, whereas control
147 embryos showed high levels of transcripts along the anterior NPB including the ANF at
148 the 5s stage (Fig. 1F-G). At this stage, phenotypical changes following *Tcf711* deletion
149 became apparent; the shape of neural folds changed from rounded into more a narrow
150 morphology and the neural plate expanded laterally at the prosencephalic-mesencephalic
151 boundary (dashed lines in frontal views in Fig. 1F,G). At later stages (E10.5), we
152 observed a variability in the penetrance of morphological changes among individual
153 mutants. Therefore, we decided to classify the defects into two categories: (i) a strong
154 phenotype, represented by a severe reduction of the telencephalic tissue and
155 exencephaly (arrow Fig. 1H); and (ii) a mild phenotype, with reduced telencephalon and
156 bilateral anophthalmia (arrowhead Fig. 1H). Quantification of phenotype incidence,
157 between E10.5-E13.5, revealed that the strong phenotype was present in 60.5% and the
158 mild phenotype in 39.5% of the analyzed embryos (n=38) (Fig. 1I). Mutant embryos with
159 the strong phenotype did not survive beyond E13.5, exhibiting massive exencephaly and
160 severe defects in craniofacial structures (Fig. S1D, E). These data demonstrate that
161 Tcf711 function in the ANF is crucial for the development of the mouse forebrain.

162

Mašek et al.

163 **Tcf711 is required for the expression of anterior neural markers**

164 Tcf711 has been implicated in A-P patterning of the developing brain in both
165 zebrafish and mouse since its loss-of-function mutations result in severe reductions of
166 anterior neural regions, accompanied with apparent expansion of midbrain and hindbrain
167 markers towards the anterior (Dorsky et al., 2003; Merrill et al., 2004). In contrast to
168 published data, we did not observed any shift in mRNA expression of the core regulators
169 of the midbrain-hindbrain boundary (MHB). *Fgf8*, *Gbx2* and *Wnt1* were expressed
170 anteriorly when comparing Tcf711 conditional mutant embryos and controls at E9.5
171 (arrowheads in Figs 2A-B', S3C). Remarkably, we observed a progressive loss of the
172 posterior prosencephalon marker *Tcf712* (*Tcf4*) mRNA (Fig. 2C-C'), illustrating the
173 gradual loss of anterior neural tissue in AP2 α -Cre;Tcf711^{fl/fl} mutants with mild (C') or
174 strong (C'') phenotype at E9.5. Furthermore, the expression of the ANF specific
175 transcripts, *Six3* (Lagutin et al., 2003), *FoxG1* (Hanashima et al., 2004) and *Fgf8* (Meyers
176 et al., 1998) was lost or strongly reduced in mutants at the 8s stage (Fig. 2D-F'). Next we
177 tested whether the ANF cells affected by Tcf711 deletion retained their neural character.
178 Reduced expression of the neural marker *Sox2*, revealed by RNA *in situ* hybridization,
179 uncovered an expansion of *Sox2* negative cells along the whole lateral border of the ANF
180 in AP2 α -Cre;Tcf711^{fl/fl} mutants (Fig. 2G,G'), suggesting that the cells had lost their neural
181 identity.

182 **Tcf711 deletion results in aberrant trans-differentiation of the ANF cells into the NC**

183 NC cells need to lose their neuroepithelial character in order to undergo EMT and
184 migrate towards their target destinations. We decided to investigate the expression of the
185 transcription factors *FoxD3*, *Sox9* and *Sox10*, key regulators of the NC specification,
186 responsible for initiation of EMT in *Xenopus* and chicken (Cheung et al., 2005; Dottori et
187 al., 2001; Liu et al., 2013), in the absence Tcf711. As can be seen from the whole-mount
188 immunostaining, *Sox9* positive NC cells expanded into the *Sox1* positive ANF region in
189 AP2 α -Cre;Tcf711^{fl/fl} mutants compared with controls at the 5s stage (Fig. 3A). Examination
190 under higher magnification showed decreased neural *Sox1* staining towards the anterior
191 part of the mutant embryo. A frontal view on the same embryos clearly showed ectopic
192 *Sox9*-positive NC cells along the ANF in mutants (Fig. 3B). This was further confirmed by

7

Mašek et al.

193 *in situ* hybridization of *Sox9* mRNA (arrowhead Fig. S2A). Consistently, the expression of
194 *Foxd3* mRNA also shifted anteriorly in mutant embryos compared to controls at the 10s
195 stage (Fig. 3C). Later at E9.0, aberrant *Foxd3* mRNA was detected in the rostral part of
196 the head in mutants (arrowhead Fig. S2B), while it was completely absent in controls.
197 Expression of *Sox10* mRNA was apparently delayed in the absence of Tcf711, being
198 barely detectable at the 6s stage (Fig. 3D). Two days later, at E9.5, however, RNA *in situ*
199 hybridization revealed robust ectopic expression of *Sox10* in the anterior part of the head
200 of mutant embryos (arrowhead Fig. 3D). Interestingly, we also observed a cell fate shift,
201 characterized by the change from Sox1 to Sox9, in caudal neural tissue. Coronal
202 sectioning of the developing hindbrain at E9.0 also uncovered aberrant Sox9-
203 positive/Sox1-negative cells in the mutants (arrowheads Fig. S2C). Taken together, the
204 expression of several genes responsible for the NC specification and EMT initiation is
205 expanded towards ANF in the AP2 α -Cre;Tcf711^{fl/fl} mutants, suggesting that Tcf711
206 maintains the neuroepithelial character of the ANF and restricts spreading of NC within
207 the anterior head.

208 **Trans-differentiation of the ANF is driven by aberrant Wnt/ β -catenin signaling**

209 Tcf711 is a very efficient repressor of Wnt/ β -catenin signaling target genes, as has
210 been shown in both mouse embryonic stem cells and *in vivo* (Cole et al., 2008; Shy et al.,
211 2013; Wu et al., 2012). Gain- and loss-of-function experiments in non-mammalian
212 vertebrates have shown that the Wnt/ β -catenin pathway is required for physiological, and
213 sufficient for ectopic, induction and expansion of the NC (Garcia-Castro et al., 2002;
214 Heeg-Truesdell and LaBonne, 2006; Steventon et al., 2009; Taneyhill and Bronner-
215 Fraser, 2005; Wu et al., 2005). In our transient reporter assays using the SuperTopFlash
216 reporter in HEK293 cells, Tcf711 was able to compete with other Tcf/Lefs, reducing Wnt
217 reporter signal significantly (Fig. S3A). Therefore we asked, whether the expansion of NC
218 cells in AP2 α -Cre;Tcf711^{fl/fl} mutants, was caused by upregulation of Wnt/ β -catenin
219 signaling. We crossed BAT-Gal reporter mice with Tcf711 conditional mutants and stained
220 whole-mount embryos with anti-galactosidase and anti-Sox9 antibodies.

221 As expected, the Wnt reporter BAT-gal immunofluorescence expanded anteriorly
222 in the AP2 α -Cre;Tcf711^{fl/fl} mutants (arrow, Fig. 4A). This was accompanied with a high

Mašek et al.

223 number of ectopic Sox9-positive cells, as clearly visible from the frontal view of the 8s
224 stage embryos (white arrowheads, Fig. 4A). The coexpression of Sox9 and BAT-gal
225 positive cells does not seem to be aberrant, as cross-sections from the 8s old wild-type
226 embryos showed large overlaps between the Sox9 and BAT-gal immunofluorescence
227 (Fig. S3B), indicating that Sox9 may be induced by Wnts. Furthermore, expression of *Sp5*
228 mRNA, a known Wnt/ β -catenin target gene, was also upregulated and expanded rostrally
229 in the mutant embryos at 6s stage (arrowheads, Fig. 4B), confirming the ectopic increase
230 of the Wnt/ β -catenin signaling activity in the anterior neuroectoderm. Apart from its role in
231 MHB formation (McMahon and Bradley, 1990; Thomas and Capecchi, 1990) is *Wnt1*
232 required also during NC development (Ikeya et al., 1997; Saint-Jeannet et al., 1997).
233 Interestingly, we found aberrant *Wnt1* mRNA expression in the ANF of the Tcf711 mutants
234 at the 5-6s stage (Fig. 4C). The ectopic pattern of *Wnt1* mRNA expression along the NPB
235 of the prosencephalon was even more obvious later, at E9.0 (arrowheads, Fig. 4C). We
236 observed no difference in *Wnt1* mRNA expression in the MHB between controls and
237 Tcf711 mutants (arrowheads, Fig. S3C) at the same stage, suggesting that the aberrant
238 expression of *Wnt1* reflects the NC phenotype, rather than changes in A-P patterning.

239 To confirm that the phenotype observed in AP2 α -Cre;Tcf711^{fl/fl} mutants resulted
240 from an aberrant activation of the Wnt/ β -catenin pathway, we activated the signaling
241 using β -cat ^{Δ Ex3^{fl/fl}} mice (Harada et al., 1999), in which a truncated, non-degradable form of
242 β -catenin is produced upon AP2 α -Cre-mediated recombination. The AP2 α -Cre; β -
243 cat ^{Δ Ex3^{fl/+}} embryos exhibited neural tube closure defects and did not survive beyond
244 E10.5. The crossing of the BAT-gal reporter into AP2 α -Cre;Tcf711^{fl/fl} mutants revealed
245 activation of the reporter in the forebrain, which was even more pronounced in AP2 α -
246 Cre; β -cat ^{Δ Ex3^{fl/+}} mutants that also showed a strong over-activation of the signal in most of
247 the head ectoderm when compared with controls (Fig. 4D-F). A lateral view of the Tcf711
248 and β -cat ^{Δ Ex3^{fl/+}} mutants clearly showed an aberrant population of BAT-gal-positive cells
249 migrating towards the branchial arches (arrowheads, Fig. 4D'-F'). Cross sections of these
250 embryos uncovered aberrant BAT-gal staining in the forebrain of both Tcf711 and β -
251 cat ^{Δ Ex3} mutants (Fig. 4D''-F'').

Mašek et al.

252 Next we assayed the EMT using immunofluorescence of neuroepithelial cells
253 marked with N-cadherin and migrating NC cells labelled with Sox9 antibodies. In control
254 embryos, we observed only a thin layer of Sox9 positive cells between the N-cadherin
255 positive forebrain tissue and the epidermis. The hindbrain in controls labeled with N-
256 cadherin was found to be completely devoid of Sox9 positive cells at E9.5. (Fig. 4G). In
257 contrast, AP2 α -Cre;Tcf7l1^{fl/fl} mutants clearly displayed aberrant Sox9-positive cells in the
258 hindbrain prior to EMT (arrowheads, Figs 4H, S2C). Concomitantly, N-cadherin
259 expression was weaker in the anterior forebrain and the dorsal hindbrain mutants with
260 “strong” phenotype (arrows Fig. 4H). Intriguingly, the same analysis of AP2 α -Cre; β -
261 cat^{Ex3fl/+} embryos revealed that almost the whole mutant forebrain converted into Sox9
262 positive NC. Similarly to Tcf7l1 conditional mutants, we also detected aberrant Sox9
263 expressing cells in the hindbrain, accompanied with a massive decrease in the levels of
264 N-cadherin (arrows, Fig. 4I). Further, protein levels of the Wnt/ β -catenin transcriptional
265 activator and target gene Lef1 (Galceran et al., 1999; Kratochwil et al., 2002; Liu et al.,
266 2005), were increased in the forebrain of the Tcf7l1 mutants in comparison with controls
267 (Fig. 4J,K). β -cat^{Ex3} mutants displayed very strong upregulation of Lef1 in the
268 mesenchyme adjacent to the hindbrain as well as in the forebrain (Fig. 4L). Whole-mount
269 immunofluorescence of wild-type embryos revealed colocalization of Lef1 and Sox10-
270 positive cells at the 8s stage (arrowhead, Fig. S3C). It should be noted that in addition to
271 the effects on NC population, the strong activation of the Wnt/ β -catenin pathway in the
272 AP2 α -Cre; β -cat^{Ex3fl/+} mutants disorganized both the A-P patterning of the neural tissue
273 and the non-neural ectoderm surrounding the NC. This was clearly visible from the
274 expansion of *Gbx2* and *Fgf8* mRNA at E9.5 (Fig. S3E,F). Taken together, deletion of
275 Tcf7l1 resulted in an ectopic activation of the Wnt/ β -catenin pathway, suppression of
276 neuroepithelial character and premature initiation of NC cell fate. Similar observations
277 were made in conditional AP2 α -Cre; β -cat^{Ex3fl/+} mutants that yielded even more profound
278 changes in the expression of described cell markers and in larger areas than in Tcf7l1
279 mutants.

280 **The phenotype can be rescued with a truncated form of TCF4 but not with Tcf7l1**
281 **fused with β -catenin**

10

Mašek et al.

282 Our data suggest that the loss of Tcf711-mediated repression of Wnt targets is the
 283 primary cause of NC cell fate expansion. In order to verify this hypothesis, we performed
 284 rescue experiments using two mouse strains, conditionally expressing either dominant
 285 Tcf repressor or activator. As a dominant repressor we used a mouse strain
 286 $Rosa26^{dnTCF4fl/+}$ containing the N-terminally truncated form of the human TCF7L2 targeted
 287 into the ROSA26 locus 3' to the lox-STOP TdTomato (TdT) cassette (originally referred to
 288 as $Rosa26^{+/tdTomato}$). This form cannot bind β -catenin and thus acts as dominant repressor
 289 of Wnt/ β -catenin targets (Janeckova et al., in press). Secondly, we generated the mouse
 290 strain $Rosa26^{ct\beta cat-Tcf711fl/+}$, allowing conditional expression of full-length mouse Tcf711
 291 fused with the transactivation domain of β -catenin (aa696-781), analogous to the
 292 described Cat-Lef fusion (Hsu et al., 1998). This construct, that mimics the β -catenin
 293 binding to Tcf711, was able to deliver activation of the Wnt reporter (Fig. S4A). Details
 294 about the strain generation and characterization are present in the supplementary (Fig.
 295 S4B-G). Following Cre recombination, the TdT cassette is excised, allowing production of
 296 either dnTCF4 or ct β cat-Tcf711 mRNA (Fig. 5A).

297 We crossed the $Tcf711^{fl/fl};Rosa26^{dnTCF4fl/fl}$ and $AP2\alpha-Cre;Tcf711^{fl/+}$ strains and
 298 evaluated the strength of the phenotype in $AP2\alpha-Cre;Tcf711^{fl/fl};Rosa26^{dnTCF4fl/+}$ compound
 299 mutants at E10.5 stage. Intriguingly, overexpression of the dnTCF4 was able to reduce
 300 the occurrence of the strong phenotype by more than half (27.3%), compared with the
 301 60.5% incidence in the $AP2\alpha-Cre;Tcf711^{fl/fl}$ mutant. The effect of the rescue on NC
 302 population was further analyzed by *in situ* hybridization showing no or very little ectopic
 303 *Sox10* mRNA in the $AP2\alpha-Cre;Tcf711^{fl/fl};Rosa26^{dnTCF4fl/+}$ 'rescued' mutants (Fig. 5B,D). On
 304 the contrary, the β cat-Tcf711 fusion protein showed significantly ($P=0.049$, Fishers test)
 305 decreased capability to rescue the phenotype than the dnTCF4, as demonstrated by
 306 85.7% of analyzed embryos displaying the strong phenotype in the $AP2\alpha-Cre;Tcf711^{fl/fl};$
 307 $Rosa26^{ct\beta cat-Tcf711fl/+}$ compound mutants. Expression of ct β cat-Tcf711 was also unable to
 308 reduce the aberrant, *Sox10* mRNA positive, NC population (Fig. 5C,D). In summary,
 309 using transgenic mice strains, we have genetically confirmed that Tcf711, acting as a
 310 repressor of Wnt/ β -catenin signaling, protects anterior neural tissue from conversion to a
 311 NC cell fate.

Mašek et al.

312 **Discussion**

313 **How does the progressive activation of Wnt/ β -catenin pathway affect development**
314 **of the anterior neural tissue and neural crest?**

315 Spatio-temporal regulation of Wnt/ β -catenin pathway activation, required for proper
316 development of the prosencephalon, is secured by expression of several ANF specific
317 negative regulators of the Wnt/ β -catenin signaling. Our data (Figs 4,5,S3), and evidence
318 from others (Cole et al., 2008; Liu et al., 2005; Ombrato et al., 2012; Wu et al., 2012)
319 characterize Tcf711 as a Wnt/ β -catenin target gene repressor, implicating aberrant
320 activation of the Wnt/ β -catenin pathway as the cause of strong A-P patterning defects
321 that follow Tcf711 deficiency both in zebrafish (Dorsky et al., 2003; Kim et al., 2000) and
322 mouse (Merrill et al., 2004). In zebrafish, the Tcf711a loss-of-function in headless (*hdl*)
323 mutants, as well as MO-mediated knock-down of Tcf711a and Tcf711b variants, result in
324 the expansion of MHB markers, *Pax2.1* and *Gbx1* mRNA expression anteriorly,
325 accompanied by the loss of *Six3* and *Rx3* expression (Dorsky et al., 2003). The Tcf711
326 mutants in mouse also displayed the expansion of the midbrain mRNA marker *Engrailed*,
327 joined with the downregulation of *Hesx1* expression (Merrill et al., 2004). Similarly, the
328 loss of anterior neural tissue in mouse follows deletion of *Dkk1* (Mukhopadhyay et al.,
329 2001), *Six3* (Lagutin et al., 2003), *Hesx1* (Andoniadou et al., 2007) and *ICAT* (Sato et
330 al., 2004) and has been interpreted as a defect in A-P patterning induced by aberrant
331 Wnt/ β -catenin signaling. We contend that this is too generalized view and that, in the
332 context of the ANF phenotypes, is only partially true. In *Xenopus*, low levels of ectopic
333 Wnt/ β -catenin activation enrich the NC population without affecting A-P patterning, while
334 high doses affect both (Wu et al., 2005). This might be also valid for mammals, as mice
335 carrying ENU-induced activating point-mutations in Lrp6 and β -catenin display a gradual
336 loss of the prospective prosencephalon, depending on the strength of the Wnt/ β -catenin
337 pathway overactivation, but does not manifest a shift of posterior markers towards the
338 anterior part of the embryo (Fossat et al., 2011). Furthermore, compound deletion of one
339 *Hesx1* allele and both alleles of *Tcf711* in mouse, using prosencephalon-specific *Hesx1*-
340 Cre, results in the aberrant activation of Wnt/ β -catenin signaling, accompanied with loss
341 of anterior neural tissue without affecting the A-P patterning (Andoniadou et al., 2011).

12

Mašek et al.

342 Similarly, we did not detect any changes in the expression of the MHB markers *Fgf8* or
343 *Gbx2* in AP2 α -Cre;Tcf711^{fl/fl} mutants. Nevertheless, we do observe a gradual loss
344 (depending on the strength of the phenotype) of the posterior prosencephalon marker
345 *Tcf712* and the ANF markers *Six3*, *Fgf8* and *FoxG1* (Fig. 2). This was accompanied by the
346 expansion of *Sox9*, *FoxD3* and *Sox10*-positive NC populations along the NPB anteriorly
347 (Figs 3,S2). Therefore we conclude that the loss of Tcf711 mediated repression of Wnt
348 target genes in the AP2 α -Cre;Tcf711^{fl/fl} mutants allows the gradient of Wnt ligands to
349 influence cell fate in a wider region of the ANF than in controls, without having an effect
350 on A-P patterning. This is not the case in AP2 α -Cre; β -cat^{Ex3fl/+} mutants, in which ectopic
351 stabilization of β -catenin facilitates strong over-activation of Wnt/ β -catenin driven
352 transcription, affecting both NC (Fig. 4) and A-P patterning (Fig. S3). Notably, we
353 observed effects on the population of undifferentiated *Sox9*-positive NC cells in AP2 α -
354 Cre; β -cat^{Ex3fl/+} mutants at E9.5 and earlier (data not shown). In contrast, the imbalance in
355 NC differentiation observed in Wnt1-Cre/ β -cat^{Ex3fl/+} mutants occurred one day later at
356 E10.5 (Lee et al., 2004). This merely reflects the earlier onset of the AP2 α -Cre (Macatee
357 et al., 2003) mediated Cre recombination (Fig. 1) than in the widely used Wnt1-Cre
358 (Danielian et al., 1998; Lewis et al., 2013), making AP2 α -Cre a more suitable tool for
359 studying early events of NC development. Our data provide clear evidence for a notably
360 earlier role of the Wnt/ β -catenin pathway in NC development in regard to previously
361 published findings from the mouse model showing the requirement of the Wnt/ β -catenin
362 pathway in NC maintenance and differentiation (Brault et al., 2001; Gay et al., 2015; Lee
363 et al., 2004).

364 The effects of the Tcf711 deficiency in mice and zebrafish on NC development
365 were not, until now, characterized in detail. Analogously to the NC expansion in AP2 α -
366 Cre;Tcf711^{fl/fl} mutant mice (Figs 3,4,S2), we observed ectopic expression of *FoxD3*, *Pax3*
367 and *Sox9* mRNA along the entire anterior NPB upon Tcf711a MO-mediated knock-down
368 in zebrafish (Fig. S2D), implicating the conservation of Tcf711 function across vertebrate
369 species. In accord with this, the enrichment of the NC population, marked by the
370 expansion of *Snail2* mRNA expression towards the anterior portion of the embryo, follows
371 the MO-mediated knock-down of *Dkk1* in *Xenopus* (Carmona-Fontaine, 2007). In mouse,
372 *Hesx1* mutants display expansion of Wnt target genes as well as the NC mRNA markers

13

Mašek et al.

373 *Pax3* and *FoxD3* anteriorly (Andoniadou et al., 2007) and the loss of the Wnt inhibitor
 374 *Dkk1* leads to the expansion of the NC mRNA marker *Sox10* (Carmona-Fontaine et al.,
 375 2007), completely in agreement with the interpretation of the data presented here.
 376 Furthermore, mutual dispensability of these factors was demonstrated in zebrafish, where
 377 injection of either *Six3* or *Hesx1* mRNA rescued the *hdl* phenotype (induced by *Tcf711a*
 378 deletion) (Andoniadou et al., 2011; Lagutin et al., 2003).

379 In summary, collective evidence point towards a coordinated expression of several
 380 Wnt/ β -catenin pathway inhibitors in the anterior neuroectoderm that together define,
 381 under physiological conditions, a spatial border to the expansion of the NC. Similarity in
 382 the phenotypes following their deficiency signifies that the ANF region is very close to a
 383 threshold of the NC inducing Wnt/ β -catenin activation. Therefore, from the evolutionary
 384 perspective, attenuation of the sensitivity to Wnt/ β -catenin signaling in the ANF region by
 385 fine-tuning the expression levels of Wnt signaling inhibitors may represent a very
 386 sensitive tool that allows simultaneous modification of two prominent features of the
 387 vertebrates, the neural crest and the forebrain.

388 **Key question remains: which Wnt/ β -catenin target genes act as NC inducers?**

389 Our analysis of the AP2 α -Cre;*Tcf711*^{fl/fl} mutants identify *Tcf711* as a negative
 390 regulator of the NC population, suggesting that other *Tcf/Lefs* are responsible for
 391 activation of Wnt/ β -catenin targets in the NC. It is likely that *Lef1*, *Tcf7* and *Tcf712* are
 392 redundant in NC cells since whole body double knock-outs of *Lef1/Tcf7* and *Tcf7/Tcf712*
 393 in mouse do not display any obvious NC phenotype (Galceran et al., 1999; Gregorieff et
 394 al., 2004). Ectopic *Sox9*-positive cells (Fig. 4K,L) in AP2 α -Cre; β -cat ^{Δ Ex3fl/+} mutants
 395 spatially overlap with the elevation of the BAT-gal reporter (Fig. 4H',I'), *Lef1*, *Tcf7* but not
 396 *Tcf712* proteins (Fig. 4N,O and data not shown), suggesting that *Lef1* and *Tcf7* are
 397 positively regulated by Wnt/ β -catenin signaling and probably participate in the expression
 398 of Wnt responsive NC specific genes. *Sp5*, another well-defined Wnt target gene and
 399 transcriptional repressor (Fujimura et al., 2007) was strongly upregulated in AP2 α -
 400 Cre;*Tcf711*^{fl/fl} mutants spreading its expression across the entire ANF (Fig. 4). Work in
 401 *Xenopus* has identified *Sp5* as a novel NC specific inducer (Park et al., 2013). MO-
 402 mediated knock-down of *Sp5* leads to the upregulation of *Zic1*, making it a candidate

14

Mašek et al.

403 target of Sp5 repression. Zic1 acts as a NC inducer only when expressed in appropriate
 404 balance with Pax3, another NC inducer (Hong and Saint-Jeannet, 2007; Park et al.,
 405 2013). Pax3 has been recently identified as a direct target of Tcf/Lefs (Zhao et al., 2014),
 406 providing an additional link to the GRN driving NC induction. It is quite possible that
 407 aberrant induction of Sp5 mediated repression of Zic1, in combination with the ectopic
 408 expression of Wnt1 ligand (Fig. 4) enhancing the β -catenin/Tcf/Lef driven transcription of
 409 Pax3, might serve as an artificial positive feedback loop, further potentiating the effects
 410 on NC induction. Additionally, the aberrant Wnt/ β -catenin signaling present in AP2 α -
 411 Cre;Tcf7l1^{fl/fl} mutants might upregulate the expression of the transcription factor Axud1, a
 412 novel Wnt dependent, positive regulator of NC specification (Simoes-Costa et al., 2015).

413 In summary, we demonstrated that Tcf7l1 mediated repression of β -catenin target
 414 genes protects the anterior neuroectoderm from converting into NC and through that we,
 415 (i) help to eliminate the ambiguity in the interpretation of NC development in mouse and
 416 other vertebrate model organisms and, (ii) provide a model explaining the phenotypes
 417 previously acquired in mouse after de-repression of the Wnt/ β -catenin signaling pathway
 418 during early brain development.

419

420 **Materials and methods**

421 **Mouse strains**

422 Housing of mice and *in vivo* experiments were performed in compliance with the
 423 European Communities Council Directive of 24 November 1986 (86/609/EEC) and
 424 national and institutional guidelines. All procedures involving experimental animals were
 425 approved by the Institutional Committee for Animal Care and Use (permission PP-
 426 071/2011, PP-281/2011). This work did not include human subjects. AP2 α -IRESCre
 427 (AP2 α -Cre) was described previously (Macatee et al., 2003), Cre reporter lines
 428 Rosa26^{EYFPfl/+} (B6.129X1-Gt(ROSA)26Sor^{tm1(EYFP)Cos}/J, stock No: 00614) and ROSA26
 429 (B6.129S4-Gt(ROSA)26Sor^{tm1Sor}/J), stock No: 003474) were purchased from The
 430 Jackson Laboratory. Tcf7l1^{fl/+} strain (Tcf7l1^{tm1a(EUCOMM)Wtsi}) was purchased from the
 431 EUCOMM. Transgenic mouse strain BAT-gal (Maretto et al., 2003) was kindly provided

15

Mašek et al.

432 by S. Piccolo. Mice with a conditional “floxed” β -catenin (β -cat^{Ex3fl/+}) were kindly provided
 433 by Dr. M. M. Taketo (Harada et al., 1999). Generation of Rosa26^{dnTCF4fl/fl} was described in
 434 (Janeckova et al., in press). Briefly, human TCF7L2 coding sequence lacking N-terminal
 435 domain (aa 1-31) was cloned into the ROSA26 targeting vector containing arms for
 436 homologous recombination into ROSA26 locus in a same way as when generating the
 437 Rosa26^{ct β cat-Tcf711fl/+}. Details about the Rosa26^{ct β cat-Tcf711fl/+} mouse line generation are
 438 present in Fig. S4. A C-terminal part of β -catenin (aa 696-781) was fused with the mouse
 439 full length Tcf711 and inserted into ROSA26 locus using homologous recombination in ES
 440 cells. The construct carries tdTomato coding sequence flanked with the LoxP sites
 441 serving as a stop cassette for ct β cat-Tcf711. Excision of the tdTomato cassette via Cre-
 442 mediated recombination, allows transcription of ct β cat-Tcf711 mRNA (Fig. 5A). PGK-Neo
 443 cassette was removed using FLP-FRT recombination, F1 animals were crossed to the
 444 Actb:FLPe strain (Rodriguez et al., 2000) and kept on a C57BL/6J background. Primers
 445 for genotyping Rosa26^{ct β cat-Tcf711fl/+} allele: JM21F GAGGAGCCATAACTGCAGAC, JM23R
 446 CCTGGCTATCCTAGATAGAAC and JM27R GTAAGTGTCCACGATGGT the expected
 447 size of the PCR product is 965bp in the mutant and 300bp in the wild-type.

448 **MO knock-down in zebrafish**

449 Zebrafish wild-type, single-cell embryos were injected with combination of previously
 450 described Tcf711a (5' CTCCGTTTAACTGAGGCATGTTGGC 3') and Tcf711b (5'
 451 CGCCTCCGTTAAGCTGCGGCATGTT 3') morpholinos (Dorsky et al., 2003), in 1:1 ratio
 452 at a final concentration of 1.6ng/nl (1-2nl injected) (Gene Tools). Embryos were then
 453 raised at 28°C and harvested at 12hpf.

454 **Immunohistochemistry and RNA in situ hybridization**

455 At least three embryos of each genotype and similar developmental stage were analyzed
 456 per staining. All used primary antibodies are listed in Supplementary Table S1.
 457 Secondary antibodies: anti-mouse (-chicken, -rabbit, -goat) Alexa Fluor488 or 594 (Life
 458 Technologies), Biotinylated anti-rabbit (Vector Laboratories), Vectastain ABC Elite kit and
 459 ImPACT DAB substrate (all Vector Laboratories). For wholemount immunohistochemistry
 460 we used the protocol published by Sandell et al. (Sandell et al., 2014). Briefly, embryos

16

Mašek et al.

461 were fixed overnight in 4% PFA, permeabilized using Dent's bleach and 100% methanol
462 and rehydrated. Blocking for 2 hours and antibody incubation overnight were performed
463 in 3% BSA in 0.1M Tris-Cl, pH 7.5, 0.15 M NaCl, 0.03% Triton X-100. After 5 times of 1-
464 hour washing in PBS, overnight incubation with secondary antibody in the blocking buffer
465 followed. The next day, embryos were stained for nuclei using Hoechst (Life
466 technologies), washed three times in PBS (20 minutes each) and stored in 2%
467 formaldehyde (Sigma). Whole-mount immunofluorescence was captured using binocular
468 microscope Apotome.2 Ax10 zoom.V16 (Zeiss). Fluorescence and bright-field light
469 images were acquired in Nikon Diaphot 300 with objectives 4x/0.1 and 10x/0.25 and
470 confocal Leica SP5.

471 Whole-mount *in situ* hybridization was performed using standard protocols. Riboprobes
472 were cloned into pGEM-T-easy vector (Promega) using primers specified in the
473 Supplementary Table S1.

474 **SuperTop Flash reporter assay.**

475 HEK293 cells (30 000 cells/well/96-well plate) were transiently transfected using
476 Lipofectamine 2000 (Invitrogen) with 30 ng of Super8X TopFlash and 1 ng of Renilla
477 luciferase constructs and indicated amount of the expression vector, filled with mock DNA
478 to final concentration of 200ng DNA per well. Luciferase assays were performed 48h later
479 with a Dual-Glo luciferase kit (Promega). The luciferase signal was normalized to a co-
480 transfected Renilla readout. Experiments were performed on at least 6 biological
481 replicates per condition.

482 **Acknowledgments**

483 The work was supported the by Grant Agency of the Czech Republic (P305/12/2042)
484 (OM), (GACR 14-33952S) (VK), Ministry of Education, Youth and Sports of the Czech
485 Republic (LK11214) (OM), (LO1419) (ZK), Grant Agency of Charles University
486 (GAUK-521212) (JM), and by BIOCEV – Biotechnology and Biomedicine Centre of the
487 Academy of Sciences and Charles University (CZ.1.05/1.1.00/02.0109) (ZK). We are
488 grateful to K. Kovacova, J. Lachova and V. Noskova for excellent technical support. We
489 are also grateful to S. Piccolo for providing the BAT-gal.

Mašek et al.

490 **Competing interest statement**

491 The authors declare no competing financial interests.

492 **Author contribution**

493 J.M., O.M., and Z.K. conceived and designed the experimental approach. V.K. and
494 M.M.T. provided new analytic tools. J.M. and O.M. performed the experiments and
495 analyzed the data. J.M., O.M. and Z.K. wrote the manuscript.

496 **Supplementary material**

497 Supplementary material for this article is available at

498

Mašek et al.

499 **References**

- 500 **Andoniadou, C.L., Signore, M., Sajedi, E., Gaston-Massuet, C., Kelberman, D., Burns, A.J., Itasaki, N.,**
501 **Dattani, M., and Martinez-Barbera, J.P.** (2007). Lack of the murine homeobox gene *Hesx1* leads to a
502 posterior transformation of the anterior forebrain. *Development* **134**, 1499-1508.
- 503 **Andoniadou, C.L., Signore, M., Young, R.M., Gaston-Massuet, C., Wilson, S.W., Fuchs, E., and Martinez-**
504 **Barbera, J.P.** (2011). HESX1- and TCF3-mediated repression of *Wnt*/beta-catenin targets is required for
505 normal development of the anterior forebrain. *Development* **138**, 4931-4942.
- 506 **Bang, A.G., Papalopulu, N., Goulding, M.D., and Kintner, C.** (1999). Expression of *Pax-3* in the lateral
507 neural plate is dependent on a *Wnt*-mediated signal from posterior nonaxial mesoderm. *Dev Biol* **212**,
508 366-380.
- 509 **Barriga, E.H., Trainor, P.A., Bronner, M., and Mayor, R.** (2015). Animal models for studying neural crest
510 development: is the mouse different? *Development* **142**, 1555-1560.
- 511 **Brault, V., Moore, R., Kutsch, S., Ishibashi, M., Rowitch, D.H., McMahon, A.P., Sommer, L., Bousadia,**
512 **O., and Kemler, R.** (2001). Inactivation of the beta-catenin gene by *Wnt1*-*Cre*-mediated deletion results in
513 dramatic brain malformation and failure of craniofacial development. *Development* **128**, 1253-1264.
- 514 **Burstyn-Cohen, T., Stanleigh, J., Sela-Donenfeld, D., and Kalcheim, C.** (2004). Canonical *Wnt* activity
515 regulates trunk neural crest delamination linking *BMP*/*noggin* signaling with *G1/S* transition. *Development*
516 **131**, 5327-5339.
- 517 **Cadigan, K.M., and Waterman, M.L.** (2012). TCF/LEFs and *Wnt* signaling in the nucleus. *Cold Spring Harb*
518 *Perspect Biol* **4**.
- 519 **Carmona-Fontaine, C., Acuna, G., Ellwanger, K., Niehrs, C., and Mayor, R.** (2007). Neural crests are
520 actively precluded from the anterior neural fold by a novel inhibitory mechanism dependent on *Dickkopf1*
521 secreted by the prechordal mesoderm. *Dev Biol* **309**, 208-221.
- 522 **Castrop, J., van Norren, K., and Clevers, H.** (1992). A gene family of HMG-box transcription factors with
523 homology to TCF-1. *Nucleic Acids Res* **20**, 611.
- 524 **Cheung, M., Chaboissier, M.C., Mynett, A., Hirst, E., Schedl, A., and Briscoe, J.** (2005). The transcriptional
525 control of trunk neural crest induction, survival, and delamination. *Dev Cell* **8**, 179-192.
- 526 **Clevers, H., and Nusse, R.** (2012). *Wnt*/beta-catenin signaling and disease. *Cell* **149**, 1192-1205.
- 527 **Cole, M.F., Johnstone, S.E., Newman, J.J., Kagey, M.H., and Young, R.A.** (2008). *Tcf3* is an integral
528 component of the core regulatory circuitry of embryonic stem cells. *Genes Dev* **22**, 746-755.
- 529 **Danielian, P.S., Muccino, D., Rowitch, D.H., Michael, S.K., and McMahon, A.P.** (1998). Modification of
530 gene activity in mouse embryos in utero by a tamoxifen-inducible form of *Cre* recombinase. *Curr Biol* **8**,
531 1323-1326.
- 532 **Dorsky, R.I., Itoh, M., Moon, R.T., and Chitnis, A.** (2003). Two *tcf3* genes cooperate to pattern the
533 zebrafish brain. *Development* **130**, 1937-1947.
- 534 **Dottori, M., Gross, M.K., Labosky, P., and Goulding, M.** (2001). The winged-helix transcription factor
535 *Foxd3* suppresses interneuron differentiation and promotes neural crest cell fate. *Development* **128**, 4127-
536 4138.
- 537 **Fossat, N., Jones, V., Khoo, P.L., Bogani, D., Hardy, A., Steiner, K., Mukhopadhyay, M., Westphal, H.,**
538 **Nolan, P.M., Arkell, R., et al.** (2011). Stringent requirement of a proper level of canonical *WNT* signalling
539 activity for head formation in mouse embryo. *Development* **138**, 667-676.
- 540 **Fujimura, N., Vacik, T., Machon, O., Vlcek, C., Scalabrin, S., Speth, M., Diep, D., Krauss, S., and Kozmik, Z.**
541 (2007). *Wnt*-mediated down-regulation of *Sp1* target genes by a transcriptional repressor *Sp5*. *J Biol Chem*
542 **282**, 1225-1237.
- 543 **Galceran, J., Farinas, I., Depew, M.J., Clevers, H., and Grosschedl, R.** (1999). *Wnt3a*^{-/-}-like phenotype and
544 limb deficiency in *Lef1*^(-/-)*Tcf1*^(-/-) mice. *Genes Dev* **13**, 709-717.

19

Mašek et al.

- 545 **Garcia-Castro, M.I., Marcelle, C., and Bronner-Fraser, M.** (2002). Ectodermal Wnt function as a neural
546 crest inducer. *Science* **297**, 848-851.
- 547 **Garnett, A.T., Square, T.A., and Medeiros, D.M.** (2012). BMP, Wnt and FGF signals are integrated through
548 evolutionarily conserved enhancers to achieve robust expression of Pax3 and Zic genes at the zebrafish
549 neural plate border. *Development* **139**, 4220-4231.
- 550 **Gay, M.H., Valenta, T., Herr, P., Paratore-Hari, L., Basler, K., and Sommer, L.** (2015). Distinct adhesion-
551 independent functions of beta-catenin control stage-specific sensory neurogenesis and proliferation. *BMC*
552 *Biol* **13**, 24.
- 553 **Gregorieff, A., Grosschedl, R., and Clevers, H.** (2004). Hindgut defects and transformation of the gastro-
554 intestinal tract in Tcf4(-)/Tcf1(-) embryos. *EMBO J* **23**, 1825-1833.
- 555 **Groves, A.K., and LaBonne, C.** (2014). Setting appropriate boundaries: fate, patterning and competence at
556 the neural plate border. *Dev Biol* **389**, 2-12.
- 557 **Hanashima, C., Li, S.C., Shen, L., Lai, E., and Fishell, G.** (2004). Foxg1 suppresses early cortical cell fate.
558 *Science* **303**, 56-59.
- 559 **Harada, N., Tamai, Y., Ishikawa, T., Sauer, B., Takaku, K., Oshima, M., and Taketo, M.M.** (1999).
560 Intestinal polyposis in mice with a dominant stable mutation of the beta-catenin gene. *EMBO J* **18**, 5931-
561 5942.
- 562 **Heeg-Truesdell, E., and LaBonne, C.** (2006). Neural induction in *Xenopus* requires inhibition of Wnt-beta-
563 catenin signaling. *Dev Biol* **298**, 71-86.
- 564 **Hong, C.S., and Saint-Jeannet, J.P.** (2007). The activity of Pax3 and Zic1 regulates three distinct cell fates
565 at the neural plate border. *Mol Biol Cell* **18**, 2192-2202.
- 566 **Hsu, S.C., Galceran, J., and Grosschedl, R.** (1998). Modulation of transcriptional regulation by LEF-1 in
567 response to Wnt-1 signaling and association with beta-catenin. *Mol Cell Biol* **18**, 4807-4818.
568 <http://web.stanford.edu/group/nusselab/cgi-bin/wnt/>.
- 569 **Ikeya, M., Lee, S.M., Johnson, J.E., McMahon, A.P., and Takada, S.** (1997). Wnt signalling required for
570 expansion of neural crest and CNS progenitors. *Nature* **389**, 966-970.
- 571 **Janssens, S., Van Den Broek, O., Davenport, I.R., Akkers, R.C., Liu, F., Veenstra, G.J., Hoppler, S.,
572 Vlemingck, K., and Destree, O.** (2013). The Wnt signaling mediator tcf1 is required for expression of foxd3
573 during *Xenopus* gastrulation. *Int J Dev Biol* **57**, 49-54.
- 574 **Kim, C.H., Oda, T., Itoh, M., Jiang, D., Artinger, K.B., Chandrasekharappa, S.C., Driever, W., and Chitnis,
575 A.B.** (2000). Repressor activity of Headless/Tcf3 is essential for vertebrate head formation. *Nature* **407**,
576 913-916.
- 577 **Kleber, M., Lee, H.Y., Wurdak, H., Buchstaller, J., Riccomagno, M.M., Ittner, L.M., Suter, U., Epstein, D.J.,
578 and Sommer, L.** (2005). Neural crest stem cell maintenance by combinatorial Wnt and BMP signaling. *J*
579 *Cell Biol* **169**, 309-320.
- 580 **Korinek, V., Barker, N., Willert, K., Molenaar, M., Roose, J., Wagenaar, G., Markman, M., Lamers, W.,
581 Destree, O., and Clevers, H.** (1998). Two members of the Tcf family implicated in Wnt/beta-catenin
582 signaling during embryogenesis in the mouse. *Mol Cell Biol* **18**, 1248-1256.
- 583 **Kratochwil, K., Galceran, J., Tontsch, S., Roth, W., and Grosschedl, R.** (2002). FGF4, a direct target of LEF1
584 and Wnt signaling, can rescue the arrest of tooth organogenesis in Lef1(-) mice. *Genes Dev* **16**, 3173-
585 3185.
- 586 **Lagutin, O.V., Zhu, C.C., Kobayashi, D., Topczewski, J., Shimamura, K., Puellas, L., Russell, H.R.,
587 McKinnon, P.J., Solnica-Krezel, L., and Oliver, G.** (2003). Six3 repression of Wnt signaling in the anterior
588 neuroectoderm is essential for vertebrate forebrain development. *Genes Dev* **17**, 368-379.
- 589 **Lee, H.Y., Kleber, M., Hari, L., Brault, V., Suter, U., Taketo, M.M., Kemler, R., and Sommer, L.** (2004).
590 Instructive role of Wnt/beta-catenin in sensory fate specification in neural crest stem cells. *Science* **303**,
591 1020-1023.

Mašek et al.

- 592 **Lewis, A.E., Vasudevan, H.N., O'Neill, A.K., Soriano, P., and Bush, J.O.** (2013). The widely used Wnt1-Cre
593 transgene causes developmental phenotypes by ectopic activation of Wnt signaling. *Dev Biol* **379**, 229-
594 234.
- 595 **Li, B., Kuriyama, S., Moreno, M., and Mayor, R.** (2009). The posteriorizing gene Gbx2 is a direct target of
596 Wnt signalling and the earliest factor in neural crest induction. *Development* **136**, 3267-3278.
- 597 **Litsiou, A., Hanson, S., and Streit, A.** (2005). A balance of FGF, BMP and WNT signalling positions the
598 future placode territory in the head. *Development* **132**, 4051-4062.
- 599 **Liu, F., van den Broek, O., Destree, O., and Hoppler, S.** (2005). Distinct roles for Xenopus Tcf/Lef genes in
600 mediating specific responses to Wnt/beta-catenin signalling in mesoderm development. *Development*
601 **132**, 5375-5385.
- 602 **Liu, J.A., Wu, M.H., Yan, C.H., Chau, B.K., So, H., Ng, A., Chan, A., Cheah, K.S., Briscoe, J., and Cheung, M.**
603 (2013). Phosphorylation of Sox9 is required for neural crest delamination and is regulated downstream of
604 BMP and canonical Wnt signaling. *Proc Natl Acad Sci U S A* **110**, 2882-2887.
- 605 **Macatee, T.L., Hammond, B.P., Arenkiel, B.R., Francis, L., Frank, D.U., and Moon, A.M.** (2003). Ablation
606 of specific expression domains reveals discrete functions of ectoderm- and endoderm-derived FGF8 during
607 cardiovascular and pharyngeal development. *Development* **130**, 6361-6374.
- 608 **Maretto, S., Cordenonsi, M., Dupont, S., Braghetta, P., Broccoli, V., Hassan, A.B., Volpin, D., Bressan,
609 G.M., and Piccolo, S.** (2003). Mapping Wnt/beta-catenin signaling during mouse development and in
610 colorectal tumors. *Proc Natl Acad Sci U S A* **100**, 3299-3304.
- 611 **McMahon, A.P., and Bradley, A.** (1990). The Wnt-1 (int-1) proto-oncogene is required for development of
612 a large region of the mouse brain. *Cell* **62**, 1073-1085.
- 613 **Merrill, B.J., Pasolli, H.A., Polak, L., Rendl, M., Garcia-Garcia, M.J., Anderson, K.V., and Fuchs, E.** (2004).
614 Tcf3: a transcriptional regulator of axis induction in the early embryo. *Development* **131**, 263-274.
- 615 **Meyers, E.N., Lewandoski, M., and Martin, G.R.** (1998). An Fgf8 mutant allelic series generated by Cre-
616 and Flp-mediated recombination. *Nat Genet* **18**, 136-141.
- 617 **Mukhopadhyay, M., Shtrom, S., Rodriguez-Esteban, C., Chen, L., Tsukui, T., Gomer, L., Dorward, D.W.,
618 Glinka, A., Grinberg, A., Huang, S.P., et al.** (2001). Dickkopf1 is required for embryonic head induction and
619 limb morphogenesis in the mouse. *Dev Cell* **1**, 423-434.
- 620 **Ombrato, L., Lluís, F., and Cosma, M.P.** (2012). Regulation of self-renewal and reprogramming by TCF
621 factors. *Cell Cycle* **11**, 39-47.
- 622 **Park, D.S., Seo, J.H., Hong, M., Bang, W., Han, J.K., and Choi, S.C.** (2013). Role of Sp5 as an essential early
623 regulator of neural crest specification in xenopus. *Dev Dyn* **242**, 1382-1394.
- 624 **Rodriguez, C.I., Buchholz, F., Galloway, J., Sequerra, R., Kasper, J., Ayala, R., Stewart, A.F., and Dymecki,
625 S.M.** (2000). High-efficiency deleter mice show that FLPe is an alternative to Cre-loxP. *Nat Genet* **25**, 139-
626 140.
- 627 **Saint-Jeannet, J.P., He, X., Varmus, H.E., and Dawid, I.B.** (1997). Regulation of dorsal fate in the neuraxis
628 by Wnt-1 and Wnt-3a. *Proc Natl Acad Sci U S A* **94**, 13713-13718.
- 629 **Sakai, D., Tanaka, Y., Endo, Y., Osumi, N., Okamoto, H., and Wakamatsu, Y.** (2005). Regulation of Slug
630 transcription in embryonic ectoderm by beta-catenin-Lef/Tcf and BMP-Smad signaling. *Dev Growth Differ*
631 **47**, 471-482.
- 632 **Sandell, L.L., Butler Tjaden, N.E., Barlow, A.J., and Trainor, P.A.** (2014). Cochleovestibular nerve
633 development is integrated with migratory neural crest cells. *Dev Biol* **385**, 200-210.
- 634 **Satoh, K., Kasai, M., Ishida, T., Tago, K., Ohwada, S., Hasegawa, Y., Senda, T., Takada, S., Nada, S.,
635 Nakamura, T., et al.** (2004). Anteriorization of neural fate by inhibitor of beta-catenin and T cell factor
636 (ICAT), a negative regulator of Wnt signaling. *Proc Natl Acad Sci U S A* **101**, 8017-8021.
- 637 **Shy, B.R., Wu, C.I., Khramtsova, G.F., Zhang, J.Y., Olopade, O.I., Goss, K.H., and Merrill, B.J.** (2013).
638 Regulation of Tcf7l1 DNA binding and protein stability as principal mechanisms of Wnt/beta-catenin
639 signaling. *Cell Rep* **4**, 1-9.

Mašek et al.

- 640 **Simoës-Costa, M., and Bronner, M.E.** (2015). Establishing neural crest identity: a gene regulatory recipe.
641 *Development* **142**, 242-257.
- 642 **Simoës-Costa, M., Stone, M., and Bronner, M.E.** (2015). Axud1 Integrates Wnt Signaling and
643 Transcriptional Inputs to Drive Neural Crest Formation. *Dev Cell* **34**, 544-554.
- 644 **Steventon, B., Araya, C., Linker, C., Kuriyama, S., and Mayor, R.** (2009). Differential requirements of BMP
645 and Wnt signalling during gastrulation and neurulation define two steps in neural crest induction.
646 *Development* **136**, 771-779.
- 647 **Taneyhill, L.A., and Bronner-Fraser, M.** (2005). Dynamic alterations in gene expression after Wnt-
648 mediated induction of avian neural crest. *Mol Biol Cell* **16**, 5283-5293.
- 649 **Thomas, K.R., and Capecchi, M.R.** (1990). Targeted disruption of the murine int-1 proto-oncogene
650 resulting in severe abnormalities in midbrain and cerebellar development. *Nature* **346**, 847-850.
- 651 **Travis, A., Amsterdam, A., Belanger, C., and Grosschedl, R.** (1991). LEF-1, a gene encoding a lymphoid-
652 specific protein with an HMG domain, regulates T-cell receptor alpha enhancer function [corrected].
653 *Genes Dev* **5**, 880-894.
- 654 **Vallin, J., Thuret, R., Giacomello, E., Faraldo, M.M., Thiery, J.P., and Broders, F.** (2001). Cloning and
655 characterization of three *Xenopus* slug promoters reveal direct regulation by Lef/beta-catenin signaling. *J*
656 *Biol Chem* **276**, 30350-30358.
- 657 **van de Wetering, M., Oosterwegel, M., Dooijes, D., and Clevers, H.** (1991). Identification and cloning of
658 TCF-1, a T lymphocyte-specific transcription factor containing a sequence-specific HMG box. *EMBO J* **10**,
659 123-132.
- 660 **Wu, C.I., Hoffman, J.A., Shy, B.R., Ford, E.M., Fuchs, E., Nguyen, H., and Merrill, B.J.** (2012). Function of
661 Wnt/beta-catenin in counteracting Tcf3 repression through the Tcf3-beta-catenin interaction.
662 *Development* **139**, 2118-2129.
- 663 **Wu, J., Yang, J., and Klein, P.S.** (2005). Neural crest induction by the canonical Wnt pathway can be
664 dissociated from anterior-posterior neural patterning in *Xenopus*. *Dev Biol* **279**, 220-232.
- 665 **Zhao, T., Gan, Q., Stokes, A., Lassiter, R.N., Wang, Y., Chan, J., Han, J.X., Pleasure, D.E., Epstein, J.A., and**
666 **Zhou, C.J.** (2014). beta-catenin regulates Pax3 and Cdx2 for caudal neural tube closure and elongation.
667 *Development* **141**, 148-157.

668

Mašek et al.

669 **Fig. 1**

670 **Tcf711 is expressed in a mutually exclusive manner with markers of specified NC and**
671 **is required for proper forebrain development**

672 (A-D) Expression of *Tcf711* mRNA, early NC marker Tfp2 α protein, marker of specified NC Sox9
673 mRNA and Wnt reporter BAT-gal in the NPB and the ANF (encircled) of developing mouse
674 embryo. Please note the overlap of *Tcf711* transcript and Tfp2 α protein, and of Sox9 mRNA and
675 BAT-gal signal.

676 (E) Mapping of recombination delivered by AP2 α -Cre using Rosa26^{EYFP^{fl/fl}} reporter mouse at
677 various stages E7.0-E10.5. EYFP was detected either directly or using anti-GFP antibody. The
678 recombination occurred along the entire NPB (arrowheads, 10s stage). Co-staining of GFP with
679 anti-Sox10 antibody revealed recombination in the whole cranial NC population at 10s stage.

680 (F-G) *In situ* hybridization shows loss of *Tcf711* mRNA expression in AP2 α -Cre;Tcf711^{fl/fl} mutants.
681 ANF in mutant is wider at PM, but narrower towards anterior tip of the ANF (dashed line) than in
682 the control at 5s stage, scale 30 μ m. Control embryo (left) and typical examples of strong (middle)
683 and mild (right) AP2 α -Cre;Tcf711^{fl/fl} phenotype.

684 (I) Quantification of strong and mild phenotype incidence between E10.5-E13.5 ANF- anterior
685 neural fold, NPB-neural plate border, NC-neural crest, NNE-non-neural ectoderm, PM-
686 prosencephalic-mesencephalic boundary, s-somite pairs. All embryos are shown from a lateral
687 view if not stated otherwise. Nuclei were stained with Hoechst. See also Fig. S1.

688 **Fig. 2**

689 **Tcf711 deletion induces loss of ANF specifiers, without affecting more posterior brain**
690 **structures**

691 (A-B') *In situ* hybridization shows unchanged expression of *Fgf8* and *Gbx2* mRNA in MHB
692 (arrowheads), all lateral view.

693 (C-C') *Tcf712* mRNA in the posterior prosencephalon of control and AP2 α -Cre;Tcf711^{fl/fl} embryos
694 displaying mild and strong phenotype at E9.5, all lateral view.

695 (D-G') Tcf711 deletion resulted in marked reduction of endogenous mRNA expression of *Six3* and
696 *Sox2* at 7-8s stage, *FoxG1* at 11-12s stage and of *Fgf8* at E9.0 in the ANF of AP2 α -Cre;Tcf711^{fl/fl}
697 embryos, all frontal view.

23

Mašek et al.

698 **Fig. 3**

699 **The NC population expands anteriorly in the absence of Tcf711**

700 (A) Whole mount immunohistochemical staining of Sox1 and Sox9 protein at 5s stage, lateral
701 view. Higher magnification reveals reduction of Sox1 staining in the ANF (dashed line) of the
702 AP2 α -Cre;Tcf711^{fl/fl} mutants. Nuclei were stained with Hoechst.

703 (B) Same embryos as shown in (A), frontal view, higher magnification documents the expansion
704 (dashed line) of Sox9 positive cells along the ANF border in mutants.

705 (C) Lateral and frontal views revealed aberrant expression of the NC markers *FoxD3* along the
706 ANF in the mutants while it is absent in the control embryos at 10s stage.

707 (D) *Sox10* mRNA is less abundant in the Tcf711 mutants at 6s stage but becomes ectopically
708 expressed later in anterior head (arrowhead) of AP2 α -Cre;Tcf711^{fl/fl} embryos at E9.5. V-trigeminal
709 ganglion. See also Fig. S2.

710 **Fig. 4**

711 **The ectopic activation of Wnt/ β -catenin pathway promotes NC formation in mouse**

712 (A) BAT-gal signal (detected with β -galactosidase antibody) and Sox9 staining expands anteriorly
713 in AP2 α -Cre;Tcf711^{fl/fl} mutants at the 8s stage.

714 (B, C) *In situ* hybridization shows upregulation of the Wnt target *Sp5* and Wnt ligand *Wnt1* along
715 the NPB of the ANF in Tcf711 mutants at 5s and E9.5 stage.

716 (D-F') Frontal and lateral view on the whole mount BAT-gal staining of the control, AP2 α -
717 Cre;Tcf711^{fl/fl} and AP2 α -Cre; β -cat^{Ex3fl/+} embryos at E9.5.

718 (D''-F'') Coronal sections in the dashed line shown in (D-F), respectively. Different embryos were
719 used in F, F' and F''.

720 (G-I) Coronal sections immunostained with antibodies against N-Cadherin and Sox9 at E9.5.
721 Sox9⁺ population is increased and N-Cadherin staining decreased in the AP2 α -Cre;Tcf711^{fl/fl} and
722 AP2 α -Cre; β -cat^{Ex3fl/+} mutants, but not in control embryos.

723 (J-L) Lef1 immunostaining of coronal sections of the control (M), AP2 α -Cre;Tcf711^{fl/fl} (N) and
724 AP2 α -Cre; β -cat^{Ex3fl/+} (O) embryos at E9.5. fb-forebrain, t-tail. See also Fig. S3.

24

Mašek et al.

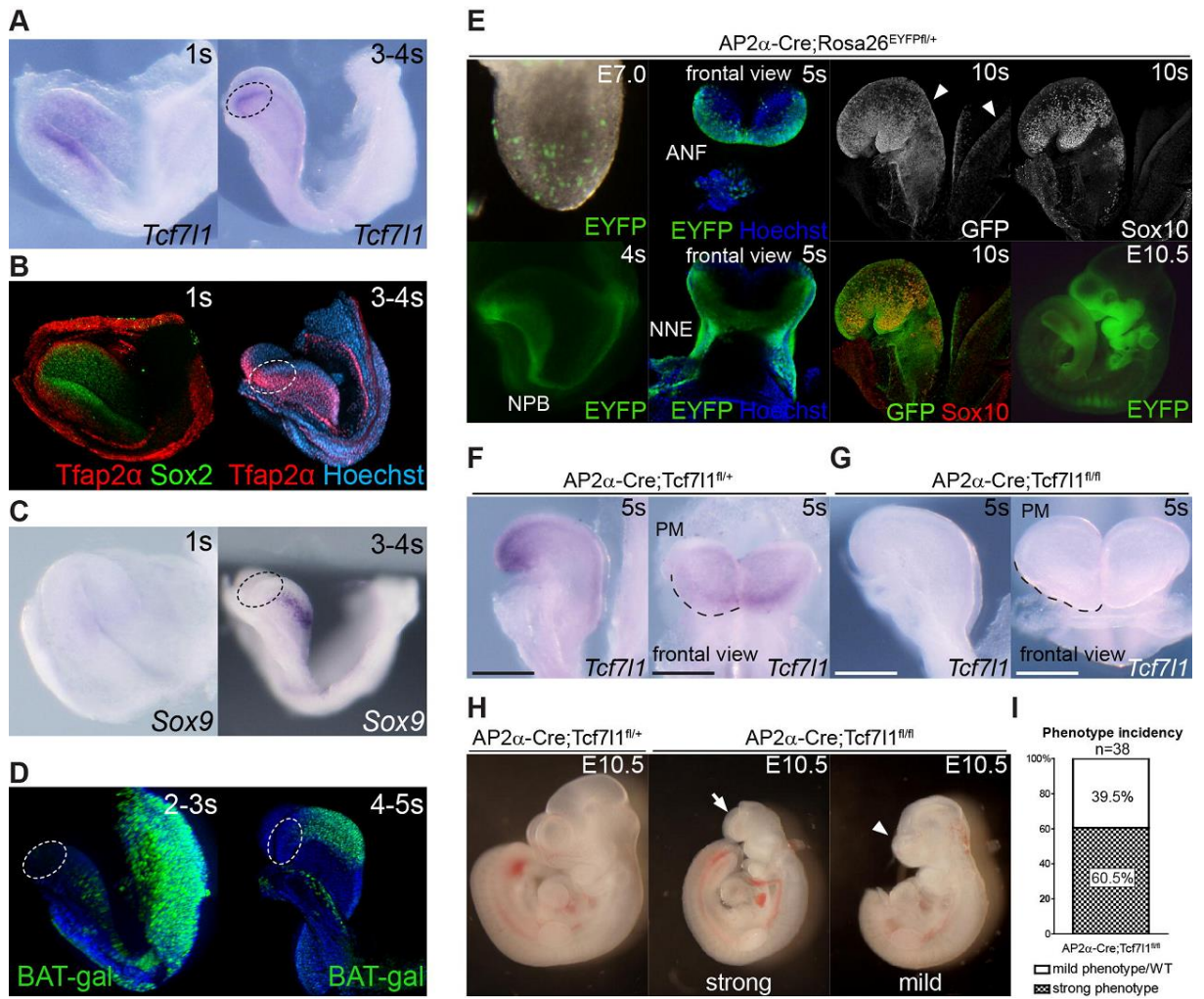
725 **Fig. 5**

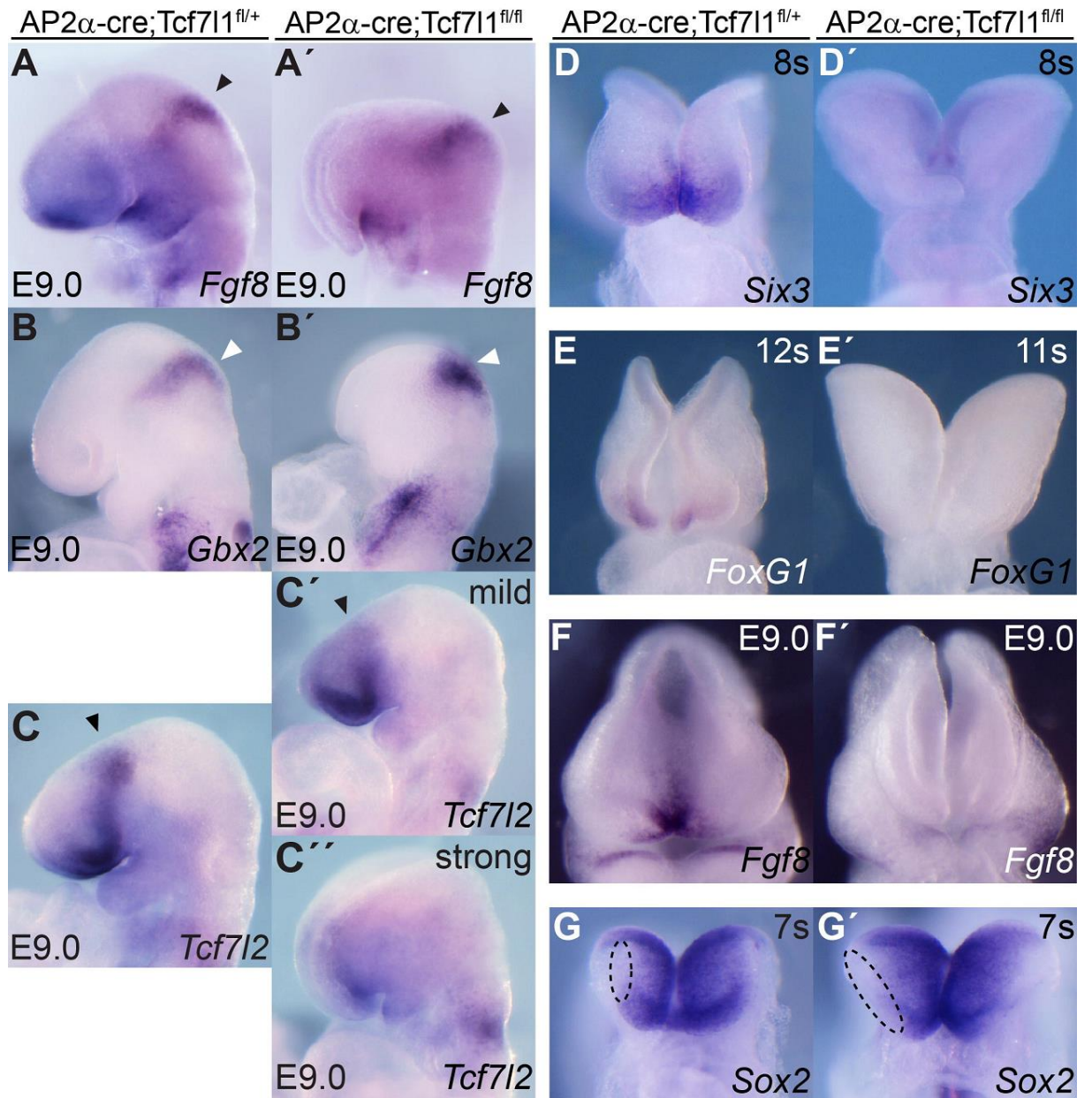
726 **A constitutively repressing form of Tcf is able to rescue ANF absence in AP2 α -Cre;Tcf7l1^{fl/fl}**
727 **mutants**

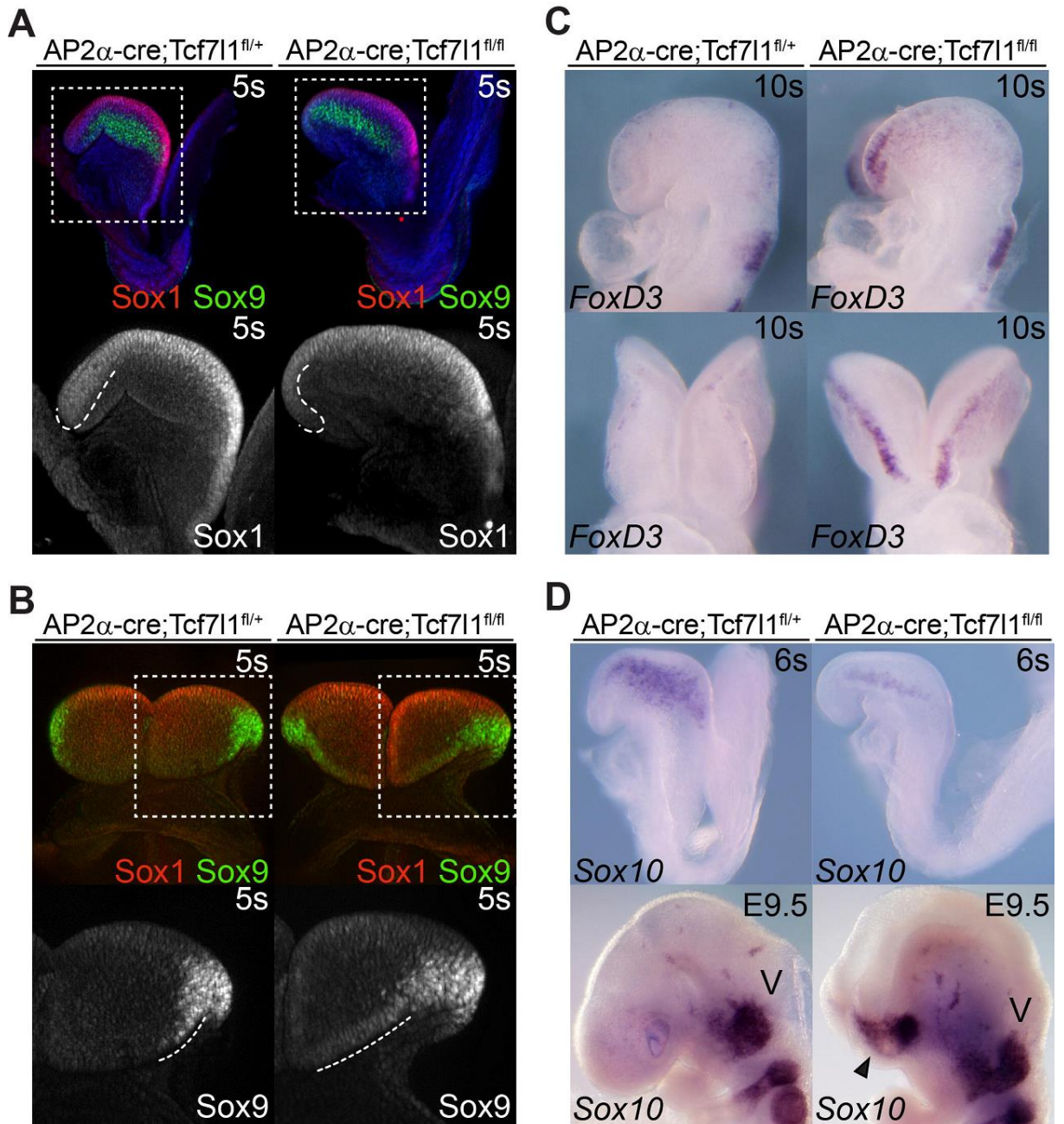
728 (A) Diagram describing Rosa26^{dnTCF4fl/+} and Rosa26^{ct β cat-Tcf7l1fl/+} mouse strains used in the rescue
729 experiments. SA-splice acceptor, pA-poly-adenylation signal.

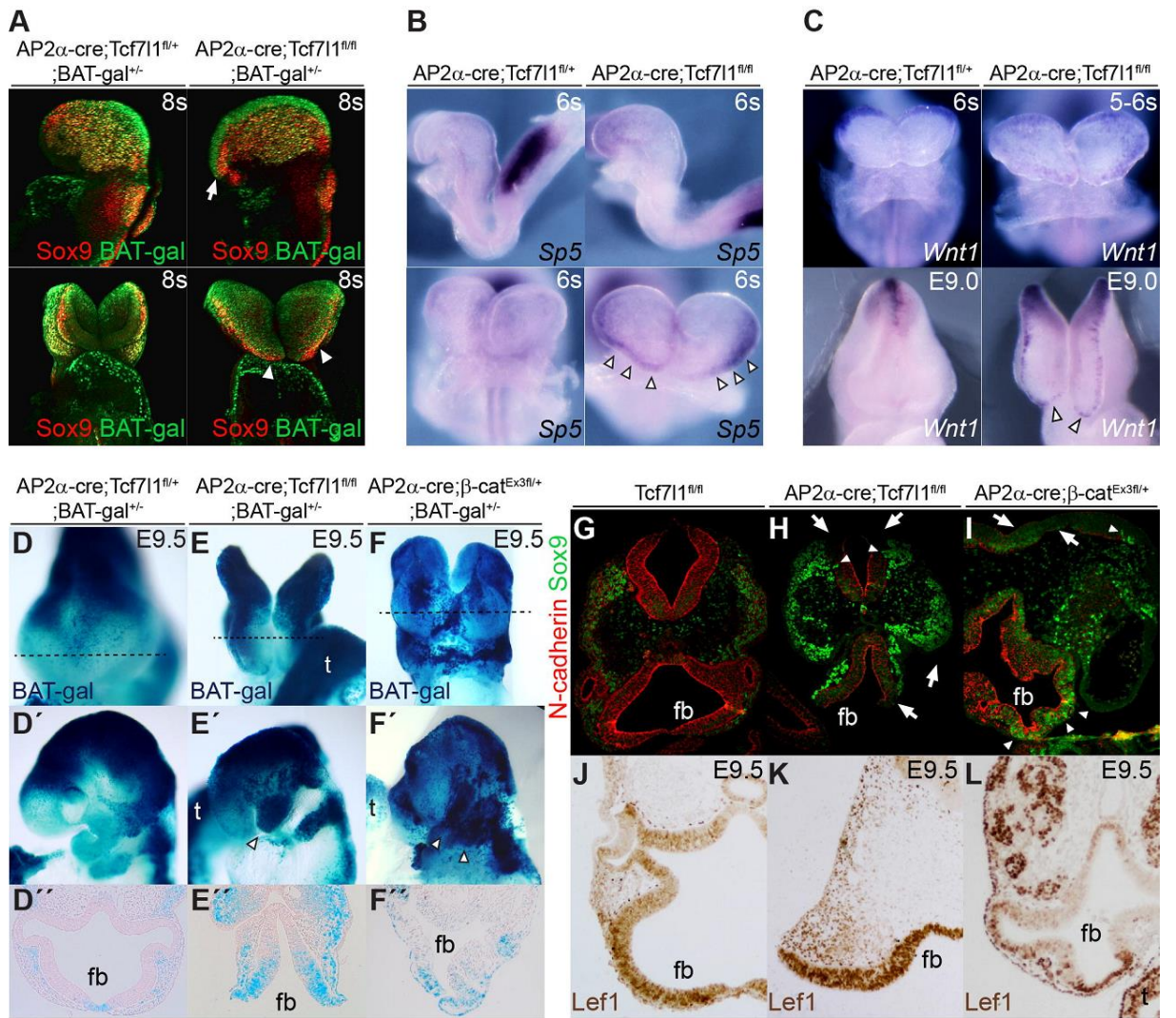
730 (B,C) Expression of Sox10 transcripts was either unaffected or only mildly affected in the AP2 α -
731 Cre;Tcf7l1^{fl/fl};Rosa26^{dnTCF4fl/+} compound mutants, confirming the rescue capability of dnTCF4.
732 AP2 α -Cre;Tcf7l1^{fl/fl}; Rosa26^{ct β cat-Tcf7l1fl/+} compound mutants, displayed no rescue or even stronger
733 phenotype. * indicates artifact caused during preparation.

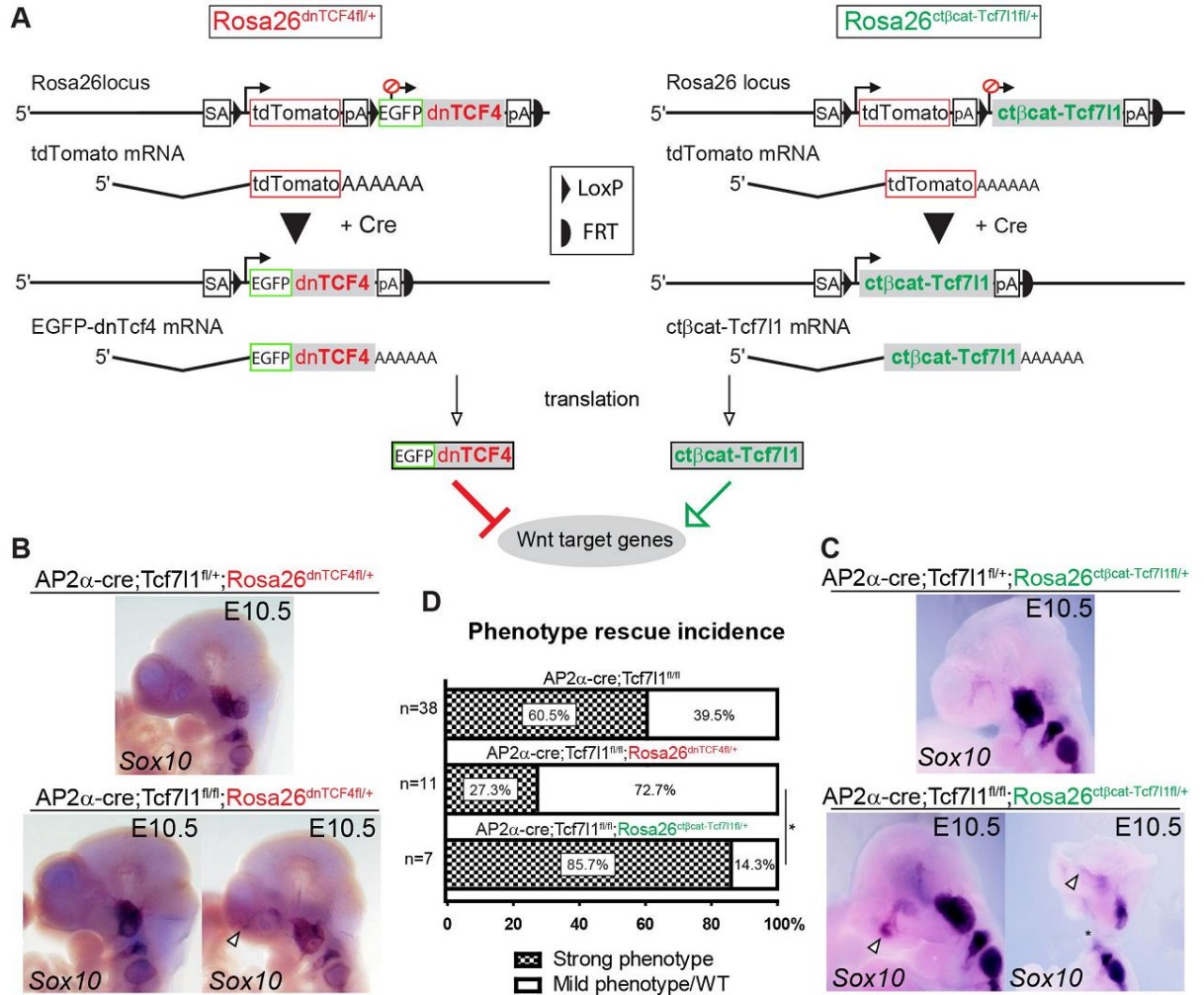
734 (D) Quantification of the strong and mild phenotype incidence and rescue capability of dnTCF4
735 and ct β cat-Tcf7l1, scored at E10.5-13.5. *(P=0.049, Fishers test), n-number of embryos analyzed.
736 See also Fig. S4.





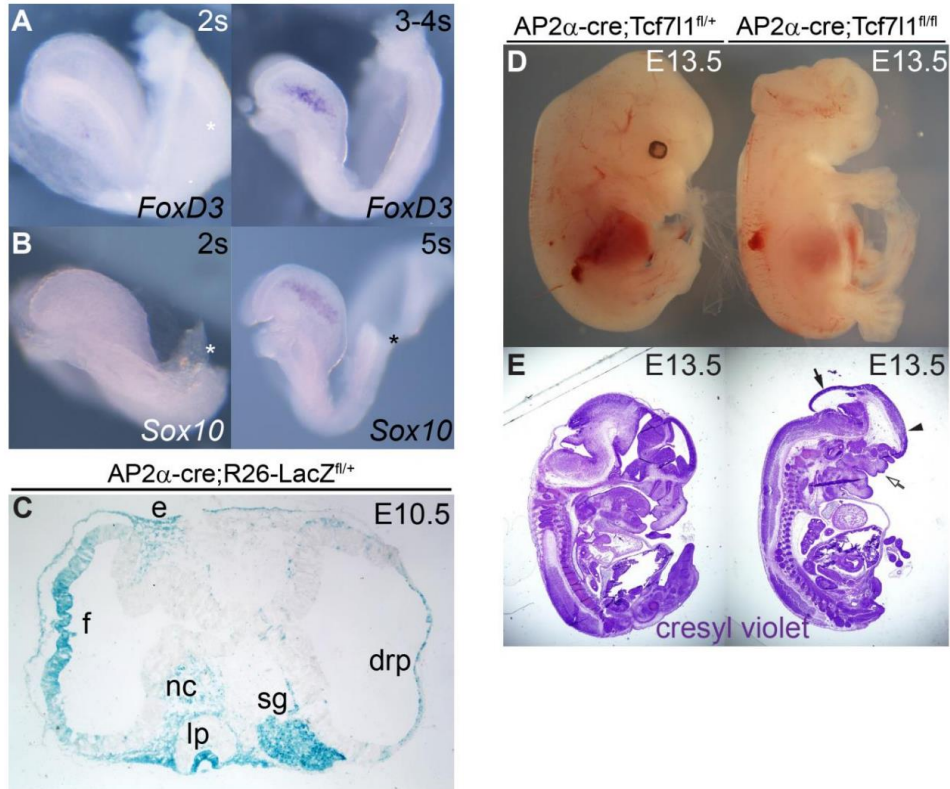






Mašek et al.

1 **Fig. S1, related to Fig. 1**



2

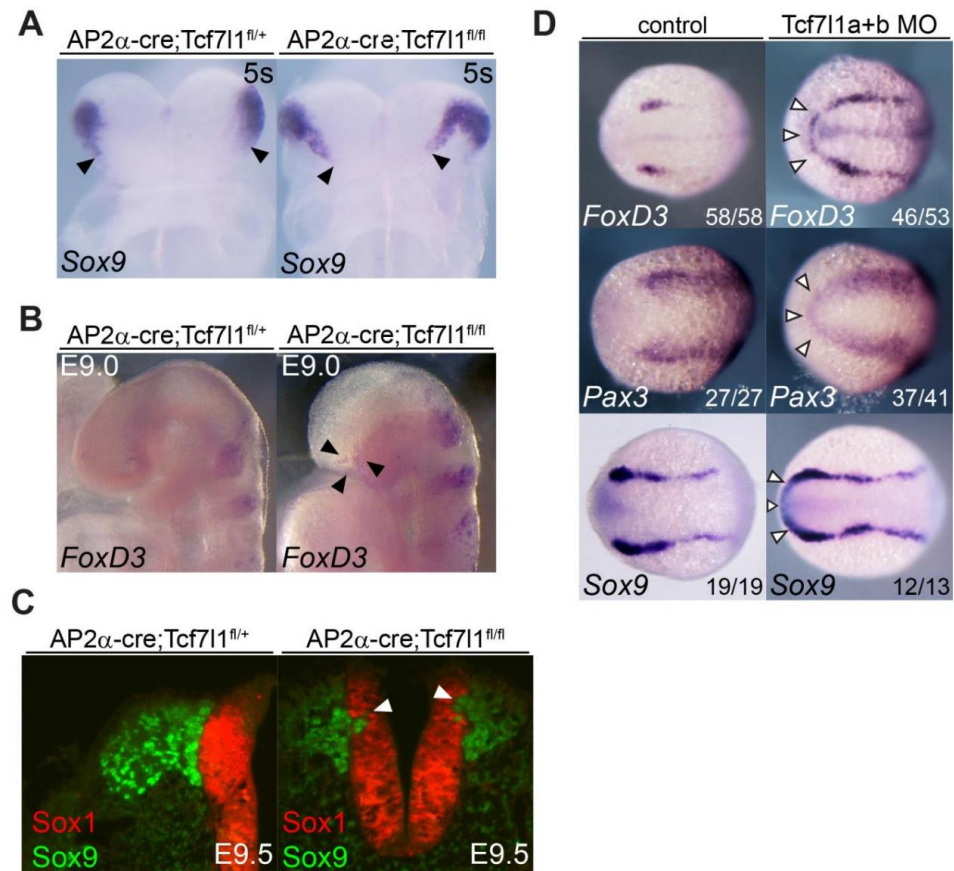
3 **Expression of NC genes during early mouse embryogenesis.**

4 **(A-B)** RNA *in situ* hybridisation of *FoxD3* at 2s and 3-4s stage, and *Sox10* transcripts at 2s and 5s
 5 stage, respectively. **Mapping of AP2α-Cre delivered recombination (C)** Coronal section of AP2α-
 6 Cre;*Rosa26^{LacZ}^{fl/+}* at E10.5 stage. Recombination was detected enzymatically with β-galactosidase.
 7 drp-dorsal roof plate, e-ectoderm, f-forebrain, lp-lens pit, nc-neural crest, sg-sensory ganglion.
 8 **Tcf711 deletion results in exencephaly (D,E)** Histological analysis of saggittal sections from the
 9 AP2α-Cre;*Tcf711^{fl/fl}* 'strong' mutant at E13.5, sections stained with cresyl violet show severe defects
 10 in the splanchnocranium (white arrow), forebrain (black arrowhead) and midbrain (black arrow) of
 11 the mutant embryo.

12

Mašek et al.

13 Fig. S2, related to Fig. 3



14

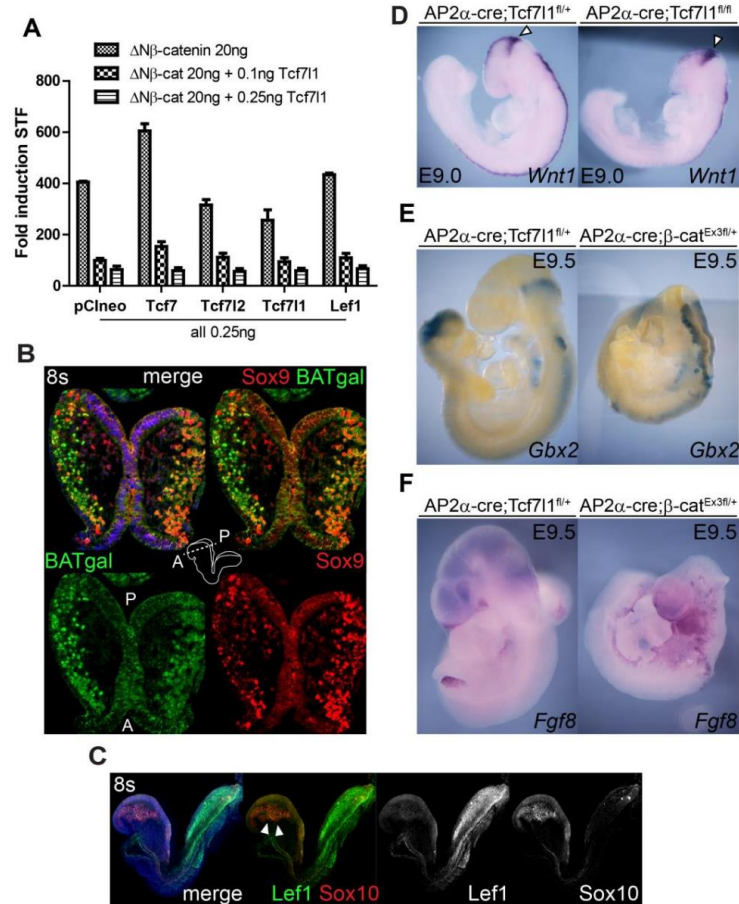
15 **Expansion of NC markers follows Tcf711 deletion in mouse and zebrafish**

16 **(A-C)** Expression of Sox9 transcripts expanded rostrally in AP2 α -Cre;Tcf711^{fl/fl} mutant at 5s stage.
 17 Abberant FoxD3 mRNA expressing cells are present in the Tcf711 mutant at E9.0.
 18 Immunohistological staining of coronal sections from the E9.0 hindbrain revealed ectopic Sox9-
 19 positive/Sox1-negative cells in AP2 α -Cre;Tcf711^{fl/fl} mutants. **(D)** Expression of FoxD3, Pax3 and
 20 Sox9 mRNA expands along the anterior NPB upon MO-mediated knock-down of both Tcf711a and
 21 Tcf711b variants in zebrafish at 12h stage.

22

Mašek et al.

23 Fig. S3, related to Fig. 4



24

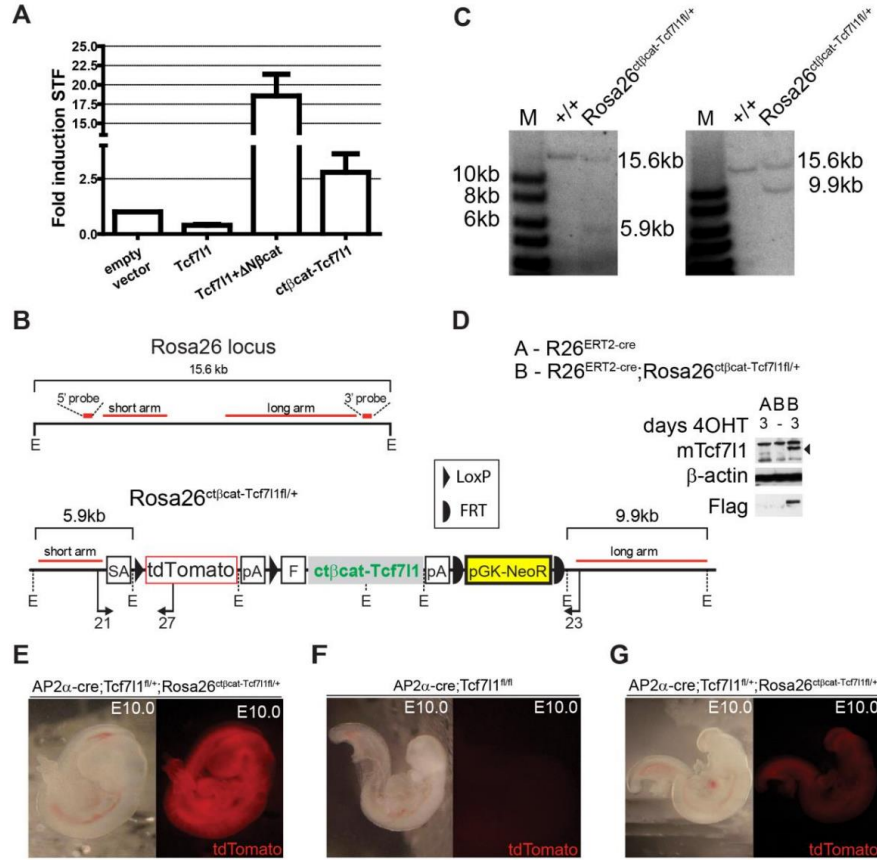
25 **Balance between Wnt/β-catenin pathway activation and Tcf711 delivered repression**
 26 **regulates NC specification.**

27 **(A)** SuperTopFlash luciferase reporter assay in HEK293 cells documents Tcf711 ability to repress
 28 Tcf/Lef driven gene expression. **(B)** Immunostaining of coronal sections from 8s stage wild-type
 29 embryos, A-anterior, P-posterior. Please note a large overlap between the Sox9-positive and BAT-
 30 gal-positive delaminating cells. Nuclei were stained with DAPI. **(C)** Whole mount
 31 immunofluorescence revealed overlap of Lef1 and Sox10-positive cells in wild-type embryo at 8s
 32 stage. Nuclei were stained with Hoechst. **(D)** The expression of *Wnt1* transcripts is unchanged in
 33 the MHB of AP2α-Cre;Tcf711^{fl/fl} mutants at E9.0. **Ectopic activation of the Wnt/β-catenin pathway**
 34 **severely affects NPB development.** **(E-F)** RNA *in situ* hybridisation of the MHB markers *Gbx2* (E)
 35 and *Fgf8* (E) in the AP2α-Cre;β-cat^{Ex3fl/+} mutants at E9.5.

3

Mašek et al.

36 Fig. S4, related to Fig. 5



37

38 **Generation and validation of the mouse strain *Rosa26^{ctβcat-Tcf711fl/+}*.**

39 **(A)** SuperTopFlash assay in HEK293 cells showed *ctβcat-Tcf711* mediated activation of the Tcf/Lef
40 driven luciferase reporter. **(B)** Scheme of the *Rosa26* locus and the targeting vector, homology
41 arms are depicted in red. E-EcoRI cleavage site, SA-splice acceptor, pA-poly-adenylation signal,
42 pGK-NeoR-neomycin expressing cassette, F-Flag tag sequence, primers for genotyping 21-
43 JM21F, 23-JM23R and 27-JM27R. **(C)** Southern blotting analysis confirms correct homologous
44 recombination into mES cells, short arm is on the left. **(D)** Western blotting of lysates from mouse
45 embryonic fibroblasts (MEFs) isolated from the *R26^{ERT2-cre};Rosa26^{ctβcat-Tcf711fl/+}* embryos revealed
46 presence of the *ctβcat-Tcf711* fusion protein 3 days after administration of 4-OHT (4-
47 *hydroxitamoxifen*). **(E-G)** *Rosa26^{ctβcat-Tcf711fl/+}* mice ubiquitously express fluorescent protein
48 tdTomato, the expression is lost in the regions where recombination occurs, visible in the *AP2α-
49 Cre;Tcf711^{fl/fl}; Rosa26^{ctβcat-Tcf711fl/+}* compound mutants, *AP2α-Cre;Tcf711^{fl/fl}* serves as a negative
50 control.

4

Mašek et al.

51 **Supplemental Table S1 (Related to Materials and methods)**

ISH probes		
Gene	forward	reverse
FoxD3	GGACCGCAAGAGTTCGCGGA	TCCGGAGCTCCCCTGTCGTT
Sox9	GAGCACTCTGGGCAATCTCAG	CTCAGGGTCTGGTGAGCTGTG
Gbx2	Gift from Peter Rathjen	Adelaide University
Sp5	CGTGAAGACGCACCAAAATA	TATTTTCACGCTGCCAACTG
Fgf8	CAGGTCCTGGCCAACAAG	GAGCTCCCGCTGGATTCTT
Sox10	Gift from Anthony Firulli	Indiana University, USA
Sox2	Open Biosystems	BC057574
FoxG1	Gift from Stefan Krauss	OUS, Oslo, Norway
Six3	Gift from Guillermo Oliver	St. Jude Hospital, Memphis, USA
Wnt1	Gift from Andy McMahon	USC, USA
Tcf7l1	Open Biosystems	BC128306
Tcf7l2	Open Biosystems	BC052022
Antibodies		
Gene	Company	Dilution
Sox1	R&D AF3369	1:1000
Tfap2a	Sanata Cruz Biotech SC-184	1:1000
Sox10	Santa Cruz Biotech SC-17342	1:1000
Sox9	Millipore AB5535	1:1000
N-cadherin	BD Transduction Lab. 610920	1:2000
GFP	Life Technologies A11122	1:1000
β -galactosidase	Abcam ab9361-250	1:1000
Lef1	Cell Siganling C12A5	1:1000

52

53